

Synaptotagmin 1 and Synaptic Vesicle Protein 2-like in Arabidopsis

Dissertation

zur

Erlangung des Doktorgrades (Dr. rer. nat.)

der

Mathematisch-Naturwissenschaftlichen Fakultät

der

Rheinischen Friedrich-Wilhelms-Universität Bonn

vorgelegt von

Wei Siao

aus

Taipei, Taiwan

Bonn 2016

Angefertigt mit Genehmigung der Mathematisch-Naturwissenschaftlichen
Fakultät der Rheinischen Friedrich-Wilhelms-Universität Bonn

1. Gutachter: PD Dr. Frantisek Baluska
2. Gutachter: Prof. Dr. Diedrik Menzel

Tag der Promotion: 20.05.2016

Erscheinungsjahr: 2016

Gedruckt mit Unterstützung des Deutschen Akademischen
Austauschdienstes

Summary

The process of synaptic transmission at neuronal synapses is mediated by synaptic vesicle cycle. Synaptotagmins (SYTs) and Synaptic Vesicle Protein 2 (SV2), widely studied in animals since the 1990s, are important synaptic vesicle proteins that regulate synaptic neurotransmission in animal neurons. However, functions of these synaptic vesicle protein homologs in plants remain to be elucidated. In order to gain a better understanding of signal transmission in plants, this study focuses on the subcellular localizations of synaptotagmin 1 and SV2-like in Arabidopsis as well as the functions of these proteins.

Arabidopsis synaptotagmin 1 (SYT1) is localized on the ER-PM contact sites in leaf and root cells. The ER-PM localization of Arabidopsis SYT1 resembles that of the extended synaptotagmins (E-SYTs) in animal cells. In mammals, E-SYTs have been shown to regulate calcium signaling, lipid transfer, and endocytosis. Arabidopsis SYT1 was reported to be essential for maintaining cell integrity by stabilizing the cytoskeleton. Our data provide detailed insight into the subcellular localization of SYT1 and VAP27-1, another ER-PM tethering protein. SYT1 and VAP27-1 were shown to be located on distinct ER-PM contact sites. The VAP27-1-enriched ER-PM contact sites (VECSs) were always associated with the SYT1-enriched ER-PM contact sites (SECSs), but not *vice versa*. The VAP27-1-enriched contact sites still existed in the leaf epidermal cells of *SYT1* null mutant. However, the VAP27-1-enriched contact sites in *SYT1* null mutant were less stable than that in the wild type. The polygonal networks of cortical ER disassembled and the

mobility of VAP27-1 protein on the ER-PM contact sites increased in leaf cells of *SYT1* null mutant. These results suggest that SYT1 is responsible for modulating the stability of ER network and the VAP27-1-enriched contact sites. Furthermore, cells of *SYT1* mutant line have smaller BFA-induced compartments in the transition zone of root apices, indicating that the endocytic pathway is modulated by SYT1.

Arabidopsis Synaptic Vesicle Protein 2-Like (SVL) belongs to the major facilitator superfamily and has been shown to be a niacin/trigonelline transporter. However, physiological studies of SVL in Arabidopsis still remain scarce. Our data have shown that Arabidopsis SVL protein is localized on the trans-Golgi network (TGN) and FM-dye stained early endosomes. The subcellular localization pattern of Arabidopsis SVL is similar to mammalian Synaptic Vesicle Protein 2 (SV2) and SV2-related Protein (SVOP) in neurons. The gene expression of SVL is developmental stage-dependent and can be detected in roots, hypocotyls, leaves, and anthers. One SVL mutant (*svl-1*) was identified and the transgenic Arabidopsis expressing SVL-GFP fusion protein was generated for functional and cytological studies. We have demonstrated that the primary root of SVL mutant grew slightly faster than the wild type during the early seedling stage in the control condition. The subcellular localization of SVL was sensitive to brefeldin A (BFA) treatment. In summary, Arabidopsis SVL participates in the endocytotic pathway in roots. Further studies on other possible functions of SVL in signal transduction and stress responses are still required. These data provide first insights into the sensory functions of SVL in Arabidopsis roots.

Table of Contents

1. Introduction.....	1
1.1. Arabidopsis Synaptotagmin 1	1
1.1.1. Mammalian Synaptotagmins	3
1.1.2. Mammalian Extended Synaptotagmins	5
1.1.3. ER-PM Contact Sites in Mammalian Cells	6
1.1.4. ER-PM Contact Sites in Plant Cells	9
1.1.5. Arabidopsis Synaptotagmins.....	11
1.2. Arabidopsis Synaptic Vesicle Protein 2-Like	13
1.2.1. Synaptic Vesicle Protein 2 and Synaptic Vesicle Protein 2-like	13
1.2.2. Endosomal Trafficking Pathways in Plant Cells	15
2. Material and Methods.....	18
2.1. Plant Material and Growth Conditions	18
2.2. Constructs	20
2.3. Agrobacterium-Mediated Transient Expression in Tobacco Leaves	21
2.4. Transient Transformation of Arabidopsis Leaves by Biolistic Bombardment	22
2.5. FRAP Analysis	22
2.6. Western Blot.....	23
2.7. Immunogold Labeling	24
2.8. Whole Mount Immunofluorescence Labeling.....	25
2.9. Analysis of BFA Compartments.....	26
2.10. Phylogenetic Analysis	26
2.11. Histochemical GUS Assay	28
2.12. RT-PCR.....	28
2.13. Confocal Microscopy	28
2.14. Accession Numbers	29
3. Results	30
3.1. Tethering of Arabidopsis SYT1 on the PM Maintains the Stability of ER Network and ER-PM Contact Sites	30
3.1.1. Arabidopsis SYT1 is Localized on the ER-PM Contact Sites	30
3.1.2. SYT1 and VAP27-1 are Localized on Different Regions of ER-PM Contact Sites	32

3.1.3.	Spatial Distributions of SECSs, VECs, and Plant Cytoskeleton	39
3.1.4.	Disruption of VAP27-1 Tethering to PM has no Obvious Effects on Formation of SECSs.....	44
3.1.5.	SYT1 Stabilizes VECs by Maintaining Patterns of Polygonal ER Networks	48
3.1.6.	SYT1-Mediated Regulation of Vesicle Trafficking.....	55
3.2.	Trans-Golgi Network-Localized Synaptic Vesicle Protein 2-like in Root Apex Cells	63
3.2.1.	Phylogenetic Relationship of SV2 and SV2-like Proteins in Eukaryotes	63
3.2.2.	Expression of SVL is Developmental Stage-Dependent	64
3.2.3.	SVL Null Mutant Showed no Apparent Phenotype	66
3.2.4.	SVL is Localized on the Trans-Golgi Network	68
4.	Discussion	76
4.1.	Arabidopsis SYT1.....	76
4.1.1.	Subcellular Localization of SYT1.....	76
4.1.2.	Tethering of SYT1 and VAP27-1 on ER-PM Contact Sites	80
4.1.3.	ER-PM Contact Sites and Vesicle Trafficking	83
4.2.	Arabidopsis SVL	85
4.2.1.	Physiological Functions of Arabidopsis SVL	85
4.2.2.	Subcellular Localization of Arabidopsis SVL	86
5.	Conclusions.....	88
6.	References.....	90
7.	Appendix.....	102
7.1.	Abbreviation	101
7.2.	List of Figures.....	104
7.3.	List of Tables.....	106
	Acknowledgements	107

Curriculum Vitae

1. Introduction

Both plants and animals are sensitive to environmental stimuli and respond accordingly. Animals have developed sophisticated nervous systems for sensing, hunting, escaping, memory, communication, and learning. The rapid electrical signal transduction and synaptic neurotransmission are two essential elements for the function of the nervous system. It has been shown that plants are able to sense environmental stimuli and respond rapidly within seconds or store the information for future reactions. Plants are also able to recognize, communicate, and interact with organisms, including other individual plants, bacteria, and animals. This indicates that plants possess systems, which have not yet been fully studied, for information transmission and integration. Several types of long-distance electrical signals have been identified in plants. These signals mediate movements, growth, and a variety of physiological processes in plants. However, the process of converting electrical signals into chemical signals in plants is still unclear. This study aims at investigating whether synaptic transmission is existent in Arabidopsis.

1.1. Arabidopsis Synaptotagmin 1

Proteins with multiple C2 domains are often found to participate in membrane trafficking or membrane tethering processes in eukaryotic cells (Min et al., 2007). These functions are credited to the ability of their C2 domains to bind negatively charged phospholipids mostly in a Ca^{2+} -dependent manner or interact with other protein partners (Nalefski and Falke, 1996). Arabidopsis

Synaptotagmin 1 (SYT1) belongs to a five-member gene family (SYT1-5) in *Arabidopsis thaliana*. All proteins in this gene family contain an N-terminal transmembrane domain (TM), a synaptotagmin-like mitochondrial and lipid-binding protein (SMP) domain, and two tandem C2 domains at its C-terminus (Yamazaki et al., 2010). The protein structure of *Arabidopsis* SYT1 is similar to both metazoan synaptotagmins (SYTs) and metazoan extended synaptotagmins (E-SYTs) (Craxton, 2010). Protein domains of *Arabidopsis* SYT1, human SYT1, human E-SYT1-3, and the homologs in yeast are illustrated in Figure 1, which is based on NCBI protein database and the previous studies (Giordano et al., 2013; Levy et al., 2015; Min et al., 2007; Perez-Sancho et al., 2015).

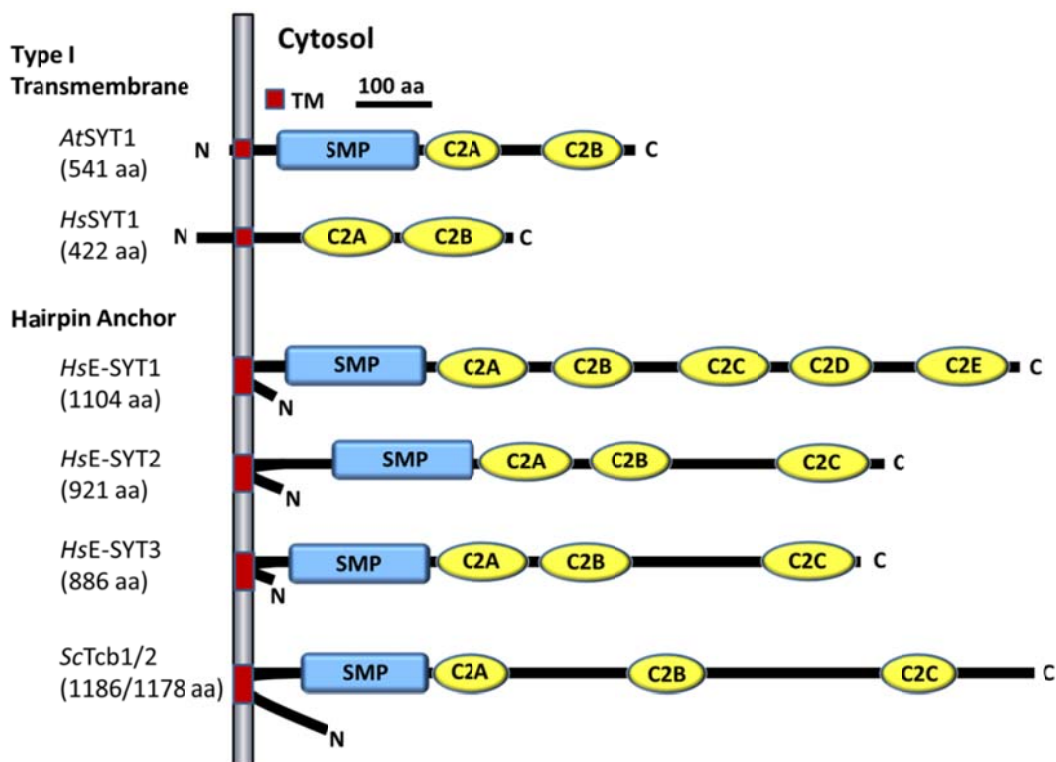


Figure 1. Protein Domains of *Arabidopsis thaliana* SYT1 (AtSYT1), *Homo sapiens* SYT1 (HsSYT1), *Homo sapiens* E-SYT1, 2 and 3 (HsE-SYT1-3), and *Saccharomyces cerevisiae* Tricalbin-1 and -2 (ScTcb1/2). AtSYT1 and

HsSYT1 are type I transmembrane protein with the N-terminus facing the non-cytosolic space. *HsE-SYTs* and *ScTcbs* are inserted in the membrane by a hydrophobic hairpin structure with the N-terminus in the cytosol.

Transmembrane domain (TM); synaptotagmin-like mitochondrial and lipid-binding protein domain (SMP); C2 domains (C2A-E).

1.1.1. Mammalian Synaptotagmins

Mammalian SYTs are integral synaptic vesicle proteins with an N-terminal TM, a variable-length linker domain, and two cytoplasmic C2 domains in tandem (Südhof, 2002). At least 17 SYT isoforms have been found in mammals. Most of these proteins are expressed in neurons or neuroendocrine cells, and play essential roles in Ca^{2+} -regulated neurotransmission and hormone secretion (Moghadam and Jackson, 2013). The binding of Ca^{2+} to the C2 domains of SYTs is required to trigger vesicle fusion to the plasma membrane (PM) in exocytosis (Mackler et al., 2002). Human SYT1, the most characterized isoform, is a Ca^{2+} sensor for fast synchronous neurotransmitter release in forebrain neurons (Geppert et al., 1994; Südhof, 2013). Human SYT2, with no invertebrate homolog, is the predominant isoform that triggers very fast synaptic vesicle exocytosis in the brainstem (Saraswati et al., 2007; Südhof, 2013). Human SYT7 is abundant in brain neurons and pancreatic cells, functions in slow asynchronous release in neuroendocrine cells and Ca^{2+} -induced exocytosis of insulin and glucagon secretion in pancreatic cells (Bacaj et al., 2015; Gustavsson et al., 2009; Sugita et al., 2001). Similar to SYT1, human SYT9 is also a Ca^{2+} sensor mediating synchronous

neurotransmitter release; however, it exhibits intermediate Ca^{2+} -regulated membrane binding in endocrine cells (Zhang et al., 2011b). The tissue distribution and the subcellular localization of SYT isoforms are varied in the human body (Moghadam and Jackson, 2013; Südhof, 2002). SYT proteins are widely studied in neuroscience and medical research because of their important functions in regulating the neurotransmission and endocrine exocytosis. The domain structure of rat SYT1 is shown in Figure 2 (Lin et al., 2014).

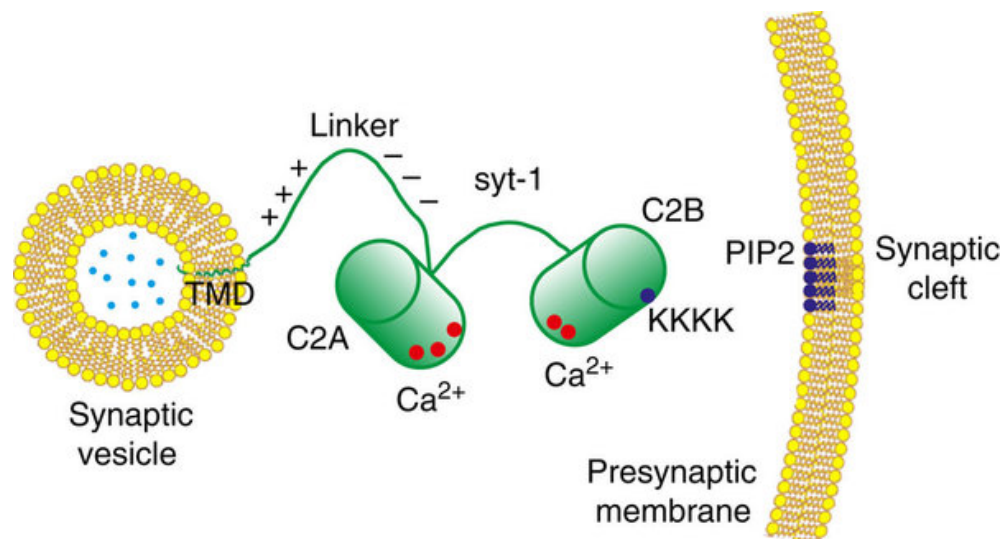


Figure 2. Domain Structure of Rat SYT1. Ca^{2+} -binding sites of C2A and C2B (red dots); Poly-lysine patch (KKKK) of the C2B domain (dark blue dots); Clusters of positive and negative charges on the linker domain (+ or - signs). Neurotransmitter molecules (bright blue dots); phosphatidylinositol(4,5)-bisphosphate (PIP2); transmembrane domain (TMD). Adopted from (Lin et al., 2014).

1.1.2. Mammalian Extended Synaptotagmins

Mammalian E-SYTs are endoplasmic reticulum (ER) membrane proteins that contain an N-terminal hairpin transmembrane domain, a SMP domain, and five (E-SYT1) or three (E-SYT2/3) C-terminal C2 domains (Min et al., 2007). Human *E-SYT1* is expressed almost ubiquitously while human *E-SYT2* and *E-SYT3* are expressed mainly in cerebellum (Min et al., 2007). On the other hand, mouse *E-SYT1* and *E-SYT2* are expressed primarily in spleen and lung of adult mice, and mouse *E-SYT3* is expressed predominantly in testis and lung (Herdman et al., 2014). Mouse *E-SYT2* is expressed ubiquitously and highest in the neural tube of mouse embryos while mouse *E-SYT3* is expressed mainly at the midbrain-hindbrain boundary (Herdman et al., 2014). Mammalian E-SYTs are known as to participate in the ER-PM tethering (Stefan et al., 2013). Human E-SYT2 and E-SYT3 bind PM-enriched phospholipid PIP₂ at resting Ca²⁺ levels while the tethering of human E-SYT1 to the PM is triggered by elevation of cytosolic Ca²⁺ (Giordano et al., 2013). C2C domain of human E-SYTs is essential for the binding to the PM and the binding is not disrupted by depolymerization of actin or microtubule cytoskeletons (Giordano et al., 2013; Min et al., 2007). The SMP domain is a membrane binding domain belong to the tubular lipid-binding (TULIP) superfamily, a group of proteins that often found to bind lipids and mediate lipid transfer (Kopec et al., 2010). Proteins containing a SMP domain are found to be localized on the membrane contact sites in yeast, such as ER-mitochondrion encounter structure (ERMES) complex on the ER-mitochondria contact sites, nucleus-vacuole junction (Nvj2) on the ER-vacuole contact sites, and tricalbins (Tcb1, 2 and 3), the homologs of mammalian E-SYTs, on the

ER-PM contact sites (Toulmay and Prinz, 2012). The SMP domain of human E-SYT2 has been proposed to function in non-vesicular lipid transfer because their ability to form a hydrophobic channel by dimerization and to bind glycerophospholipids (Figure 3) (Schauder et al., 2014).

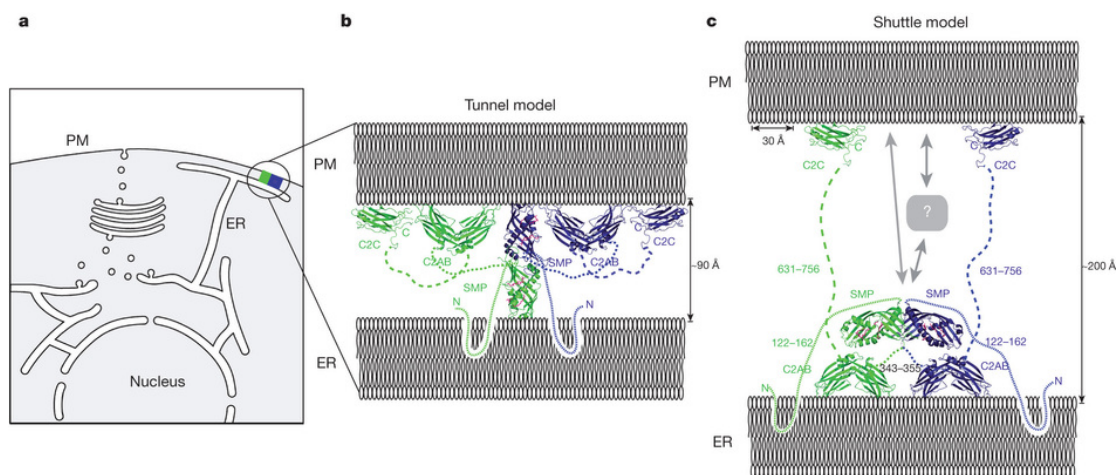


Figure 3. Models of Lipid Transfer by Human E-SYT2. (a) A diagram of an ER-PM contact site. (b) Tunnel model: The E-SYT2 dimer forms a channel between the ER and PM to transfer lipids. (c) Shuttle model. The E-SYT2 dimer shuttles lipids between the ER and PM. Putative partner proteins (question mark). Adopted from (Schauder et al., 2014).

1.1.3. ER-PM Contact Sites in Mammalian Cells

Membrane contact sites (MCSs) are regions where the membranes of two organelles are in close proximity (Helle et al., 2013). The membranes from two compartments on the MCSs do not fuse together and require specific tethering proteins to maintain the close apposition between the membranes, typically within 30 nm (Prinz, 2014). The ER is an expansive and dynamic network composed of membrane tubules and sheets that functions in protein synthesis,

protein modification, lipid biosynthesis and ion homeostasis. The ER is the origin of the secretory pathway that sends proteins and lipids to the PM by vesicle budding, sorting and fusion. ER may also form direct contact with the PM and other organelles (Friedman and Voeltz, 2011). ER-PM contact sites were first reported in 1957 by electron microscopic observation in muscle cells (Porter and Palade, 1957), and later on also in neurons (Rosenbluth, 1962). Recent studies have revealed the tethering mechanisms of ER-PM contact sites, which are now known to be a common feature in the eukaryote cells (Friedman and Voeltz, 2011; Henne et al., 2015).

Until now three groups of proteins have been shown to be involved in the formation of ER-PM contact sites in mammals: 1) Extended synaptotagmins (E-SYTs); 2) vesicle-associated membrane protein (VAMP)-associated proteins (VAPs) and 3) junctophilins (JPHs) (Henne et al., 2015). E-SYT1 binds to the PM in response to the increased cytosolic Ca^{2+} and is postulated to regulate the Ca^{2+} -dependent PM remodeling in neurons (Giordano et al., 2013). E-SYT2 binds to the PM without elevation of cytosolic Ca^{2+} and is supposed to function in lipid transfer (Schauder et al., 2014). VAP proteins contain an N-terminal major sperm protein (MSP) domain, a coiled-coil domain, and an ER-anchored C-terminal transmembrane domain (Han et al., 2012; Moriishi and Matsuura, 2012). VAP proteins interact with several proteins containing di-phenylalanine in an acidic tract (FFAT) motifs, and the MSP domain can bind phospholipids on the PM (Henne et al., 2015). Many of the proteins contain FFAT motifs are participated in lipid transfer, such as oxysterol-binding protein (OSBP)-related proteins (ORPs) and proline-rich tyrosine kinase 2 (PYK2) N-terminal domain-interacting receptors (Nir proteins) (Amarilio et al., 2005; Barajas et al., 2014). Junctophilins have a single

C-terminal transmembrane domain anchored on the sarcoplasmic reticulum (SR), a long cytoplasmic α -helix with multiple membrane occupation and recognition nexus (MORN) motifs in the N-terminus (Garbino et al., 2009). Junctophilins bind to the PM through their MORN motifs and are important for the maintenance of SR-PM contact sites and Ca^{2+} signaling in muscle cells (Takeshima et al., 2000).

Another well studied ER-PM tethering proteins in yeast is increased sodium tolerance protein 2 (Ist2), which belongs to the anoctamin (TMEM16) family of Ca^{2+} -activated Cl^- channels. Yeast Ist2 is anchored on the ER through its multi-transmembrane domain and binds to the PM by a C-terminal lipid binding polybasic (PB) domain (Schulz and Creutz, 2004). However, human TMEM16A, also called anoctamin 1 (ANO1), is a plasma membrane channel without a PB domain and may mediate Ca^{2+} signaling on the ER-PM contact sites without a membrane tethering function (Jin et al., 2016). In addition, ER-PM contact sites are the regions where the process of store-operated Ca^{2+} entry (SOCE) takes place. When Ca^{2+} levels in the ER lumen are depleted, the ER-resident protein stromal interaction molecule-1 (STIM1) oligomerizes and accumulates on the pre-existing ER-PM contact sites. STIM1 binds phosphoinositides (PIPs) on the PM through the PB domain and then activates the PM-localized Ca^{2+} release-activated Ca^{2+} (CRAC) channel Orai1 by the CRAC activation domain, leading to Ca^{2+} influx from the extracellular space to the ER (Liou et al., 2007; Stathopoulos et al., 2006). Proteins that function on the ER-PM contact sites are shown in Figure 4 (Henne et al., 2015).

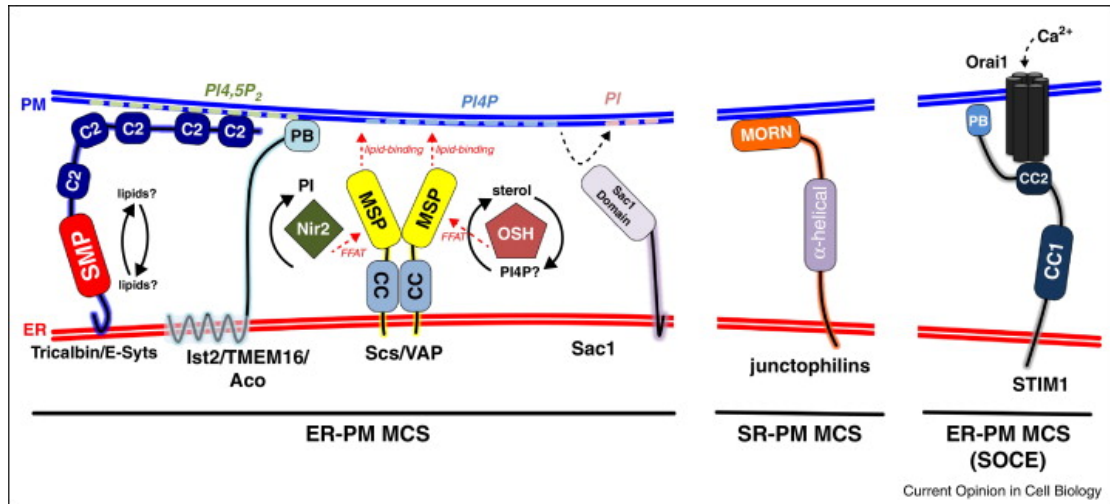


Figure 4. ER-PM Tethering Proteins in Mammals. All the proteins that mediate ER-PM tethering are ER membrane-anchored proteins and contain cytoplasmic lipid-binding domains. Coiled-coil domain (CC); oxysterol binding homology (OSH); phosphoinositide phosphatase (Sac1). Adopted from (Henne et al., 2015).

1.1.4. ER-PM Contact Sites in Plant Cells

Five proteins localized on the ER-PM contact sites in Arabidopsis are reported recently: Networked 3C (NET3C), VAMP/synaptobrevin-associated protein 27 (VAP27)-1, -3 and -4 (VAP27-1, VAP27-3 and VAP27-4), and synaptotagmin 1 (SYT1). NET3C belongs to the plant-specific NET superfamily of actin binding proteins. All the 13 members of the Arabidopsis NET family contain a NET actin-binding (NAB) domain and various numbers of coiled-coil domains that can simultaneously interact with the actin filaments and different membrane compartments (Deeks et al., 2012; Hawkins et al., 2014). NET3C contains an N-terminal NAB domain that interacts with actin cytoskeleton and a C-terminal

coiled-coil domain for self-oligomerization. The NAB domain is required for NET3C to localize on the ER-PM contact sites and a C-terminal lysine residue in the polybasic domain is important for the association of NET3C with the PM (Wang et al., 2014). Arabidopsis VAP27 proteins belongs to the VAP33-like family which are homologs of mammalian VAPs and yeast suppressor of choline sensitivity (Scs2) (Sutter et al., 2006; Saravanan et al., 2009). The conserved MSP domain is essential for VAP27-1 to anchor on the ER-PM contact sites and interaction of VAP27-1 with NET3C. VAP27-1 can form dimers or oligomers and interact with microtubules that restrain the turnover of VAP27-1 on the ER-PM contact sites (Wang et al., 2014, Wang et al., 2016). Furthermore, recent studies have shown that Arabidopsis SYT1 is co-localized with VAP27-1 on the ER-PM contact sites (Levy et al., 2015; Perez-Sancho et al., 2015). Two possible models for the plant ER-PM contacts are shown in Figure 5 (Wang et al., 2014).

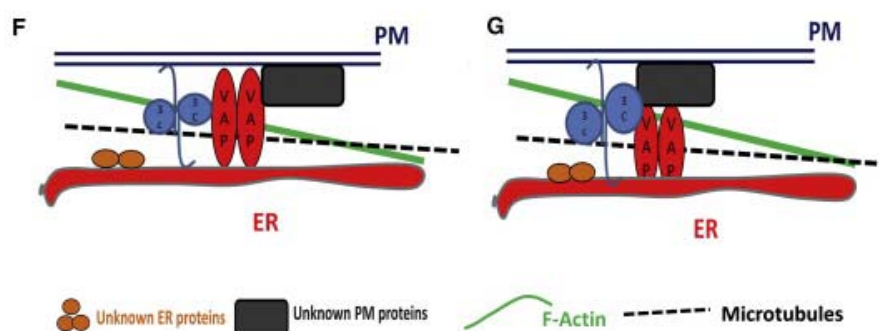


Figure 5. Schematic Depiction of NET3C, VAP27-1 and Cytoskeleton on ER-PM Contact Sites. VAP27-1 binds to the PM directly and interact with NET3C and other unknown PM proteins (left panel). NET3C forms the ER-PM contact sites with other PM proteins and recruits VAP27-1 to the contact sites (right panel). The microtubules and actin associate with VAP27-1 and NET3C, respectively. Adopted from (Wang et al., 2014).

1.1.5. Arabidopsis Synaptotagmins

Arabidopsis synaptotagmins (SYT1-5) are a family of type I membrane proteins that all contain an N-terminal transmembrane domain, a SMP domain and two C-terminal C2 domains. Arabidopsis SYT1 was thought to be a PM protein but recent studies and this study have shown that it is an ER-anchored protein. Arabidopsis *SYT1* is constitutively expressed in all the tissues and the mutants are more sensitive to salt, freezing and mechanical stresses (Levy et al., 2015; Perez-Sancho et al., 2015; Schapire et al., 2008; Yamazaki et al., 2008; Yamazaki et al., 2010). In addition, the virus infections are delayed in *SYT1* null mutant (Lewis and Lazarowitz, 2010; Uchiyama et al., 2014). The C2A domain of Arabidopsis SYT1 binds to the liposomes consisted of phosphatidylserine (PS)/phosphatidylcholine (PC) in a Ca^{2+} -dependent fashion while the C2B domain binds to the liposome in the absence of Ca^{2+} (Schapire et al., 2008). The C2AB domains of Arabidopsis SYT1 bind PIPs and PS, but not phosphatidylinositol (PI) and PC, with or without the existence of Ca^{2+} ; however, the binding of C2AB domains to PS is enhanced by Ca^{2+} (Perez-Sancho et al., 2015). The Ca^{2+} -independent binding of C2AB to PIPs indicates that Arabidopsis SYT1 may bind the PM at resting cytosolic Ca^{2+} concentrations in plant cells, a situation similar to E-SYT2/3 in human cells, or may function cooperatively in both Ca^{2+} -dependent and Ca^{2+} -independent pathways like mammalian SYT1 (Giordano et al., 2013; Südhof, 2012). In addition, expression of the truncated Arabidopsis SYT1 lacking the C2B domain disrupts the formation of PM-derived early endosomes in the leaves of *N. benthamiana* (Lewis and Lazarowitz, 2010). Arabidopsis *SYT2* has been shown to be mainly expressed in the pollen and developing embryo sacs by

RT-PCR and promoter analyses and play a role in pollen germination and pollen tube growth (Wang et al., 2015a). However, Arabidopsis SYT2 protein can be detected in the roots of wild type Arabidopsis (Zhang et al., 2011a). Arabidopsis SYT2 is localized on the Golgi-apparatus which involved in the conventional secretion and regulates the unconventional secretion of hygromycin phosphotransferase (Wang et al., 2015a; Zhang et al., 2011a). Similar to Arabidopsis SYT1, the binding of the C2A domain of Arabidopsis SYT2 to the liposome (PS/PC) is Ca^{2+} -dependent but that of the C2B domain is Ca^{2+} -independent (Wang et al., 2015a). Arabidopsis SYT2 has been shown to be delivered to the PM (Wang et al., 2015a); however, it is still unclear whether Arabidopsis SYT2, and other SYT members, can also function on the membrane contact sites. The roles of Arabidopsis SYTs in vesicle trafficking and membrane tethering remain to be elucidated. The putative roles of Arabidopsis SYT1 in the ER-PM contact sites are illustrated in Figure 6 (Perez-Sancho et al., 2015).

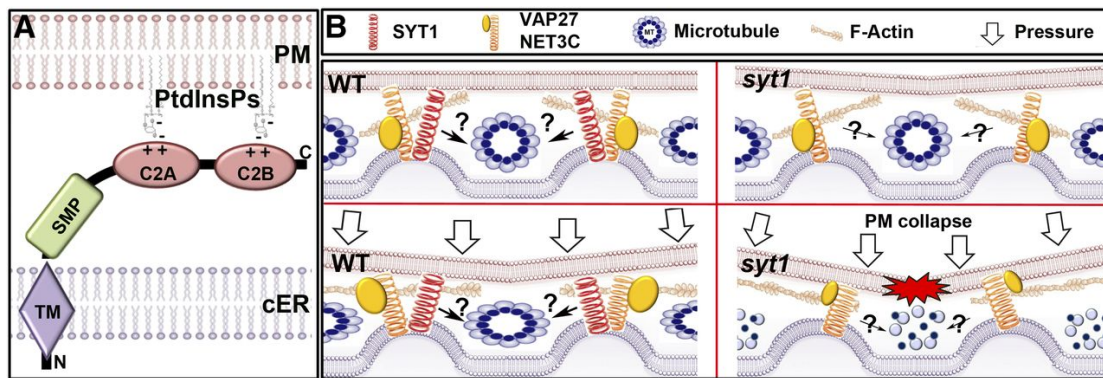


Figure 6. Schematic Depiction of SYT1 on ER-PM Contact Sites. (A)

Arabidopsis SYT1 binds phosphoinositides (PtdInsPs) on the PM through the C2 domains. (B) SYT1 maintains the PM stability by strengthening the ER-PM contact sites and distributes the mechanical forces (Left). The microtubules are depolymerized and the PM is disrupted by the mechanical stresses in the absent of SYT1 (Right). Adopted from (Perez-Sancho et al., 2015).

1.2. Arabidopsis Synaptic Vesicle Protein 2-Like

1.2.1. Synaptic Vesicle Protein 2 and Synaptic Vesicle Protein 2-like

Mammalian synaptic vesicle protein 2 (SV2), is a 12-transmembrane glycoprotein localized on the synaptic vesicles. There are three characterized isoforms in mammals, SV2A, SV2B and SV2C, which are belong to the major facilitator superfamily (MFS) of transporters (Feany et al., 1992; Janz and Südhof, 1999; Schivell et al., 1996). It has been shown that SV2A knock-out mice are prone to having severe seizures and die within a few weeks after birth (Crowder et al., 1999). Mammalian SV2A are known to interact with SYT1, and modulate Ca^{2+} -induced exocytosis, priming of synaptic vesicles and calcium channel current density (Vogl et al., 2015; Xu and Bajjalieh, 2001). Human

SV2A has been also shown to be a galactose transporter when expressing in yeast cells (Madeo et al., 2014). Furthermore, SV2A is the target for the anti-epileptic drug levetiracetam (Lynch et al., 2004), and SV2A and SV2B are the receptors for botulinum and tetanus neurotoxins (Dong et al., 2006; Yeh et al., 2010). However, the molecular mechanism of SV2 proteins underlying the regulation of the synaptic exocytosis remains uncertain.

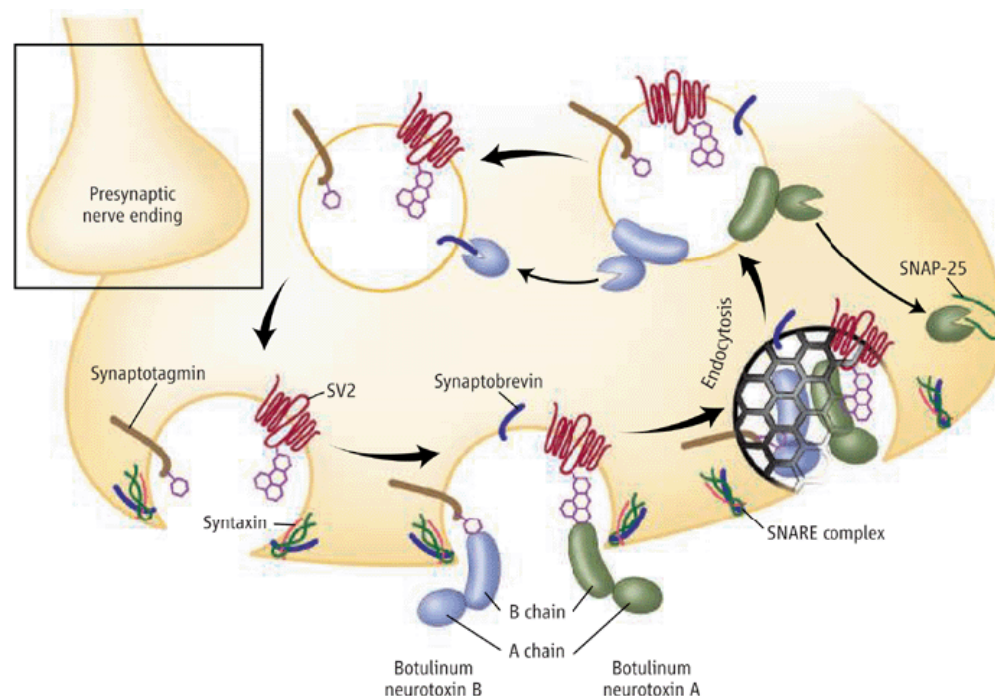


Figure 7. Botulinum Neurotoxins Entry into Neurons via SV2. SV2 and synaptotagmin are the receptors of botulinum neurotoxins A and B, respectively. The toxins are internalized by clathrin-mediated endocytosis and cleave the SNARE proteins. Adapted according Jahn (2006).

Mammalian SV2-like/SVtwO-related Protein (SVOP) is distantly related to SV2 and localized also mainly on the synaptic vesicles in brain and endocrine cells. Since the first SVOP report was published on the Journal of Neuroscience on 1998 (Janz et al., 1998), many scientists have studied the function of SVOP

protein in mammals. However, we now only know that SVOP homologs are present in all eukaryotes, but SVOP is only detected in the central nervous systems in vertebrates (Yao et al., 2013). *SVOP* is mainly expressed in the developing neurons, and its expression declines with aging (Hong et al., 2008; Logan et al., 2005). This suggests that *SVOP* may play roles in neuronal development and brain aging. Mouse SVOP has been shown to be the niacin transporter in bacteria and bind nucleotides *in vitro*. However, no measurable phenotype can be observed in *SVOP* knockout mice (Yao et al., 2013).

Arabidopsis SV2-like (SVL) protein, as well as mouse SV2-like/SVOP protein, has been shown to be a niacin transporter when it was heterogeneously expressed in lactic acid bacteria (Jeanguenin et al., 2011). However, there is no report so far pertaining to the functional study of SV2-like in plant cells.

1.2.2. Endosomal Trafficking Pathways in Plant Cells

The endomembrane system is composed of a variety of membranes-bound organelles that functions in the synthesis, sorting, transport, storage and degradation of macromolecules in eukaryotic cells. The subcellular compartments of the system included the ER, the Golgi apparatus, the trans-Golgi network (TGN), endosomes and vacuoles. These compartments can be connected either by direct contact or through vesicle trafficking. Endosomes are pivotal components of vesicle transport and involved in endocytic, biosynthetic, and recycling pathways in plant cells (Reyes et al., 2011).

Endosomes can be categorized into two groups: early endosomes (EEs)

and late endosomes (LEs). Early endosomes are characterized as the first endocytic compartments derived from the plasma membrane by endocytosis (Bolte et al., 2004). The cargo proteins endocytosed from the cell surface may be either recycled back to the PM through the recycling endosomes (REs), or may be retained in the EEs, which later on mature into LEs, and then transported to the vacuoles for degradation. Late endosomes in plant cells normally have a multivesicular structure, which then also termed as the multivesicular bodies (MVBs) (Contento and Bassham, 2012). In the biosynthetic pathway, the secretory and vacuolar proteins are synthesized in the ER lumens and exit the ER via the budding of COPII-coated vesicles. The vesicles are fused to the Golgi apparatus and the proteins pass through the Golgi complex by cisternal maturation. As the maturation proceeds, the trans-most cisternae of the Golgi stacks become the TGN, a dynamic compartment where the sorting processes of cargo proteins are active. Secretory proteins are exported from the TGN into secretory vesicles and delivered to the PM by exocytosis. In addition, the materials internalized by endocytosis are first incorporated into the TGN in plant cells, indicating that the endocytic pathway and the secretory pathway merge on the TGN (Viotti et al., 2010). The TGN is equivalent to the EEs in plant cells, which often termed TGN/EE. On the other hand, vacuolar proteins are sequestered into the TGN fragments, which then mature into the MVBs and are destined for the vacuoles (Robinson and Pimpl, 2014). The MVBs are also termed prevacuolar compartments (PVCs) in plant cells, and are the sites where the trafficking of vacuolar proteins and the endocytic pathway meet. Therefore, MVBs are equivalent to PVCs and LEs in plant cells. The endosomal trafficking pathways are shown in Figure 8 (Reyes et al., 2011).

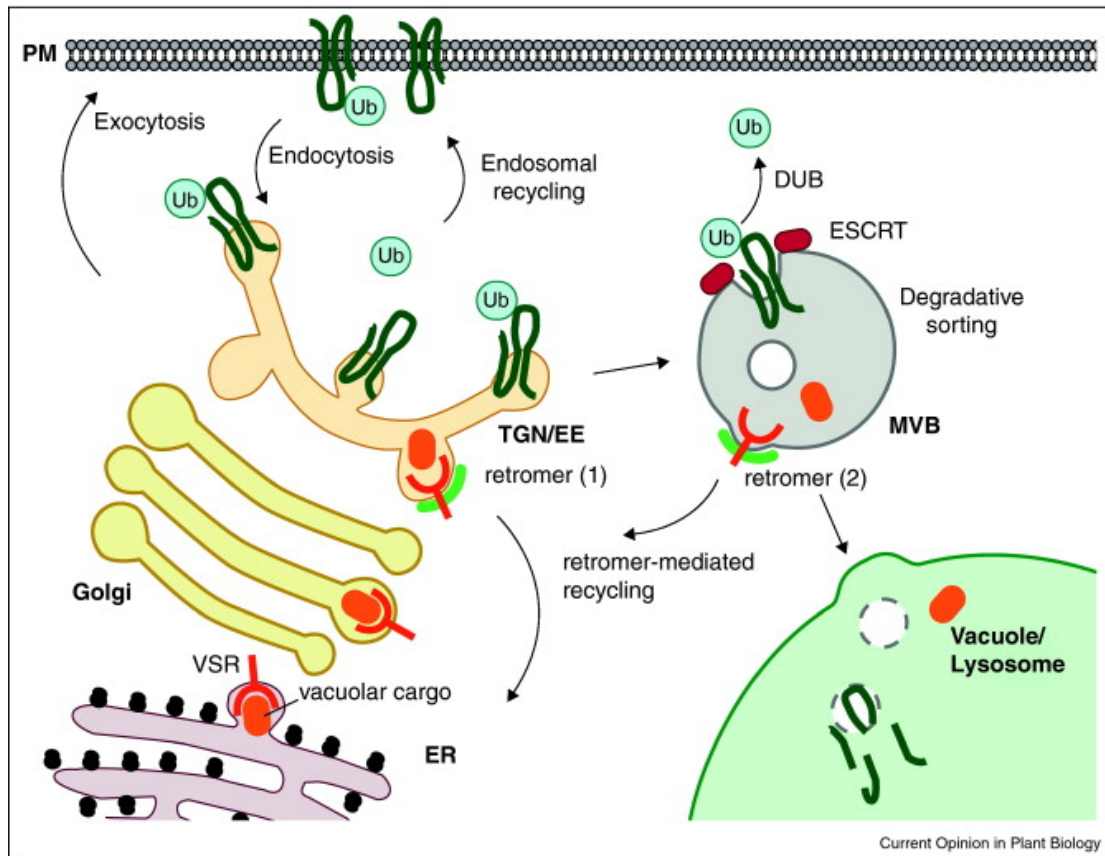


Figure 8. Endocytic and Exocytic Pathways in Plant Cells.

PM proteins are internalized by endocytosis and delivered to TGN/EE. PM proteins are either transported back to the PM (endosomal recycling) or to the MVBs and the vacuoles/lysosome for degradation (degradative sorting). The newly synthesized PM proteins are secreted to the PM by exocytosis and the vacuolar cargos are sent to the vacuoles. The vacuolar sorting receptors (VSRs) can be recycled back to cis-Golgi and/or ER (retromer-mediated recycling). Adopted according Reyes et al. (2011).

2. Material and Methods

2.1. Plant Material and Growth Conditions

Arabidopsis thaliana (L.) seedlings were grown on vertical half-strength Murashige and Skoog (1/2 MS) agar plates (pH = 5.8) in a growth chamber at 22°C under long-day conditions (16 h Light/ 8 h Dark). After 14 days, the seedlings were transferred and grown in pots in a culture room at 22°C under long-day conditions (16 h Light/ 8 h Dark). Experiments were performed using *Arabidopsis thaliana* Columbia ecotype (Col-0), *syt1-2* (SAIL_775_A08), *svl-1* (SALK_114298), *svl-2* (SALK_089824C) and *svl-3* (SALK_069071.25.70x), VAP27-1 RNAi knock-down lines and VAP27-1-YFP/Col-0 transgenic lines. VAP27-1 RNAi and VAP27-1-YFP transgenic lines were kindly provided by Dr. Pengwei Wang and Prof. Patrick J. Hussey, Durham University, UK. VAP27-1-YFP/*syt1-2* transgenic lines were obtained by agrobacterium-mediated transformation of VAP27-1-YFP into *syt1-2* using floral-dipping (Clough and Bent, 1998; Zhang et al., 2006). SVL-promoter:GUS transgenic Arabidopsis was generated by Dr. Boris Voigt. The 1541 bps of SVL promoter was amplified from genomic DNA of Arabidopsis Col-0 using primers prSVL-F and prSVL-R listed in Table 1 and then cloned into the binary vector *pΔGusBin19* (Topping et al., 1991) by BamHI/SmaI sites. The fusion construct was transformed into Col-0 using floral-dipping. SVL-GFP/*svl-1* transgenic Arabidopsis was obtained by floral-dipping transformation of SVL-promoter:SVL-GFP fusion construct into *svl-1*.

Table 1. Primer List.

The sequences of restriction enzyme cutting site, the mutated nucleotides, and the adapter sequences of attB sites are underline.

SVL Promoter GUS Analysis	
prSVL-F	5'-GCGGATCCTGTA <u>ACTCACGGACCA</u> ATTC
prSVL-R	5'-GCC <u>CCGGG</u> GAGAAAAGTGTCAACCTTTCATC
Site-directed Mutagenesis	
SpeI-SYT1-F	CGACA <u>CTAGT</u> ATGGGCTTTTTTCAGTACG
emGFP-BsrGI-R	TACTT <u>GTAC</u> AGCTCGTCCATGCCG
D370N/E372Q-F	GTGTGTATA <u>ACTGGCAAC</u> AGGT
D370N/E372Q-R	ACCTGTT <u>GCCAGT</u> IATACACAC
E378Q-F	TTGGGAATCC <u>CC</u> CAGAAGATGGG
E378Q-R	CCCATCTTCT <u>G</u> GGGATTCCCAA
Genomic DNA Amplification	
AP2 μ 2-F	5'- <u>GGGGACAAGTTTGTACAAAAAAGCAGGCTTCCCGCCAGG</u> ATCAAAGA CGGATCGAGCAA
AP2 μ 2-R	5'- <u>GGGGACCACTTTGTACAAGAAAGCTGGGTCTGCATCTGATC</u> TCGTAAGATCCC
SVL-F	5'- <u>GGGGACAAGTTTGTACAAAAAAGCAGGCTTCCCGCCATGT</u> AACTCACGGACCAATTCAA
SVL-R	5'- <u>GGGGACCACTTTGTACAAGAAAGCTGGGTCTACGGAGGC</u> TGAAGGTGGTTCT
RT-PCR	
RT SVL-F	5'-TCGTTCTCCTGAAACCGTGG
RT SVL-R	5'-CCAAGACCAACCAACAGCG

2.2. Constructs

Binary plasmids of Arabidopsis SYT1 tagged with GFP driven by native *SYT1* promoter (SYT1-GFP), VAP27-1 tagged with YFP driven by 35S promoter (VAP27-1-YFP), and NET3C fused with RFP driven by 35S promoter (RFP-NET3C) were described previously (Wang et al., 2014; Yamazaki et al., 2010). The ER marker HDEL-RFP (Lee et al., 2013; Wang et al., 2014), the microtubule marker MBD-MAP4-DsRed (Granger and Cyr, 2001; Marc et al., 1998), the actin marker ABD2-mCherry (Voigt et al., 2005b), the Golgi marker ST-RFP (Renna et al., 2005; Schoberer et al., 2010), the TGN marker VT112-mCherry (Geldner et al., 2009), the late endosome marker FYVE-mCherry (Voigt et al., 2005a), Ara6-CFP and Rha1-mCherry (Geldner et al., 2009), the recycling endosome marker RabA1e-mCherry (Geldner et al., 2009), the early endosome marker CLC-mCherry (Wang et al., 2015b; Wang et al., 2013) and AP2 μ 2-YFP (Bashline et al., 2013) were described in the indicated reports. The construct of SYT1-3M-GFP was generated by site-directed mutagenesis by overlap extension PCR (Ho et al., 1989) using primers listed in Table 1. The plasmid encoding mCherry fused to the C terminus of Arabidopsis AP2 μ 2 was constructed by cloning the genomic sequence including native *AP2* μ 2 promoter (Bashline et al., 2013) into pMDC83-mCherry vector by Gateway® Cloning system. The cDNA of *AP2* μ 2 was amplified from Arabidopsis genomic DNA using primers AP2 μ 2-F and AP2 μ 2-R listed in Table 1. *SVL-promoter:SVL-GFP* and *SVL-promoter:SVL-mCherry* fusion construct were generated by cloning the genomic sequence of *SVL* including the promoter into the binary vectors pMDC83-GFP and pMDC83-mCherry, respectively, using Gateway® Cloning system. The cDNA of *SVL* was amplified from Arabidopsis genomic DNA using primers SVL-F and SVL-R

listed in Table 1. pMDC83-GFP and pMDC83-mCherry binary vectors were kindly provided by Prof. Patrick J. Hussey, Durham University, UK (Curtis and Grossniklaus, 2003).

2.3. Agrobacterium-Mediated Transient Expression in Tobacco Leaves

Nicotiana benthamiana plants were grown in a culture room at 22°C under long-day conditions (16 h light/8 h dark) for 3-4 weeks. Each construct was transformed into *Agrobacterium tumefaciens* strain GV3101::pMP90 by electroporation followed by selection on YEB plates containing the appropriate antibiotics. Single colony was inoculated and grown overnight in 3 ml YEB liquid medium with antibiotics at 37°C. 1 ml of bacterial culture was centrifuged at 3,500 rpm for 5 min and the pellet was resuspended in 1 ml of infiltration medium (20 mM citric acid, 2% sucrose and 0.2 mM acetosyringone). The bacterial suspension was centrifuged and the pellet was resuspended again in 1 ml of infiltration medium to ensure complete removal of remnant antibiotics. Absorbance of the suspension at 600 nm was measured and the OD₆₀₀ was adjusted to the specified value for infiltration (OD₆₀₀ = 0.2 for SYT1-GFP, ABD2-mCherry, MAP4-DsRed and SVL-GFP; OD₆₀₀ = 0.1 for VAP27-1-YFP, NET3C-RFP and HDEL-RFP). Syringe infiltration of tobacco leaves was performed as previously described (Batoko et al., 2000; Sparkes et al., 2006). The plants were kept in the same culture room after infiltration for 2 days before confocal imaging.

2.4. Transient Transformation of Arabidopsis Leaves by Biolistic Bombardment

Arabidopsis thaliana Col-0 and *syt1-2* seedlings were grown on vertical 1/2 MS agar plates in a growth chamber at 22°C under long-day conditions for 2 to 3 weeks. The seedlings were transferred onto a new 1/2 MS agar plate with the abaxial sides of the leaves facing up. 0.75 mg of 0.6- μ m gold particles in 12.5 μ l of 50% glycerol was mixed with 2 μ g of VAP27-1-GFP plasmid DNA, 12.5 μ l of 2.5 M CaCl₂ and 5 μ l of 0.1 M spermidine by vortexing vigorously for 3 min. The coated gold particles were washed once with absolute ethanol and resuspended in 37.5 μ l of absolute ethanol. The suspended gold particles were loaded onto three carrier disks for three bombardments with rupture disks of 1350 psi using PDS-1000/HeTM Systems (Bio-Rad). After bombardment, the seedlings were turned back to the normal orientation on the same agar plate with the adaxial sides of the leaves facing up. The seedlings were incubated in the same growth chamber for 1 day and observed under confocal microscope.

2.5. FRAP Analysis

Stable transgenic Arabidopsis expressing VAP27-1-YFP in Col-0 (VAP27-1-YFP/Col-0) and *syt1-2* (VAP27-1-YFP/*syt1-2*) background were grown in pots for 4 weeks. One T3 homozygous line of VAP27-1/Col-0 and five T1 heterozygous lines of VAP27-1/*syt1-2* were planted. The expression levels of VAP27-1-YFP in five VAP27-1/*syt1-2* heterozygous lines were examined by confocal microscope, and one with comparable expression of VAP27-1-YFP with that in VAP27-1/Col-0 was used for FRAP experiments. Leaf discs (0.5 x 0.5 cm²) from the first or second leaf of the 4-week-old Arabidopsis were selected because the leaves have flattened surface. After incubated either with

Mock (0.1% DMSO), 20 μ M oryzalin or 25 μ M latrunculin B in Milli-Q water, the leaf discs were mounted in Milli-Q water and analyzed using confocal microscope with a 60x oil immersion objective and a zoom factor of 5.0. Confocal parameters were identical for all the FRAP experiments. 2% transmission of an argon laser at 515 nm was used for imaging and 80% transmission for photobleaching. Ten reference scans were taken before bleaching and 60 scans were taken after bleaching at 3-sec intervals. At least 20 VAP27-1-YFP-labeled puncta for each treatment were analyzed. The raw data were normalized and the best-fit curves were generated by least-squares regression using Prism (Graumann et al., 2007; Wang et al., 2011).

2.6. Western Blot

14-day-old seedlings were frozen by liquid nitrogen and grounded into powder. The total protein was extracted with protein extraction buffer (50 mM Tris-HCl, 150 mM NaCl, 10 mM MgCl₂, 0.5 % NP-40, 1 mM PMSF and 1 X protease inhibitor cocktail (P9599, Sigma). The protein samples were quantified using Bio-Rad Bradford Protein Assay and subjected to 5X sample buffer (300 mM Tris-HCl, 60% Glycerol, 10% SDS, 500 mM DTT and 0.01% bromphenol blue). The protein was denatured by heating at 70°C for 5 min and cooled down on ice. 40 μ g of protein was loaded to gels for SDS-PAGE analysis and transferred onto a PVDF membrane by eletroblotting. The membranes were first stained with Ponceau S, imaged and then blocked with 4% non-fat milk + 4% BSA in Tris-buffered saline with Tween 20 (TBST; 10 mM Tris, 150 mM NaCl and 0.1% Tween 20, pH 7.6) for 60 min. After incubation with antibodies against SYT1 (1:1000) or VAP27-1 (1:1500) at 4°C

for 16 h, the membranes were washed three times for 10 min and incubated with HRP-conjugated anti-rabbit or HRP-conjugated anti-mouse antibodies at room temperature for 1.5 h. The blots were washed three times with TBST for 10 min, and the proteins were visualized using ECL imaging system (LAS-1000, Fuji Films). The intensity of the bands was quantified using Image J. SYT1 antibody was kindly provided by Prof. Miguel A. Botella, Universidad de Malaga, Spain, and VAP27-1 anti-serum was kindly provided Dr. Pengwei Wang and Prof. Patrick J. Hussey, Durham University, UK.

2.7. Immunogold Labeling

Root tips of Arabidopsis, with or without pre-treatment of 50 μ M BFA for 2 h, were fixed using a high-pressure freezing machine (Bal-Tec HPM010, Balzers, Liechtenstein), freeze-substituted at -80°C and embedded in Lowicryl® Embedding Media HM20 (Polysciences, Warrington PA). After blocked and incubated with antibodies against SYT1 (1:150) and VAP27-1 (1:150) overnight at 4°C , the ultrathin sections were rinsed and incubated with 15-nm gold particle-conjugated anti-rabbit and 6-nm gold particle-conjugated anti-mouse antibodies at room temperature for 2 h. The sections were extensively washed and stained with uranyl acetate. The samples were imaged with an LEO 912AB electron microscope (ZEISS AG, Oberkochen). For statistical analysis, the positive gold signals were counted along the PM (within a distance of 50 nm apart from the PM). A region of interest (ROI) was defined as a rectangle area with a width of 50-nm (apart from the PM) and a length of 100-nm along the PM. More than one positive signal within a ROI was defined as a clustered labeling (co-localization).

2.8. Whole Mount Immunofluorescence Labeling

5-day-old Arabidopsis seedlings were fixed in fixation buffer (1.5% paraformaldehyde + 0.5% glutaraldehyde in 1/2 microtubule stabilizing buffer (MTSB; 50 mM PIPES, 5 mM MgSO₄ and 5 mM EGTA, pH 6.9) with vacuum filtration for 1 h, and the fixed seedlings were washed once with 1/2 MTSB and twice with phosphate-buffered saline (PBS; 140 mM NaCl, 2.7 mM KCl, 6.5 mM Na₂HPO₄ and 1.5 mM KH₂PO₄, pH 7.3) for 10 min. After three times of reduction with sodium borohydride (NaBH₄) in PBS, the roots were washed three times for 5 min and then incubated with 2% driselase + 2% cellulose + 1% pectolyase in PBS at 37°C for 30 min. The cells were permeabilized by incubating with 10 mM glycine three times for 5 min and 2% Nonidet P40 + 10% DMSO for 1 h in PBS. The roots were washed with PBS for 10 min and then blocked with 2% BSA in PBS. After incubation with antibodies against SYT1 (1:200) and VAP27-1 (1:200) at 4°C for 16 h, the roots were washed six times for 10 min and incubated with Cy5®-conjugated anti-rabbit and Alexa Fluor® 488-conjugated anti-mouse antibodies at 37°C for 1.5 h plus at room temperature for 1.5 h. For single SYT1 immunolabeling, Alexa Fluor® 488-conjugated anti-rabbit antibody was used. The roots were washed six times for 10 min, and the nuclei were stained with 5 µM DAPI in PBS. The roots were washed twice with PBS for 5 min before confocal imaging.

2.9. Analysis of BFA Compartments

Roots of 4-day-old Arabidopsis seedlings were transferred into 1/10 MS solution and pre-cooled at 6°C for 5 min. After stained with 4.1 µM of FM4-64 (SynaptoRed™ C2, Sigma) at 6°C for 10 min, the roots were incubated with 35.6 µM of BFA at room temperature for 60 min. Z-stack images of the roots at 2 µm intervals were acquired by confocal microscopy. Images were processed with ImageJ and the diameter of the BFA compartments (more than 1 µm) in root epidermis of transition zone was measured. More than 80 cells from four roots were measured. This experiment was repeated three times and showed the same trend.

2.10. Phylogenetic Analysis

The eukaryotic SV2-related proteins (Table 2) were extracted from eukaryotic protein families in a previous study (Ku et al., 2015). The prokaryotic SV2-related proteins were selected from the hits with the highest scores in a BLAST (Altschul et al., 1997) search against all prokaryotic sequences in NR (Pruitt et al., 2005) using the human SV2A and Arabidopsis SV2-like sequences as queries. The sequences were aligned using MAFFT version 7.130 (Kato and Standley, 2013) with the option 'linsi'. The maximum likelihood tree was constructed using RAxML version 7.8.6 (Stamatakis, 2006) with 100 rapid Bootstrap searches.

Table 2. List of SV2-related proteins.

<i>Bs</i> NiaP	AFQ56230_Niacin_permease_ <i>Bacillus_subtilis</i> _QB928
<i>Cm</i> MFS	WP_011519403_MFS_transporter_ <i>Cupriavidus_metallidurans</i>
<i>Ag.t</i> SVL	KJX87850_Synaptic_vesicle_2like_protein_ <i>Agrobacterium_tumefaciens</i>
<i>Rm</i> NiaP	EYD77199_Niacin_transporter_NiaP_ <i>Rubellimicrobium_mesophilum</i> _DSM_19309
<i>Tc</i> MFS	WP_013970067_MFS_transporter_ <i>Treponema_caldarium</i>
<i>An.t</i> MFS	GAP08356_arabinose_efflux_permease_ <i>Anaerolinea_thermolimosa</i>
<i>Hs</i> SV2C	NP_055794_synaptic_vesicle_glycoprotein_2C_isoform_1_ <i>Homo_sapiens</i>
<i>Gg</i> SV2AL	XP_415186_PREDICTED:_synaptic_vesicle_2related_protein_ <i>Gallus_gallus</i>
<i>Dr</i> SV2A	XP_696434_PREDICTED:_synaptic_vesicle_glycoprotein_2A_ <i>Danio_rerio</i>
<i>Hs</i> SV2A	NP_055664_synaptic_vesicle_glycoprotein_2A_isoform_1_ <i>Homo_sapiens</i>
<i>Mm</i> SV2A	NP_071313_synaptic_vesicle_glycoprotein_2A_ <i>Mus_musculus</i>
<i>Gg</i> SV2A	AER68117_synaptic_vesicle_glycoprotein_2A_partial_ <i>Gallus_gallus</i>
<i>Hs</i> SV2B	NP_055663_synaptic_vesicle_glycoprotein_2B_isoform_1_ <i>Homo_sapiens</i>
<i>Ce</i> SVOPL	NP_498960_Putative_transporter_svop1_ <i>Caenorhabditis_elegans</i>
<i>Dr.m</i> MFS	NP_611868_CG4324_isoform_A_ <i>Drosophila_melanogaster</i>
<i>Mm</i> SVOP	NP_081081_synaptic_vesicle_2related_protein_ <i>Mus_musculus</i>
<i>Gg</i> SVOP	XP_004950491_PREDICTED:_synaptic_vesicle_glycoprotein_2Alike_ <i>Gallus_gallus</i>
<i>Hs</i> SVOP	NP_061181_synaptic_vesicle_2related_protein_ <i>Homo_sapiens</i>
<i>Dr</i> SVOPL	NP_001007408_putative_transporter_SVOPL_ <i>Danio_rerio</i>
<i>Nv</i> MFS	XP_001633415_predicted_protein_partial_ <i>Nematostella_vectensis</i>
<i>Ta</i> MFS	EDV23561_hypothetical_protein_TRIADDRAFT_58334_ <i>Trichoplax_adhaerens</i>
<i>At</i> SV2L	AEE75283_nicotinate_transporter_ <i>Arabidopsis_thaliana</i>
<i>Os</i> MFS	BAT09390_Os09g0559800_ <i>Oryza_sativa</i> _Japonica_Group
<i>Zm</i> SV2L	NP_001147918_synaptic_vesicle_2related_protein_ <i>Zea_mays</i>
<i>Zm</i> SV2	DAA50364_TPA:_proteinSynaptic_vesicle_2_protein_Major_facilitator_superfamily_isoform_1_ <i>Zea_mays</i>
<i>Pa</i> MFS	XP_001770703_predicted_protein_ <i>Physcomitrella_patens</i>
<i>Sm</i> MFS	EFJ34774_hypothetical_protein_SELMODRAFT_81650_ <i>Selaginella_moellendorffii</i>
<i>Cs</i> MFS	XP_005644961_MFS_general_substrate_transporter_ <i>Coccomyxa_subellipsoidea</i> _C169

2.11. Histochemical GUS Assay

The T3 homozygous plants were used for GUS staining. Plant samples were vacuum infiltrated for 2 min in the GUS staining solution (100 mM sodium phosphate buffer, pH 7.0, 10 mM EDTA, 0.1% Triton X-100, 0.5 mM potassium ferricyanide, 0.5 mM potassium ferrocyanide, and 1 mM 5-bromo-4-chloro-3-indolyl glucuronide) and then incubated at 37°C for 16 h. The samples were transferred to 70% of ethanol for 1 h and then incubated in 100% ethanol for 1 h to remove the chlorophyll. The samples were observed with a Leica MZ FLIII stereomicroscope.

2.12. RT-PCR

7-day-old Seedlings were frozen by liquid nitrogen and grounded into powder. The total RNA was extracted using RNeasy Plant Mini Kit (Qiagen). 500 ng of RNA was used for cDNA synthesis using RevertAid RT Reverse Transcription Kit (Thermo Scientific) with Oligo(dT) primers. 0.5 µl of the cDNA was subjected to PCR amplification using primers RT SVL-F and RT SVL-R listed in Table 1. 5 µl of the PCR product was subjected to electrophoresis.

2.13. Confocal Microscopy

Confocal imaging was performed by using an Olympus FluoView™ FV1000 confocal microscope equipped with diode (405 nm), argon-ion (458, 488 and 514 nm) and helium–neon (543 nm) lasers. GFP single image was excited at 488 nm and the emission signals were collected from 500 to 600 nm. YFP was excited at 515 nm and emission was collected from 530 to 630 nm. The red fluorescent dye FM4-64 was excited at 543 nm and emission was

filtered between 660 and 760 nm. For simultaneous imaging of CFP, GFP and FM4-64 the setting of CFP (Ex 405 nm/Em 440-505 nm), GFP (Ex 488 nm/Em 510-550 nm) and FM4-64 (Ex 543 nm/Em BA560-660 nm filter) was used. For simultaneous imaging of GFP, YFP and mCherry the setting of GFP (Ex 458 nm/Em 470-515 nm), YFP (Ex 514 nm/ Em 530-560 nm) and mCherry (Ex 543 nm/Em BA560-660 nm filter) was used.

2.14. Accession Numbers

Arabidopsis *SYT1* (AT2G20990); *VAP27-1* (AT3G60600); *NET3C* (AT2G47920); *AP2* μ 2 (AT5G46630); *SVL* (AT3G13050); *VTI12* (AT1G26670); *Rha1* (AT5G45130); *Ara6* (AT3G54840); *RabA1e* (AT4G18430).

3. Results

3.1. Tethering of Arabidopsis SYT1 on the PM Maintains the Stability of ER Network and ER-PM Contact Sites

3.1.1. Arabidopsis SYT1 is Localized on the ER-PM Contact Sites

Arabidopsis Synaptotagmin 1 (SYT1) and VAP27-1 have been shown to be ER-PM tethering proteins. However, the relationship between SYT1 and VAP27-1 remains unclear. To gain a better understanding this relationship, SYT1-GFP was first transiently co-expressed with the ER lumen markers HDEL-RFP or HDEL-CFP in leaves of *Nicotiana benthamiana*. Most SYT1-GFP signals were found to accumulate on stable spots along the relatively stationary ER tubules and cisternae while fewer amount of SYT1-GFP was detected on the motile, quickly remodeling ER strands (Figure 9A). The co-expression of CFP-HDEL followed by FM4-64 staining showed that SYT1-GFP was localized on the ER and attached to the PM at specific stationary regions, i.e., the ER-PM contact sites (Figure 9B and 9C). Furthermore, the co-expression of SYT1-GFP and the Golgi marker sialyltransferase (ST)-RFP showed that the SYT1 puncta were not co-localized, but in close proximity, with the Golgi apparatus (Figure 9D).

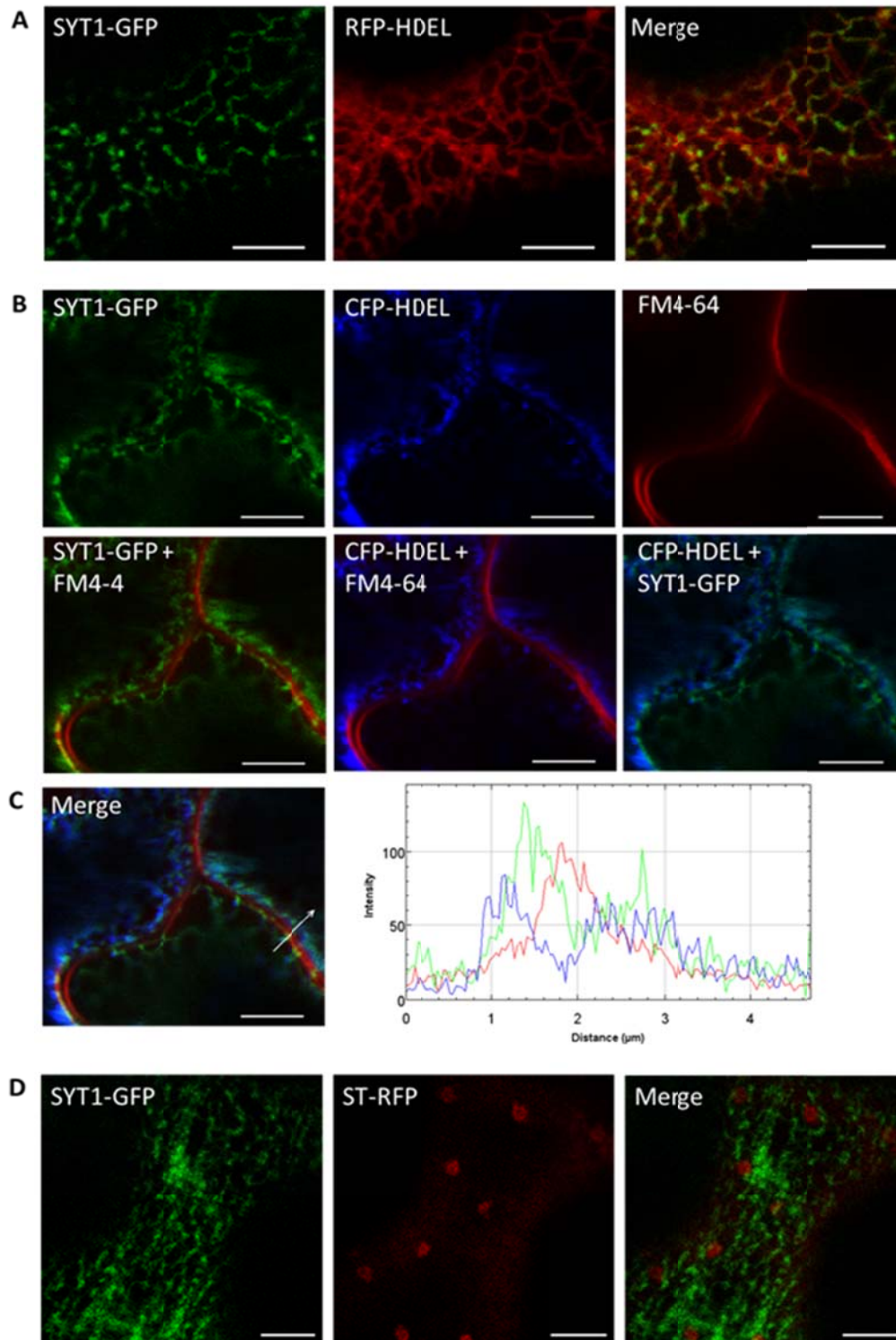


Figure 9. SYT1 Unevenly Distributes on Cortical ER Elements and Forms Stable Attachments at PM of *N. benthamiana* Leaf Epidermal Cells.

(A) Co-expression of SYT1-GFP and RFP-HDEL shows that the stable SYT1 puncta are localized on ER tubules and cisternae.

(B) ER-resident SYT1 attaches to the FM4-64-stained PM at the immobile ER-PM contact sites.

(C) The intensity profiles of the cells in (B) show that the SYT1 signal peaks between the ER lumen marker HDEL and the PM marker FM4-64 at the ER-PM contact sites.

(D) SYT1-GFP is not incorporated into the ST-RFP-labeled Golgi apparatus, even though these two compartments are very close to each other.

Scale bars = 5 μ m

3.1.2. SYT1 and VAP27-1 are Localized on Different Regions of ER-PM Contact Sites

To examine whether SYT1 and VAP27-1 are localized on the same ER-PM contact sites, SYT1-GFP and VAP27-1-YFP were co-expressed in leaves of *Nicotiana benthamiana*. The result showed that SYT1-GFP was not co-localized with VAP27-1-YFP but often surrounded VAP27-1-YFP (Figure 10A). SYT1-GFP was mainly overlapped with VAP27-1-YFP on the ER tubules or cisternae but not on ER-PM contact sites (Figure 10B and 10C).

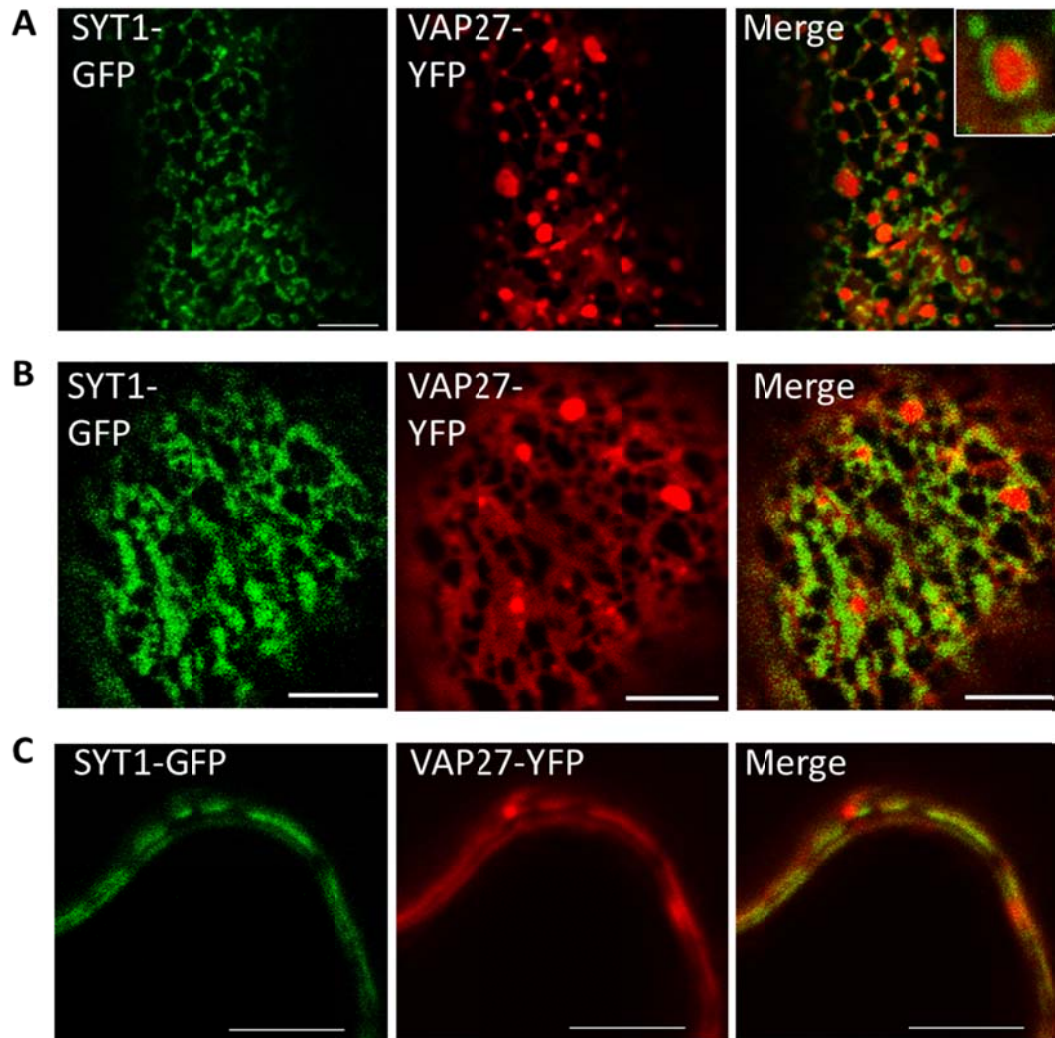


Figure 10. SYT1 and VAP27-1 Localize to Different Regions of ER-PM Contact Sites in *N. benthamiana* Leaf Epidermal Cells.

(A) The SYT1-GFP immobile puncta do not overlap with the VAP27-1-YFP immobile puncta. The inset shows a VAP27-1 punctum surrounded by the SYT1 puncta.

(B) A cell with clear ER cisternae shows that SYT1-GFP is excluded from the VAP27-1-YFP puncta, but the two signals overlap on the ER tubules and cisternae.

(C) The equatorial plane shows that SYT1 and VAP27-1 distribute on the cortical ER but these two proteins accumulate on distinct puncta.

Scale bars = 5 μ m

To obtain more convincing evidence in Arabidopsis, whole-mount Immunofluorescent labelling using SYT1- and VAP27-1-specific antibodies was conducted to probe the native SYT1 and VAP27-1 proteins in the roots of wild type Arabidopsis. The images showed that SYT1 and VAP27-1 were localized on different regions of the cortical ER (Figure 11). Immunofluorescent staining of the root cells in wild type Arabidopsis with SYT1-specific antibody showed clear puncta signals on the cell cortex (Figure 12A) and ER labeling in the cells (Figure 12B). Immunofluorescent labeling in the roots of *SYT1* null mutant, *syt1-2*, with SYT1-specific antibody undergoing the same procedure showed no fluorescent signals (Figure 12C). Western blot using VAP27-1-specific antibody showed a single band of the expected molecular weight in wild-type Arabidopsis and SYT1 null mutant. The intensity of the band was reduced in the *VAP27-1* RNAi knockdown line (Figure 12D). These data indicated that the aforementioned antibodies were specific and the localization sites of endogenous SYT1 and VAP27-1 in Arabidopsis were often in close proximity but not overlapped on the membrane contact sites.

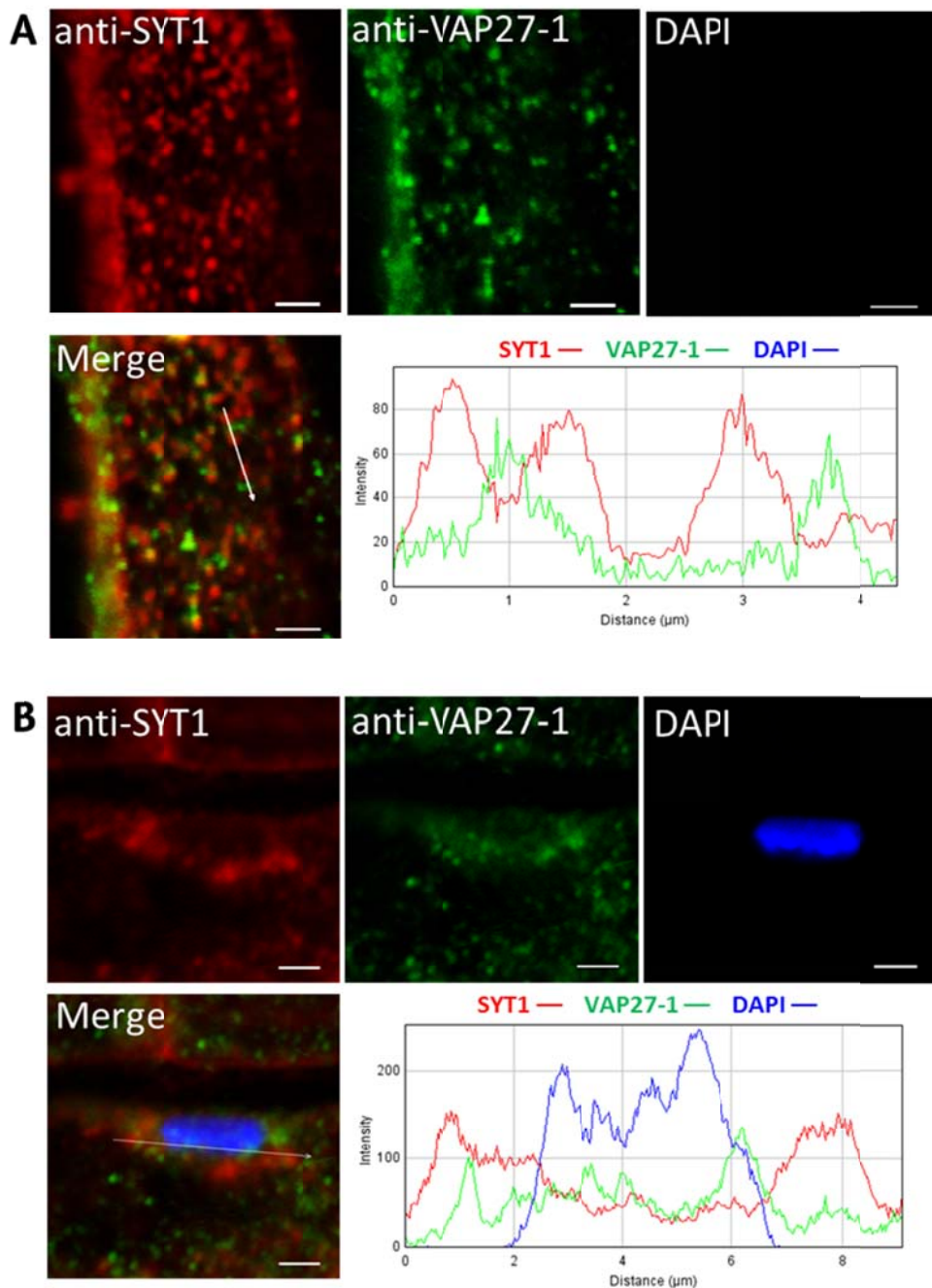


Figure 11. SYT1 and VAP27-1 Accumulate on Different Region of ER Elements in Arabidopsis Root Apex Cells.

(A) Whole-mount immunocytochemistry of the root cells in wild type

Arabidopsis root apex cells shows that SYT1 and VAP27-1 puncta are in close vicinity on the cell cortex. The intensity profiles show that the peaks of SYT1 and VAP27-1 signals are shifted.

(B) SYT1 and VAP27-1 are localized around the nucleus, which is visualized by 4',6-diamidino-2-phenylindole (DAPI) staining. These two proteins gather in different places of the nucleus membrane. The fluorescent intensities of the three signals along the white line are shown in the intensity profiles.

Scale bars = 2 μ m

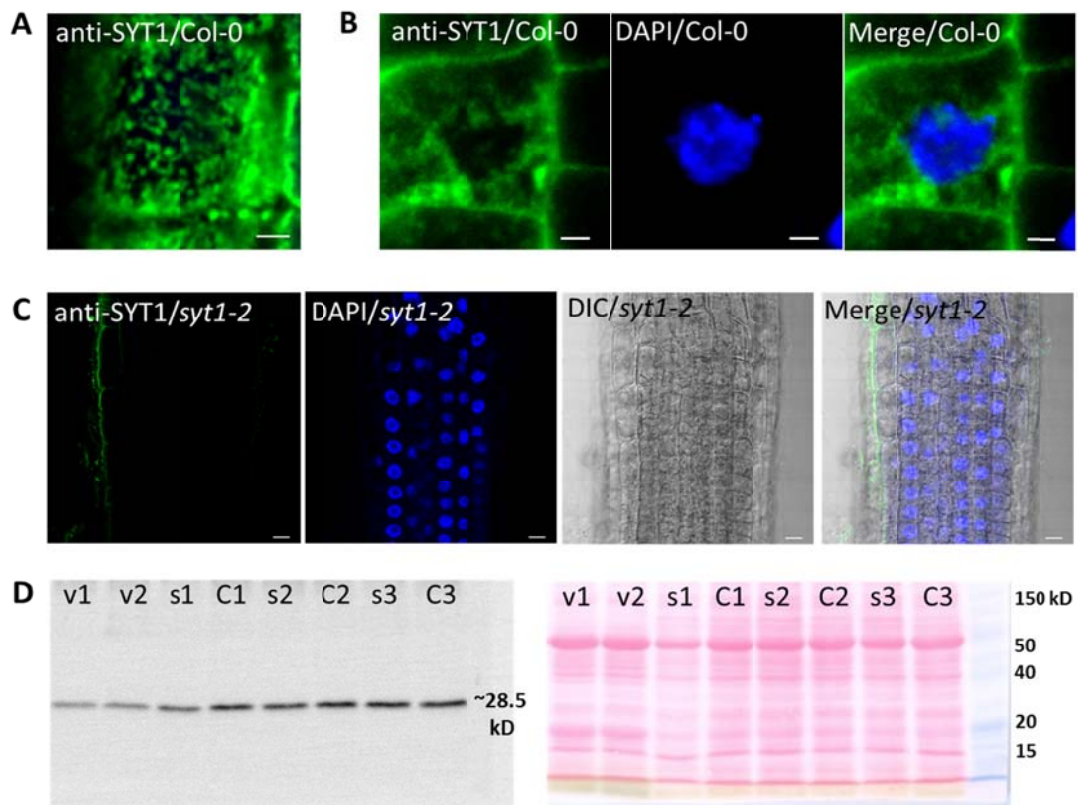


Figure 12. SYT1 and VAP27-1 Antibodies are Specific.

(A) Immunofluorescent labeling of SYT1 in wild type Arabidopsis Col-0 shows that SYT1 form punctate structures on the cell cortex in the root cells. Scale bar = 2 μ m

(B) SYT1 is localized on the ER through the cytoplasm and around the nucleus. Scale bars = 2 μ m

(C) Immunofluorescent labeling using SYT1 antibody in Arabidopsis *syt1-2* null

mutant shows no positive labeling signal. Scale bars = 10 μ m

(D) Western blot of proteins from 5-day-old seedlings of Col-0 (C1-C3), *syt1-2* (s1-s3), and VAP27-1 RNAi mutant (v1-v2) using VAP27-1 antibody shows one single band in each line (Left). The blotted proteins on the PVDF membrane are stained by Ponceau S (Right).

Ultrastructural immunogold labelling for SYT1 (15-nm gold particles) and VAP27-1 (6-nm gold particles) further confirmed that these two proteins were localized on distinct patches on the ER-PM contact sites (Figure 13). Gold particles located along the PM were counted and the result showed that 61.82% of the labeled regions were VAP27-1 single-labeled, 28.22% of the labeled regions were SYT1 single-labeled, and 9.96% of the labeled regions were VAP27-1/SYT1 dual-labeled. Statistical analyses using chi-square test showed that the localization of gold particles of two different sizes tended to localize exclusively on distinct domains; SYT1 showed no preference to cluster with SYT1 itself nor with VAP27-1 whereas VAP27-1 tended to cluster with VAP27-1 itself (Table 3). This result is consistent with the previous study showing that VAP27-1 is able to form oligomers. Based on their respective properties, the two distinct ER-PM contact sites were named as SYT1-enriched ER-PM contact sites (SECSs) and VAP27-1-enriched ER-PM contact sites (VECSs).

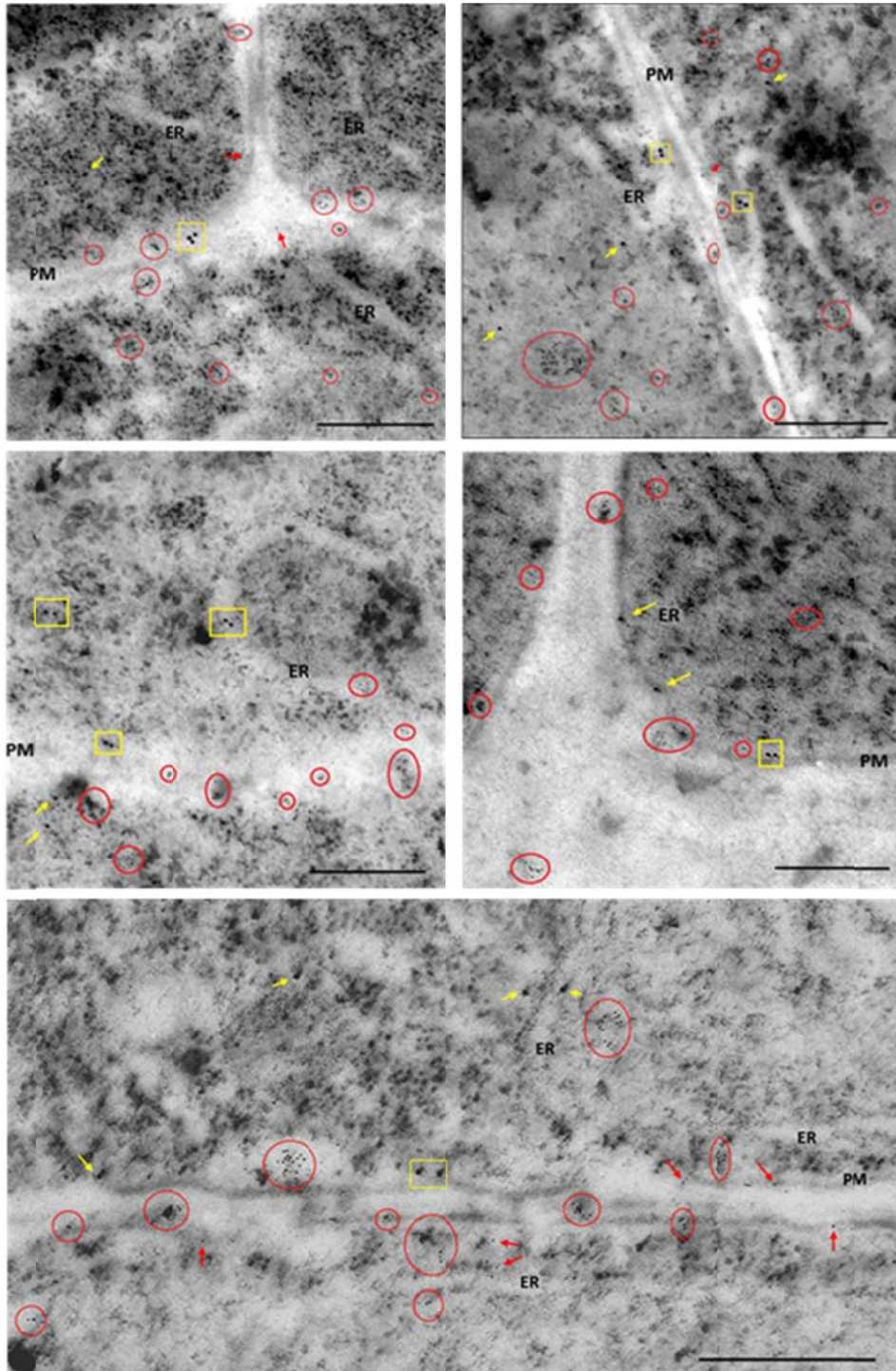


Figure 13. Double Immunogold Labeling of SYT1 and VAP27-1 in Arabidopsis Root Apex Cells.

The electron micrographs of ultrathin cryosections of wild type Arabidopsis root cells and immunogold labeling show that SYT1 (15-nm gold particles) and VAP27-1 (6-nm gold particles) are not localized on the same regions along the

PM. The clusters of gold particles are highlighted as SYT1-clusters (yellow rectangles) and VAP27-1-clusters (red circles). SYT1 single labeling (yellow arrows) and VAP27-1 single labeling (red arrows) are indicated. Scale bars = 500 nm.

Table 3. Statistical Analysis for Clustering of Gold Particles.

15-nm (SYT1) and 6-nm (VAP27-1) gold particles are counted along the PM. A 100x50 nm area with positive signal(s) is defined as one labeled ER-PM contact site. The contact sites are designated as SYT1 single labeled (SYT1+), VAP27-1 single labeled (VAP27-1+), and SYT1/VAP27-1 dual labeled (SYT1+VAP27-1+). Chi-square tests show that SYT1 particles are randomly distributed on the SYT1+ and SYT1+VAP27-1+ contact sites, but VAP27-1 particles tend to clusters together on VAP27-1+ contact sites. The values in parentheses indicate expected values of random distribution.

ER-PM Contact Sites Labeled by Gold Particles					
	SYT1+	SYT1+VAP27-1+	VAP27-1+	Total	
No. of Contact Sites	68	24	149	241	
χ^2 test for Clustering of Gold Particles					p-value
No. of SYT1 particles	161 (156.70)	51 (55.20)	–	212	0.5
No. of VAP27-1 particles	–	77 (124.86)	823 (775.14)	900	3.93E-06

3.1.3. Spatial Distributions of SECSs, VECs, and Plant Cytoskeleton

A previous study has shown that the dynamic of VAP27-1 and NET3C on the ER-PM contact sites are regulated by microtubules and actin filaments,

respectively. In order to illustrate the relationships between SYT1, VAP27-1 and the cytoskeleton, co-expression of these proteins and the cytoskeletal markers in tobacco leaves were conducted. Co-expression of SYT1-GFP and VAP27-1-YFP showed that 99.17% (476 out of 480) of the VAP27-1-enriched ER-PM contact sites (VECSs) were found to be associated with SYT1-enriched ER-PM contact sites (SECSs) whereas only 48.40% (788 out of 1628) of the SECSs were in contact with the VECSs (Table 4). Co-expression of STY1-GFP, VAP27-1-YFP and NET3C-RFP often caused the enlargement of the VECSs. VAP27-1-YFP and NET3C-RFP were co-localized on the same ER-PM contact sites that were surrounded by SYT1-GFP (Figure 14). These results implied that the formation of VECSs might be dependent on SECSs or that the stability of VECSs was regulated by SECSs.

Table 4. Spatial Relationship between VECSs and SECSs.

Almost all the VECSs are in contact with the SECSs, but about half of the SECSs are localized on the ER without connection with VECSs.

Vicinity of VECSs and SECSs					
	VECS			SECS	
	n	%		n	%
SECS accompanied	476	99.17%	VECS accompanied	788	48.40%
Non-SECS accompanied	4	0.83%	Non-VECS accompanied	840	51.60%

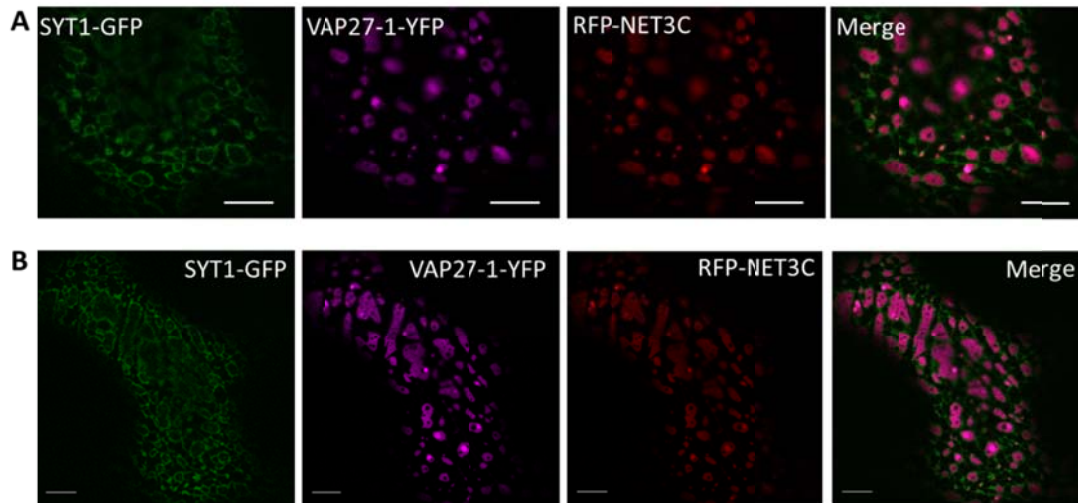


Figure 14. NET3C Co-Localize with VAP27-1 on VECs in *N. benthamiana* Leaf Epidermal Cells.

(A) Co-expression of SYT1-GFP, VAP27-1-YFP, and RFP-NET3C shows that SYT1 is excluded from the VAP27-1/NET3C-localized ER-PM contact sites.

(B) The images show another region of the cell in (A) with the wide-spreading VECs.

Scale bars = 5 μ m.

Co-expression of SYT1-GFP and the microtubule-binding domain of microtubule-associated protein 4 fused with DsRed (MBD-MAP4-DsRed) showed that most of the SYT1-enriched ER-PM contact sites were not overlapped with the microtubules but tended to localized on the regions in proximity to the microtubules, particularly in the corners of the cross-linked microtubules (Figure 15A). When SYT1-GFP was co-expressed with the actin marker actin-binding domain 2 (ABD2)-YFP or ABD2-mCherry, most of the SECSs were associated with and arranged along the F-actin (Figure 15B and 15C). These data suggested that the localization of SECSs were related to the arrangements of the cytoskeletons.

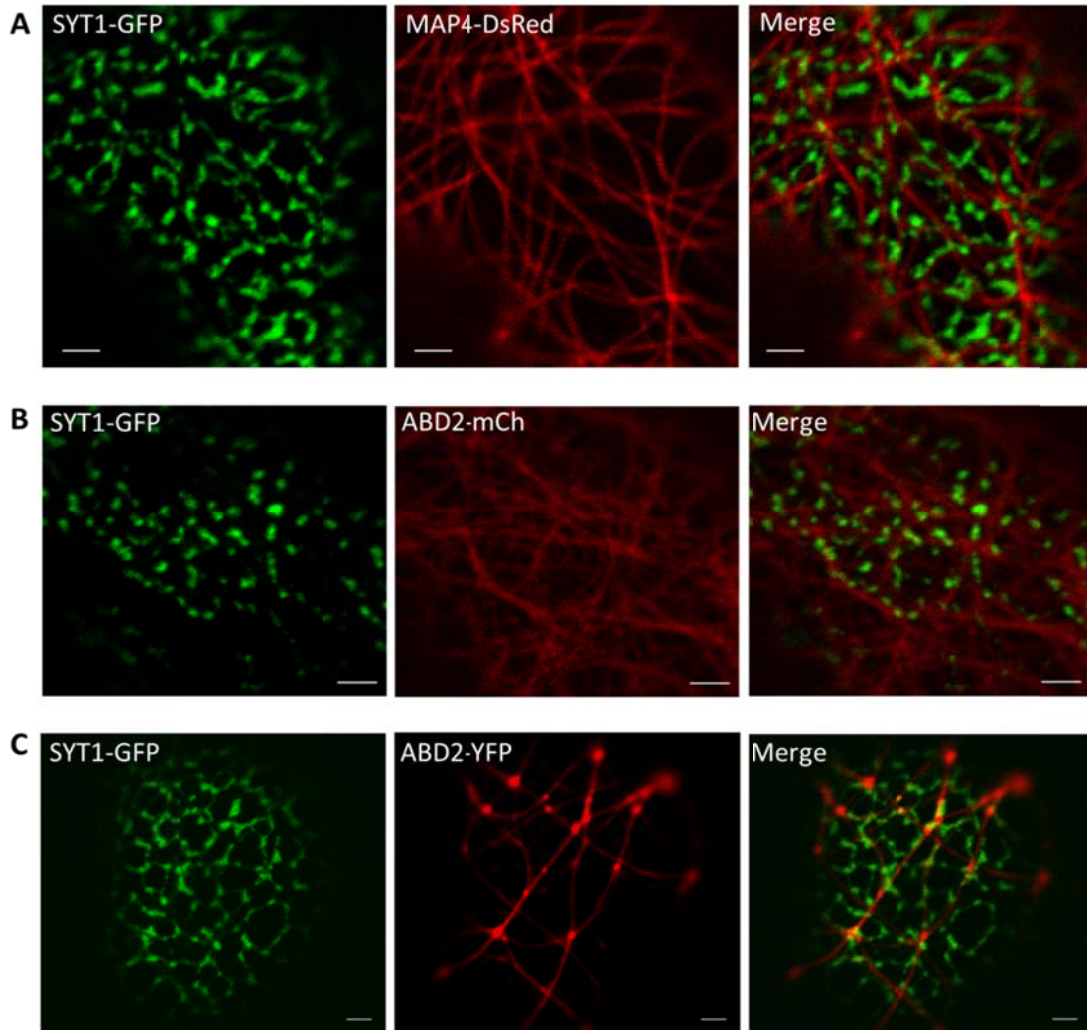


Figure 15. Spatial Relationship between SYT1 and Plant Cytoskeleton in *N. benthamiana* Leaf Epidermal Cells.

(A) Co-expression of SYT1-GFP and MAP4-DsRed shows that the localizations of SYT1 and the microtubules are almost mutually exclusive, but SYT1 tends to occupy the regions in the vicinity of the microtubules. Some overlap signals are still observed.

(B) and (C) The SYT1 puncta are very often arranged along the ABD2-labeled actin filaments.

Scale bars = 2 μ m.

The relationships between SYT1, VAP27-1, and microtubules on the

cell cortex were further demonstrated by the co-expression of SYT1-GFP, VAP27-1-YFP, and MBD-MAP4-DsRed in tobacco leaves. The result showed that VECSs were often associated with the microtubules and in close proximity to the microtubule-depleted region-located SECSs (Figure 16A). A VECS sandwiched by two SECSs and penetrated by one microtubule is shown in Figure 16B. The aforementioned data indicated that SYT1 might play a role in controlling the formation, the sizes, or the stability of VAP27-1-enriched ER-PM contact sites.

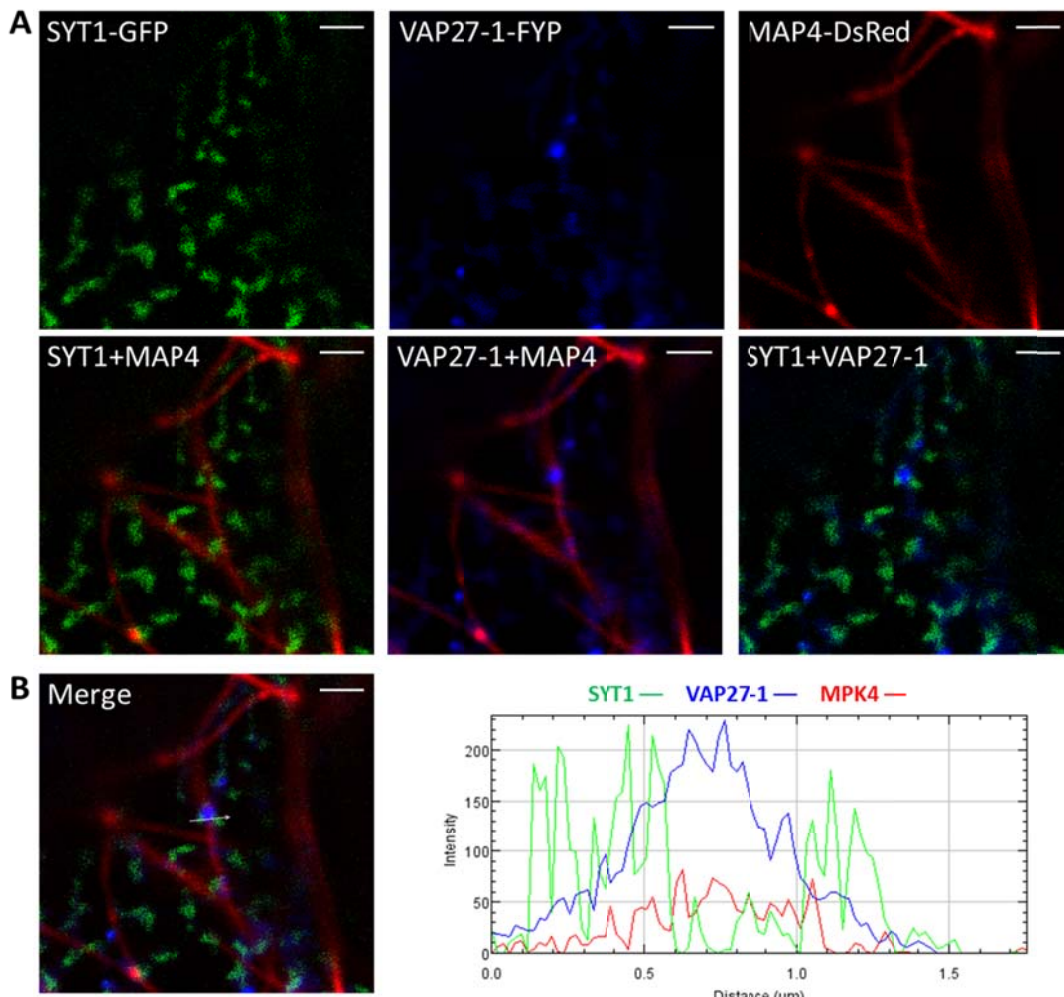


Figure 16. Spatial Relationship between SYT1, VAP27-1, and Microtubules in *N. benthamiana* Leaf Epidermal Cells.

- (A) Co-expression of SYT1-GFP, VAP27-1-YFP, and MAP4-DsRed in *N. benthamiana* leaves shows that the localizations of SYT1 and VAP27-1 are associated with the microtubules.
- (B) The intensity profiles of one VAP27-1 punctum, two SYT1 puncta, and one microtubule show that VAP27-1 overlaps with the microtubule and is sandwiched by the SYT1 puncta.

Scale bars = 2 μm .

3.1.4. Disruption of VAP27-1 Tethering to PM has no Obvious Effects on Formation of SECSs

Our results showed that SYT1 and VAP27-1 were not co-localized on the ER-PM contact sites. Nevertheless, these two contact sites were closely located; therefore, it was interesting to investigate their anchoring mechanisms. A previous study has shown that point mutations on the major sperm domain of VAP27-1 (VAP27-1-T59/60A) render the protein unable to attach to the ER-PM contact sites and co-localize with NET3C. To investigate the localization patterns of VAP27-1 mutant and SYT1, VAP27-1-T59/60A-YFP was co-expressed with SYT1-GFP in tobacco leaves. Time-lapse imaging showed that VAP27-1 T59/60A mutant aggregates were motile, moving along the ER network (Figure 17). Still, their movement was restricted within the SYT1-enriched ER-PM contact sites and unable to pass through these contact sites. The motile protein aggregates were sometimes even caged by many SECSs (Figure 17). On the other hand, after three negatively charged amino acid residues, which are essential for coordinating the Ca^{2+} in the C2A domain, of SYT1 were substituted with three uncharged residues. The SYT1 D370N/E372Q/E378Q mutant tagged with GFP (SYT1-3M-GFP) was still able

to anchor on the ER-PM contact sites but the stationary feature of the contact sites were slightly disturbed (Figure 18A). Co-expression of SYT1-3M-GFP and VAP27-1-YFP showed that VAP27-1-enriched contact sites remained stationary whereas SYT1-3M-GFP wobbled or moved nearby them (Figure 18B). These data demonstrated that the expression of VAP27-1 mutant had no dominant -negative effect on the formation of SESC, and the expression of SYT1 mutant had also no dominant-negative effect on the formation of SESC and VESC.

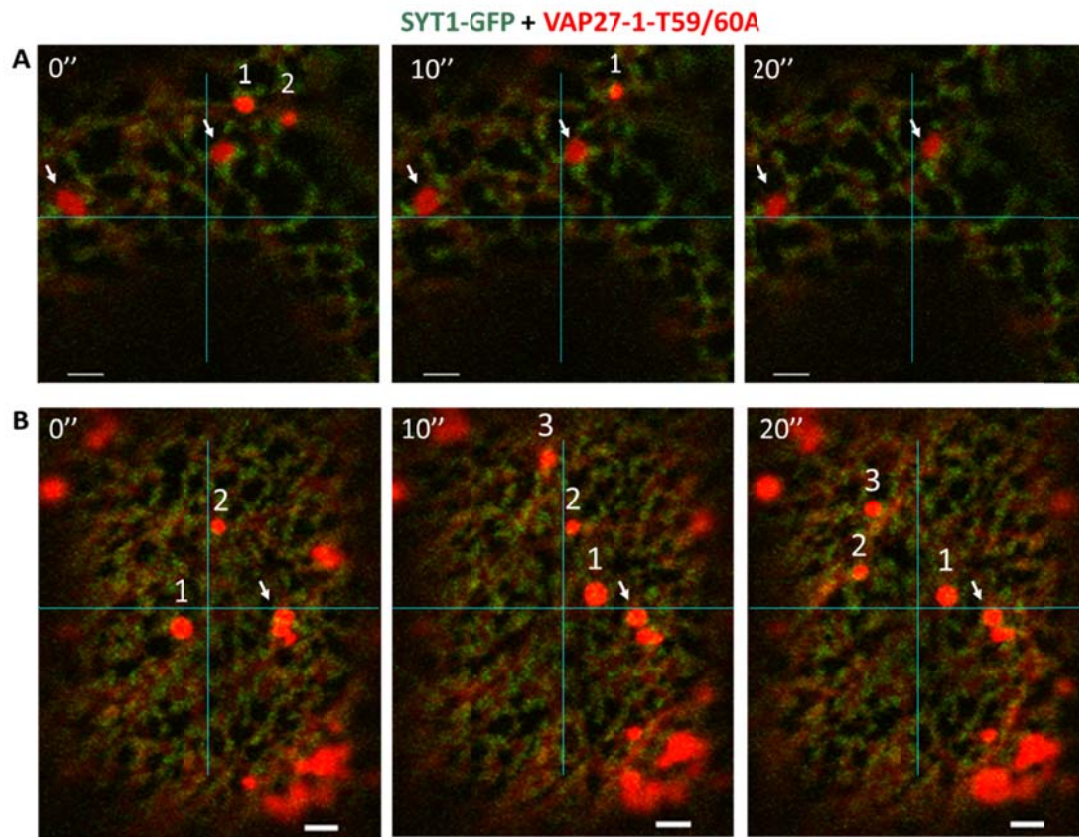


Figure 17. Anchoring of SYT1 to PM is not Affected by VAP27-1 Mutant in *N. benthamiana* Leaf Epidermal Cells.

(A) The time-lapse imaging shows that VAP27-1-T59/60A (Red) proteins are unable to stably anchor on the ER-PM contact sites. The SYT1 puncta are unaffected by the VAP27-1 mutant and still stationary. The motile VAP27-1 mutant aggregates are indicated by numbers (1-3), and the

“shape-changing” aggregates caged by SYT1 are indicated by arrows.

(B) Another cell showing the same result in (A).

Scale bars = 2 μm .

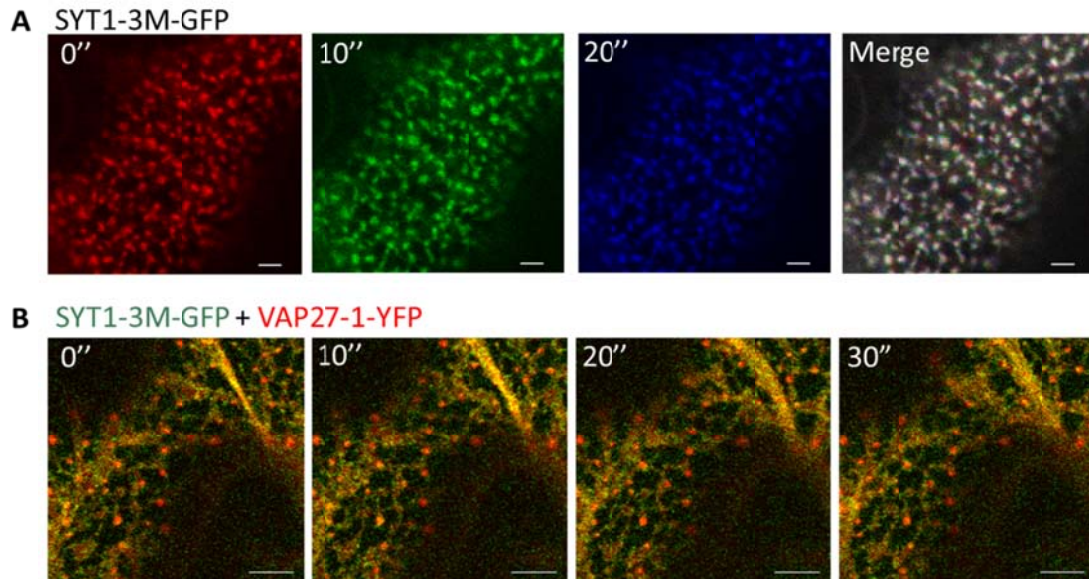


Figure 18. Mutation of SYT1 C2A Domain do not Disrupt SECSs and VECSS in *N. benthamiana* Leaf Epidermal Cells.

(A) Transient expression of SYT1-3M-GFP and time lapse images show that SYT1-3M proteins are still able to form immotile puncta structures. The puncta structures wobble on the same spots. Different colors represent images captured in different time points. The white color in the merged image indicates the overlap regions through the three time points.

(B) Co-expression of SYT1-3M-GFP and VAP27-1-YFP and time-lapse images show that the VAP27-1 puncta remain stable in the present of SYT1 mutant.

Scale bars = 5 μm .

Studies have shown that SYT1 binds to phospholipids via the C2 domains, and the C2 domains are essential for the binding of SYT1 to the PM (Perez-Sancho et al., 2015; Schapire et al., 2008; Yamazaki et al., 2010). Our data showed that the mutation on the C2A domain did not destroy the anchoring of SYT1 to the ER-PM contact sites. In order to examine whether the tethering of VAP27-1 to the PM requires the proper anchoring of SYT1 to the PM, we tried to disrupt the binding of SYT1 to the PM by depleting the cytosolic calcium and seeing if the VECs are affected. The experiment was conducted by co-expressing SYT1-GFP and VAP27-1-YFP in tobacco leaves, which were then infiltrated with the membrane permeable calcium chelator BAPTA-AM. Confocal imaging showed that both the SECSs and the VECs were not removed after the BAPTA-AM treatment for 1 min, 30min, and 60 min. However, after SYT1-GFP-labeled puncta were bleached by the laser, SYT1-GFP was often unable to recover on the same ER-PM contact sites, the SECSs were then removed. Additionally, the cortical ER was no longer stable and reticulated but started to flow dynamically (Figure 19). The dynamic ER strands were still labeled by SYT1-GFP and VAP27-1-YFP. Most of the VAP27-1-YFP-labeled puncta remained stationary within the ER streams; some of the VECs were removed together with the SECS. This result indicated that i) depletion of the cytosolic calcium did not disconnect the already established ER-PM junctions; ii) the anchoring of VAP27-1 to the PM did not require SECSs.

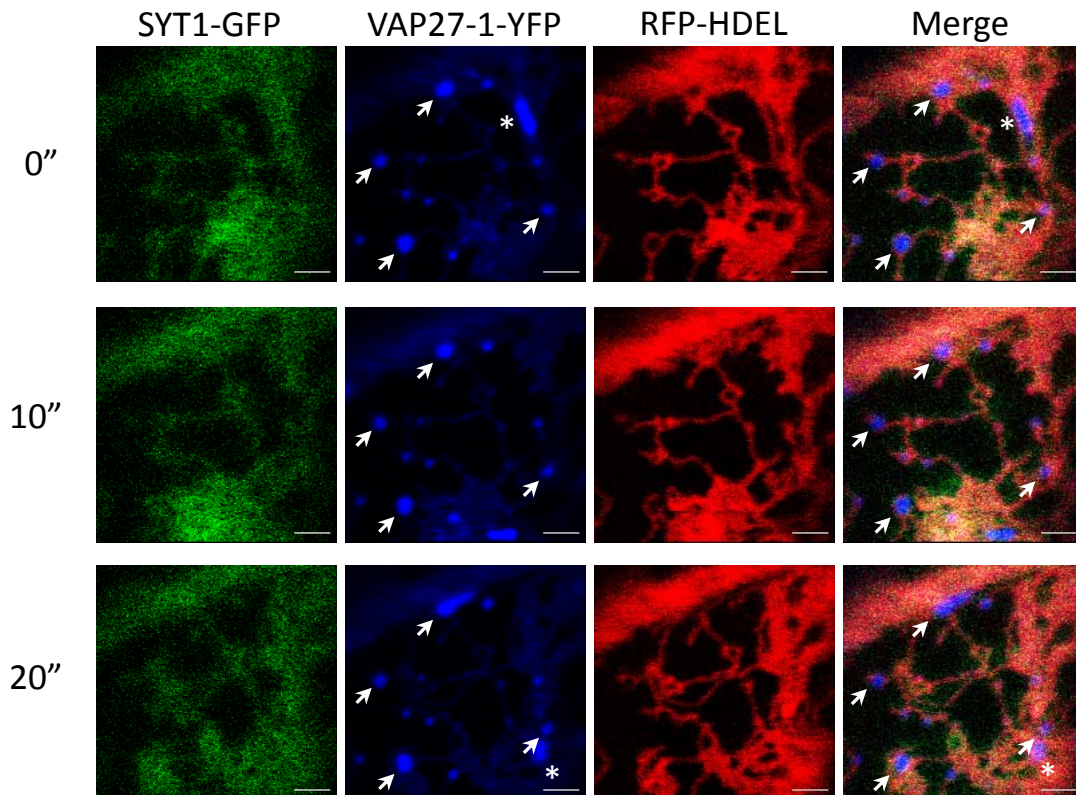


Figure 19. Removal of SECSs has Little Effect on Anchoring of VAP27-1 at Stable Puncta Structures in *N. benthamiana* Leaf Epidermal Cells.

Co-expression of SYT1-GFP, VAP27-1-YFP, and RFP-HDEL show that the SECSs are removed by the BAPTA treatment (25 μ M) for 50 min and photobleaching. The ER network is disturbed but most of the VECSS remain stable at the anchoring sites (arrows). Some VECSS become motile (asterisks).

3.1.5. SYT1 Stabilizes VECSSs by Maintaining Patterns of Polygonal ER Networks

To eliminate the possible effects of the endogenous SYT1 or VAP27-1 in tobacco, VAP27-1-YFP was transiently expressed in the leaf epidermis of Arabidopsis *SYT1* null mutant, *sy1-2*, using particle bombardment. The result showed that VECSSs still existed in *sy1-2*; however, the behavior of the VECSSs

and the ER tubules had changed (Figure 20). VAP27-1-YFP in the cells of *syt1-2* was distributed more on the stable puncta, motile puncta, and the motile ER streams compared to the ER tubules. The cortical ER became less reticulated and the polygonal network of cortical ER in *syt1-2* was not well connected (Figure 20A) compared with that in Col-0 (Figure 20B). Cells of SYT mutants have been shown to be more susceptible to several abiotic stresses; therefore, to exclude the effects of mechanical damages resulted from particle bombardments, VAP27-1-YFP was stably transformed into Col-0 and *syt1-2* using floral dipping.

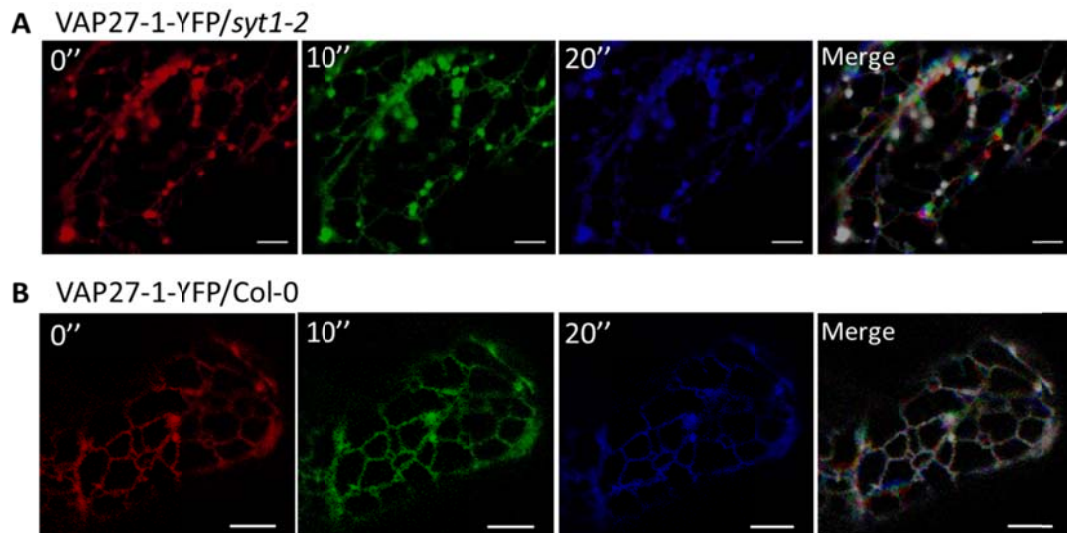


Figure 20. VAP27-1 Puncta and ER Networks are More Dynamic in Cells of Arabidopsis *syt1-2* Null Mutant.

(A) Transient expression of VAP27-1-GFP in the cotyledons of *syt1-2* by particle bombardment shows that VAP27-1 is still able to anchor on the PM, but some of the VAP27-1 puncta become motile. The ER network is also unstable in *syt1-2*. Different colors represent images captured in different time points. The white color in the merged image indicates the overlap regions through the three time points.

(B) As the control, transient expression of VAP27-1-GFP in Col-0 shows

comparably stable VAP27-1 puncta and ER network.

Scale bars = 5 μm .

The stable transformation of VAP27-1-YFP in *SYT1* null mutant showed that the ER network was less reticulated and more dynamic (Figure 21A). Quantitation of the polygonal network of the ER tubules showed that the number of the three-way junctions was reduced by 70.57% in the leaf cells of *syt1-2* compared with that in Col-0 (Figure 21B). This result indicated that the cortical ER in *syt1-2* cells was less reticulated. The stable VECSs labeled by VAP27-1-YFP were still recorded in *syt1-2* but showed a 46.61% of reduction in number (Figure 21C). This result suggested that the establishment or the stability of the VECSs was regulated by SYT1.

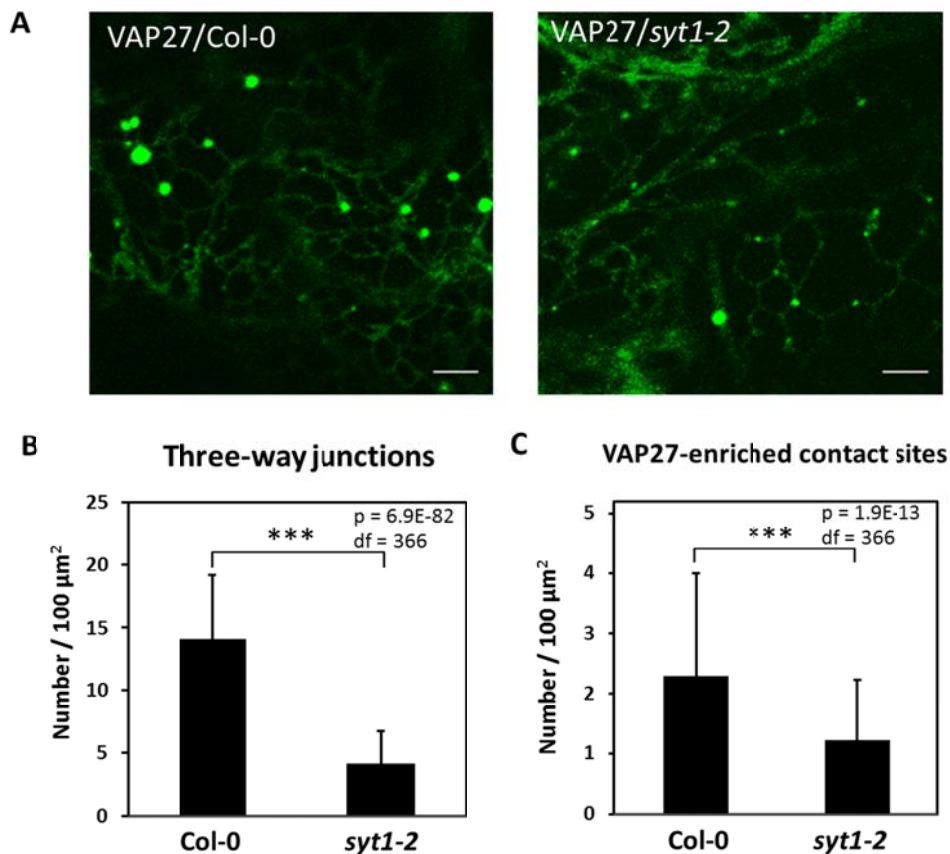


Figure 21. SYT1 is Essential for Maintaining of Polygonal ER Networks in Arabidopsis Leaf Epidermal Cells.

- (A) The stable VAP27-1 puncta are still observed in the leaf cells of VAP27-1-YFP transgenic Arabidopsis in *syt1-2* background, but the ER network in *syt1-2* background is less connected compared with that in Col-0 background.
- (B) Comparing the number of the three-way junctions of the ER in the leaf cells of VAP27-1-YFP/Col-0 and VAP27-1-YFP/*syt1-2* transgenic Arabidopsis shows that the junctions is significantly reduced in *syt1-2* background. (t-test, p-value < 0.001***)
- (C) The number of the VECSs is reduced by 46.61% in the loss of SYT1. (t-test, p-value < 0.001**) The three-way junctions and the VECSs were counted per 100 μm^2 in the first leaf cells of the transgenic plants from the confocal images. In total, 368 of the areas from 64 cells were counted.

Scale bars = 5 μm . Error bars = standard deviation (SD).

To examine if the dynamic of VAP27-1 on the VECSs was altered in the absence of SYT1, fluorescence recovery after photobleaching (FRAP) of VAP27-1-YFP was performed in the leaves of VAP27-1-YFP/Col-0 and VAP27-1-YFP/*syt1-2* transgenic Arabidopsis (Figure 22A and 22B). The results showed that the maximal recovery of VAP27-1-YFP in *syt1-2* ($69.08\% \pm 2.48\%$) was higher than that in Col-0 ($55.20\% \pm 1.73\%$, p-value < 0.0001) (Figure 22C), indicating increased mobility of VAP27-1 in *syt1-2*. In addition, 20.69% (12 out of 58) of the VECSs in *syt1-2* were completely removed after photobleaching compared to only 1.85% (1 out of 54) in Col-0 background (Figure 23), showing that the VECSs were unstable in SYT1 null mutant.

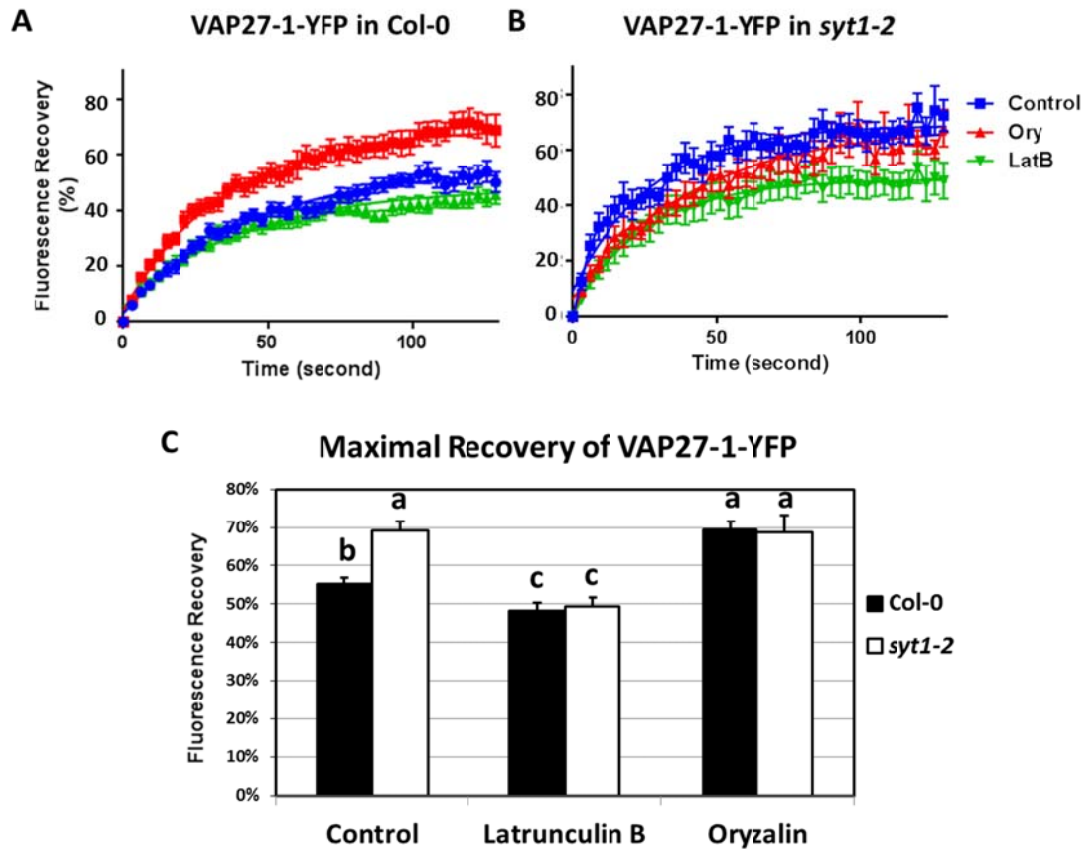


Figure 22. Motility of VAP27-1 at ER-PM Contact Sites is Restrained by Microtubules and SYT1 in Arabidopsis Epidermal Cells.

(A) FRAP of VAP27-1-YFP at the VECSs in the leaf cells of VAP27-1-YFP/Col-0 Arabidopsis shows that the maximal recovery of VAP27-1 is increased by oryzalin treatment (Ory) and slightly decreased by latrunculin B treatment (LatB).

(B) FRAP of VAP27-1-YFP in the transgenic Arabidopsis in *syt1-2* background shows that the motile fraction of VAP27-1 is already increased without drug treatment. Depolymerization of F-actin decreases the motile fraction of VAP27-1. Note that the error bars are wider in *syt1-2* background, indicating that the recovery of VAP27-1 is more various. The sample size in each group is the same (n = 13).

(C) The diagram shows that the motile fraction of VAP27-1 is enhanced in the

loss of SYT1. Latrunculin B treatment restores the enhancement and oryzalin treatment does not further increase the motile fraction. Different letters indicate significant differences between groups (p -value < 0.01) according to the extra-sum-of-squares F test of the best-fit values.

Error bars = 95% confidence intervals.

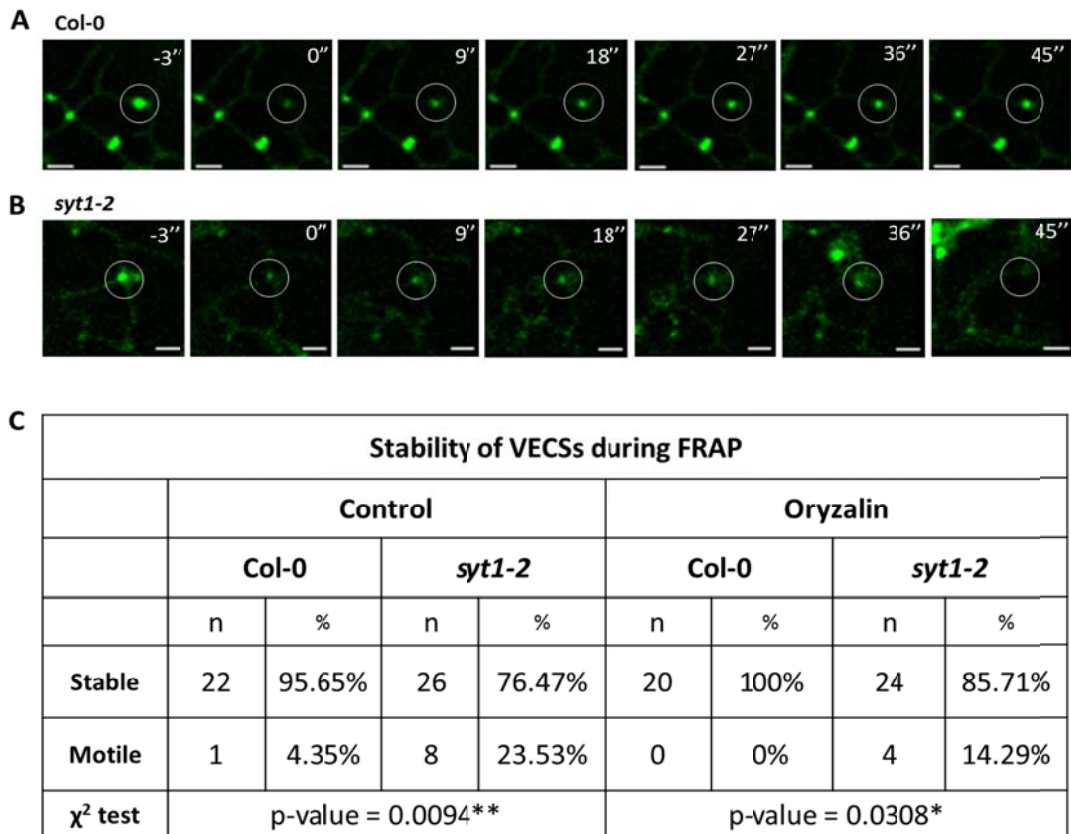


Figure 23. VAP27-1-Enriched ER-PM Contact Sites are Unstable Without SYT1 in Arabidopsis Leaf Epidermal Cells.

(A) Time-lapse images show that the fluorescence of VAP27-1-YFP is able to recovery at the same spot in Col-0 background.

(B) Time-lapse images show one example that a VAP27-1-YFP punctum moves away while recording the images in *syt1-2* background.

(C) Chi-squared tests show that there are more unsteady VAP27-1 puncta in *syt1-2* null background.

Scale bars = 2 μ m.

However, when cells were treated with the actin-depolymerizing drug latrunculin B, the maximal recovery of VAP27-1-YFP in *syf1-2* drastically decreased from $69.08\% \pm 2.48\%$ to $49.44\% \pm 2.36\%$ (p-value < 0.0001) (Figure 22B and 22C). Latrunculin B treatment slightly reduced the maximal recovery of VAP27-1-YFP in Col-o from $55.20\% \pm 1.73\%$ to $48.25\% \pm 2.01\%$ (p-value = 0.0001). After treated with latrunculin B, the maximal recovery of VAP27-1-YFP in the leaves of Col-0 and *syf1-2* showed no significant difference (p-value = 0.32). In addition, the dynamic remodeling of the ER strands in both the cells of Col-0 and *syf1-2* was remarkably arrested after treated with latrunculin B, showing that the actin-dependent movement of cortical ER was hindered by the depolymerization of F-actin. These data demonstrated that the enhanced recovery of VAP27-1 in *syf1-2* resulted from the instability and the over-remodeling of the cortical ER.

On the other hand, when microtubules were depolymerized by oryzalin treatment, the maximal recovery of VAP27-1-27 in Col-0 significantly increased ($69.44\% \pm 2.16\%$, p-value < 0.0001) (Figure 22A and 22C), which was consistent with the previous study (Wang et al., 2014). However, oryzalin did not further increase the turnover of VAP27-1-YFP in *syf1-2* ($68.70\% \pm 4.40\%$, p-value = 0.89). The oryzalin treatment did not disturb the stability of the VECSs because all the VECSs remained unmoved during the FRAP experiments (Figure 23C). Statistical analyses showed that the maximal recovery of VAP27-1-YFP in the leaf cells of oryzalin-treated Col-0, oryzalin-treated *syf1-2*, and non-treated *syf1-2* were not significantly different (p-value = 0.27) (Figure 22C). These results indicated that VAP27-1 was able to anchor on the ER-PM contact sites without SYT1 and microtubule. In summary, the above data demonstrate that SYT1 is an essential component

for maintaining the polygonal network of cortical ER and, therefore, the stability of VAP27-1 tethering on the ER-PM contact sites.

3.1.6. SYT1-Mediated Regulation of Vesicle Trafficking

Studies have shown that Arabidopsis SYT1 plays a role in regulating the endocytosis in the leaves of *N. benthamiana*. However, the functions of SYT1 on the endocytic pathway in Arabidopsis remain unclear. To investigate whether SYT1 would be incorporated in the endocytic vesicles, the roots of transgenic Arabidopsis expressing SYT1-GFP driven by *SYT1* native promoter and VAP27-1-GFP driven by 35S promoter were stained with the lipophilic styryl dye FM 4-64 followed by brefeldin A (BFA) treatment. BFA is a fungal toxin that blocks exocytosis and the return of recycling vesicles to the plasma membrane but does not abolish endocytosis. The blockage will lead to the accumulation of trans-Golgi networks/early endosomes (TGN/EE) and the Golgi apparatus and form the BFA compartments (Berson et al., 2014; Naramoto et al., 2014). The results showed that neither SYT1-GFP nor VAP27-1-GFP was co-localized with the BFA compartments (Figure 24A and 24B), indicating that these two proteins were not transported to the endosomes. Cryo-immunogold electron microscopy further confirmed that both SYT1 and VAP27-1 were still localized on the ER-PM contact sites in the BFA-treated root cells (Figure 24C and 24D).

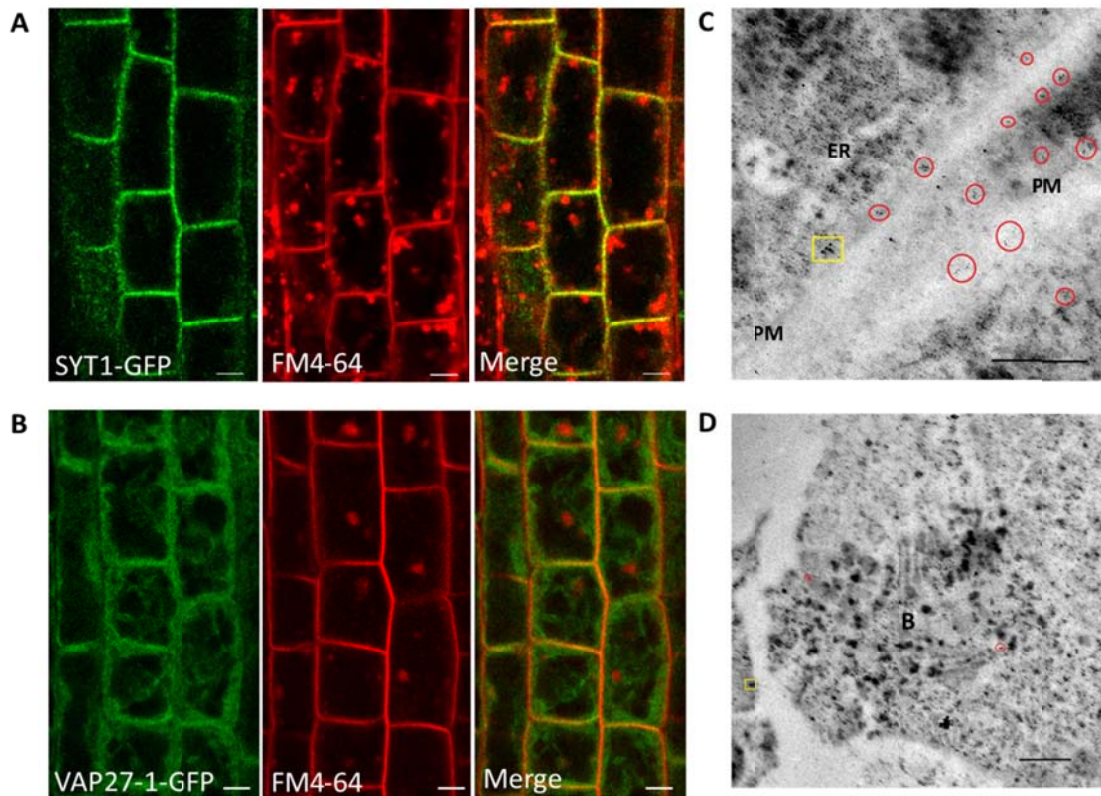


Figure 24. Tethering of SYT1 and VAP27-1 at PM is not Affected by BFA Treatment in Arabidopsis Root Apex Cells.

(A) FM4-64 staining of the roots of SYT1-GFP transgenic Arabidopsis followed by BFA treatment (35.6 μ M) for 60 min shows that SYT1 is not localized to the BFA compartments. Scale bars = 5 μ m.

(B) VAP27-1-GFP is not co-localized with the BFA compartments in the root cells of VAP27-1-GFP transgenic Arabidopsis. Scale bars = 5 μ m.

(C) Double immunogold labeling of the BFA-treated roots of wild type Arabidopsis shows that both SYT1 and VAP27-1 are still localized on the ER-PM contact sites. Scale bars = 500nm.

(D) The electron microscopic image shows an aggregate of Golgi stacks and vesicles (BFA compartment, B) in the BFA-treated root cells. No gold particles are observed in the BFA compartment by double immunogold labeling. 15-nm gold particles (SYT1) are indicated by a yellow rectangle

and 6-nm gold particles (VAP27-1) are indicated by red circles. Scale bars = 500nm.

The roles for ER-PM contact sites in vesicle trafficking in yeast and animal cells have been documented (Stefan et al., 2013; Stradalova et al., 2012). In addition, the dynamic of the ER has been shown to influence the endocytosis and the trafficking of endosomes in plant cells (Stefano et al., 2015). To determine whether the mutation of *SYT1* would affect the membrane trafficking in Arabidopsis, the sizes of the BFA-induced compartments in the cells of root transition zone in Col-0 and *sty1-2* were measured (Figure 25). The frequency distribution of different BFA compartment sizes showed that the most common size of the BFA compartments in *sty1-2* (1.5 - 2.0 μm , 39.20%) was smaller than that in Col-0 (2.0 – 2.5 μm , 25.76%). Statistics using unpaired t-test rejected the hypothesis that the two populations would be the same size (p-value < 0.0001) (Figure 25B). This result indicated that vesicle trafficking, either the endocytosis rate or the fusion of vesicles, was affected due to the loss of SYT1 protein.

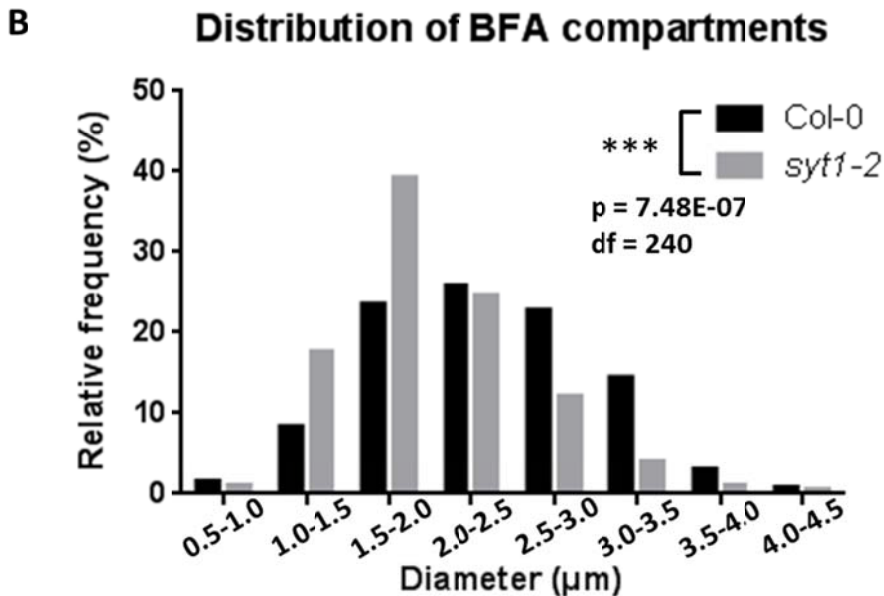
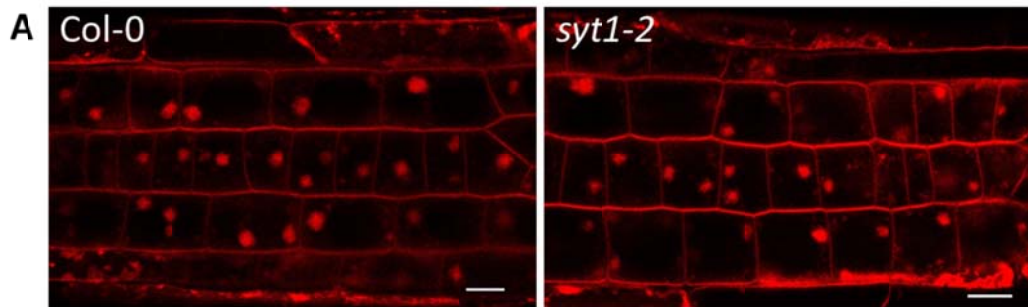


Figure 25. Vesicle Trafficking in Arabidopsis Root Apex Cells is Disturbed by the Loss of *SYT1*.

(A) FM4-64 staining followed by BFA treatment shows the BFA compartments in the root cells of transition zone of Col-0 and *syt1-2*. Scale bars = 10 μm.

(B) The frequency distribution of the sizes of BFA compartments shows that *syt1-2* has smaller BFA compartments. Only the root epidermal cells in the transition zone are measured. More than 60 cells from four roots and two independent experiments for each line are analyzed. The t-test shows that the two distributions are significantly different (p -value < 0.001***).

Other than the “beads on a string” pattern of SYT1 described in this research and in previous reports, SYT1 also often exhibited a wide-spreading

behaviour resulting in the "sheet with gaps and holes" pattern in tobacco leaf epidermis (Figure 26A and 27A). Even though this pattern might be resulted from the side effects of SYT1's overexpression, these two different patterns often co-occurred within the same cell expressing SYT1-GFP driven by native *SYT1* promoter. In addition, the similar wide-spreading pattern was also observed in immunofluorescence-labeled root cells in Arabidopsis (Figure 26B), indicating that this kind of pattern were physiological relevant.

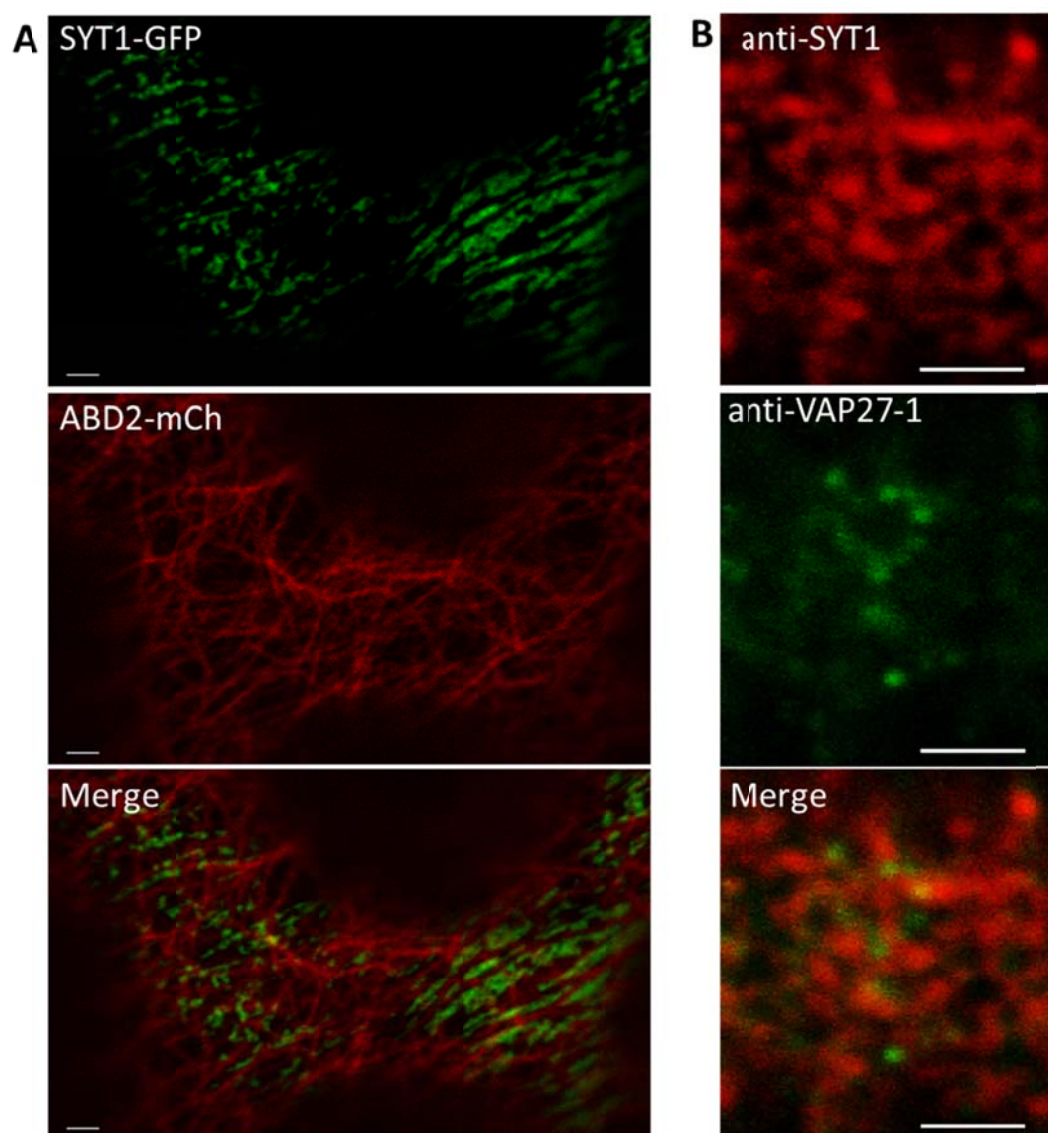


Figure 26. SYT1-Enriched ER-PM Contact Sites Show Various Patterns.

(A) Co-expression of SYT1-GFP and ABD2-mCh in *N. benthamiana* leaves shows that SYT1 may display both puncta patterns and sheet-like

structures in two parts of the same cell. The ABD2-labeled F-actin as the reference of the intracellular conditions shows that the two parts of the cell are intact and undamaged.

(B) Double immunofluorescent labeling of SYT1 and VAP27-1 in wild type Arabidopsis roots shows that SYT1 sometimes occupies huge areas of the cell cortex (in comparison with the images in Figure 11A).

Scale bars = 2 μ m.

The co-expression of SYT1-GFP, VAP27-1-YFP, and MAP4-DsRed showed that the “gaps” were occupied by microtubules. Some “holes” were filled by the VECSs (Figure 27A). When SYT1-GFP and HDEL-RFP were co-expressed in tobacco leaf cells, the wide spread of SYT1 on the cortical ER was accompanied by a disturbance of ER cisternae and tubules (Figure 27B). However, the wide spread of SECSs was not caused by the cisternalization of the ER because the SYT1 could also form puncta structures around the ER cisternae (Figure 27C). In all the cases, there were still areas on the cell cortex that were not occupied by SYT1, VAP27-1, or microtubules. These empty areas might be the regions where endocytosis and exocytosis took place. To support this hypothesis, the endosomal markers, clathrin light chain fused with mCherry (CLC-mCherry) or adaptor protein 2 μ 2 fused with mCherry (AP2 μ 2-mCherry), were co-expressed with SYT1-GFP. The results showed that the CLC- or AP2 μ 2-labeled endosomes only appeared on the cortical regions where no SYT1-labeled cortical ER was identified (Figure 28). However, the early endosomes were often in contact with the SYT1-labeled cortical ER. These data were all in line with the idea that SYT1 regulates the vesicle trafficking by confining the hot-spots for endocytosis or exocytosis.

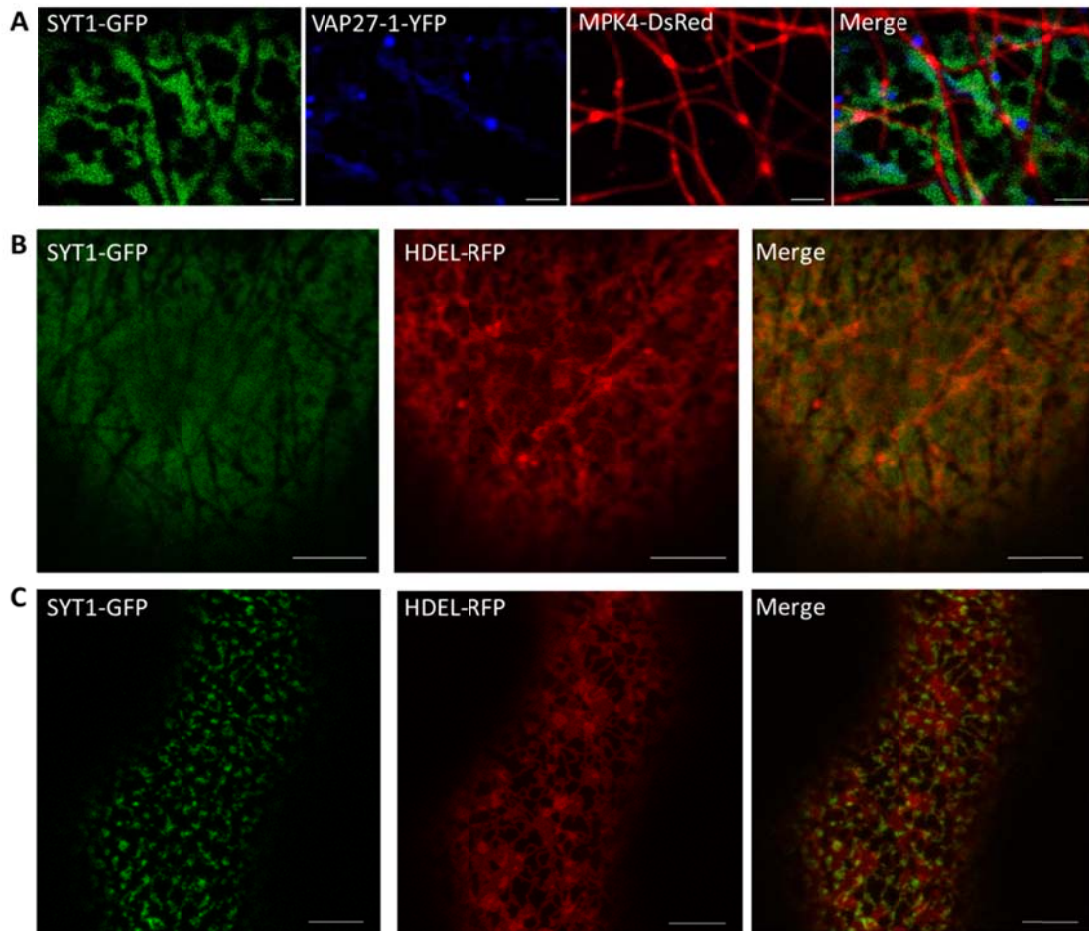


Figure 27. Some Cell Cortex Areas are Free of SYT1, VAP27-1, and Microtubules in *N. benthamiana* Leaf Epidermal Cells.

- (A) The images show the "sheet with gaps and holes" pattern of SYT1 in *N. benthamiana* leaf cells. The VECSS and the microtubules localize in some holes and gaps, respectively. Some holes are free of the three proteins. Scale bars = 2 μm .
- (B) The images show one example that the existence of the SYT1 sheets in *N. benthamiana* leaf cells is accompanied by the tangled ER networks. Scale bars = 5 μm .
- (C) The images show one example that the SYT1 puncta in *N. benthamiana* leaf cells localize on the margins of the HDEL-labeled ER cisternae. Scale bars = 5 μm .

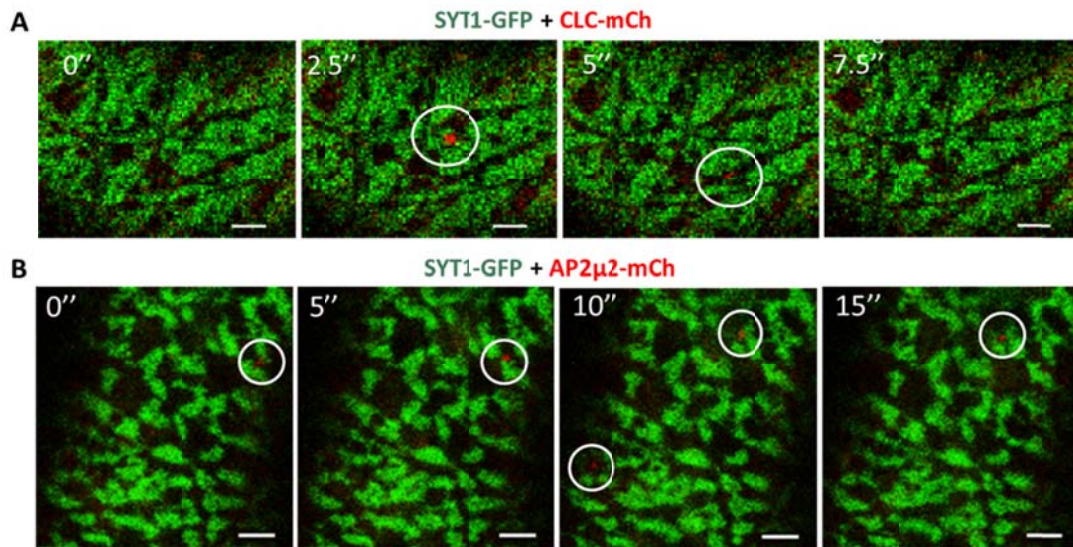


Figure 28. Spatial Relationship between SECSs and Early Endosomes in *N. benthamiana* Leaf Epidermal Cells.

(A) Co-expression of SYT1-GFP and CLC-mCherry in *N. benthamiana* leaf cells shows that the CLC-labeled early endosomes appear only on the SECS-free regions of cell cortex. The early endosomes are in close vicinity with SECSs.

(B) Co-expression of SYT1-GFP and AP2μ2-mCherry in *N. benthamiana* leaf cells shows the same result. The AP2μ2-labeled early endosomes appear on the SECS-free regions at different time points.

Scale bars = 2 μm.

3.2 Trans-Golgi Network-Localized Synaptic Vesicle

Protein 2-like in Root Apex Cells

3.2.1. Phylogenetic Relationship of SV2 and SV2-like Proteins in Eukaryotes

In order to investigate the evolutionary relationships of Arabidopsis SV2-like (SVL) and other SV2-related proteins in plant and animal kingdoms, phylogenetic analysis was conducted using the amino acid sequences of these proteins and several bacterial proteins as the outgroup. The phylogenetic tree showed that eukaryotic SV2-like proteins were divided into two clades: Animalia SV2-like and Plantae SV2-like (Figure 29). SV2 proteins existed only in vertebrates. Eukaryotic SV2 and SV2-like separated very early in the evolutionary history, before eukaryotes diverged into the two major lineages unikonts (including animals) and bikonts (including plants) (Derelle et al., 2015). Arabidopsis SV2-like belongs to the clade of Plantae SV2-like and is distantly related to the vertebrate SV2.

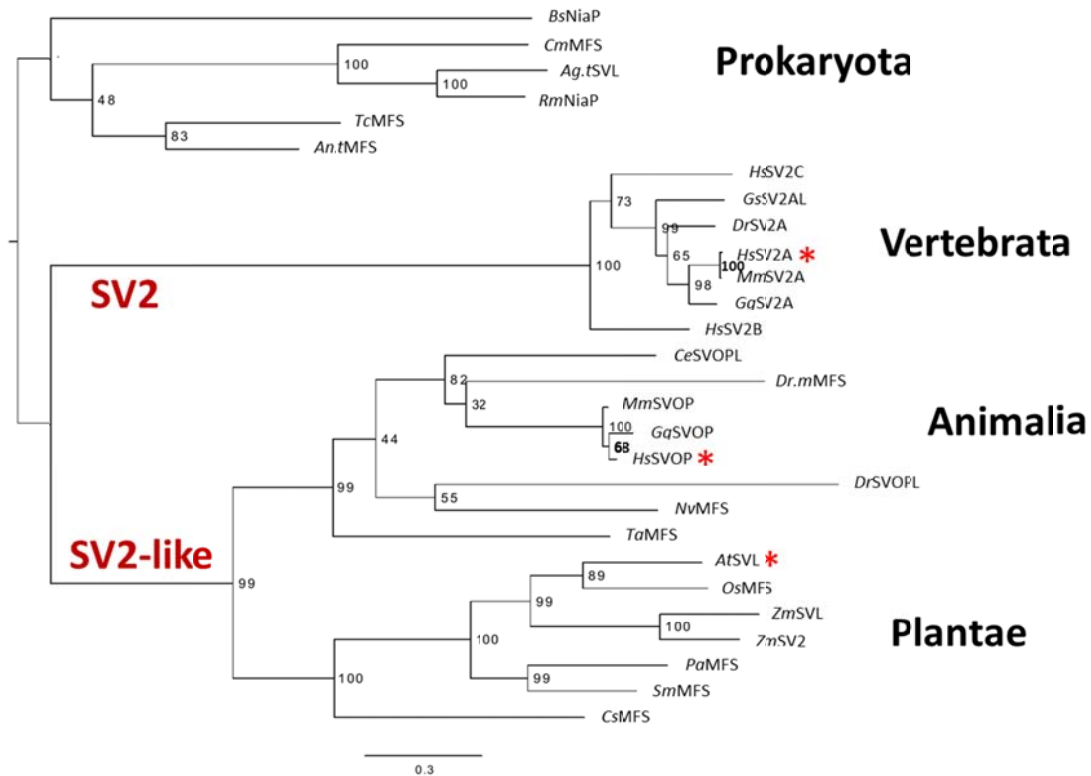


Figure 29. Phylogeny of SV2 and SV2-Like Proteins.

The maximum-likelihood tree shows that SV2 proteins exist only in vertebrate animals whereas SV2-like homologs exist in both animal and plant kingdoms. SV2 and SV2-like are distantly related. Arabidopsis SV2-like (*AtSVL*), human SV2A (*HsSV2A*), and human SV2-like (*HsSVOP*) are marked with asterisks. Bootstrap values are shown next to each node.

3.2.2. Expression of SVL is Developmental Stage-Dependent

To examine the gene expression patterns of Arabidopsis *SVL*, the cloned *SVL* promoter was fused to the β -glucuronidase (*GUS*) reporter gene and transformed into wild type Arabidopsis. The histochemical staining for *GUS* activity showed that *SVL* was mainly expressed at root tips and hypocotyls in the early growing stage (Figure 30). The expression of *SVL* expanded through the whole root after four days of germination. *SVL* was expressed almost in all

the tissues, such as leaves, hypocotyls and roots, after six to seven days of germination. At the flowering stage, the GUS activity was mainly detected in anthers and sepals (Figure 30). These results indicated that the expression of *SVL* was developmentally regulated.

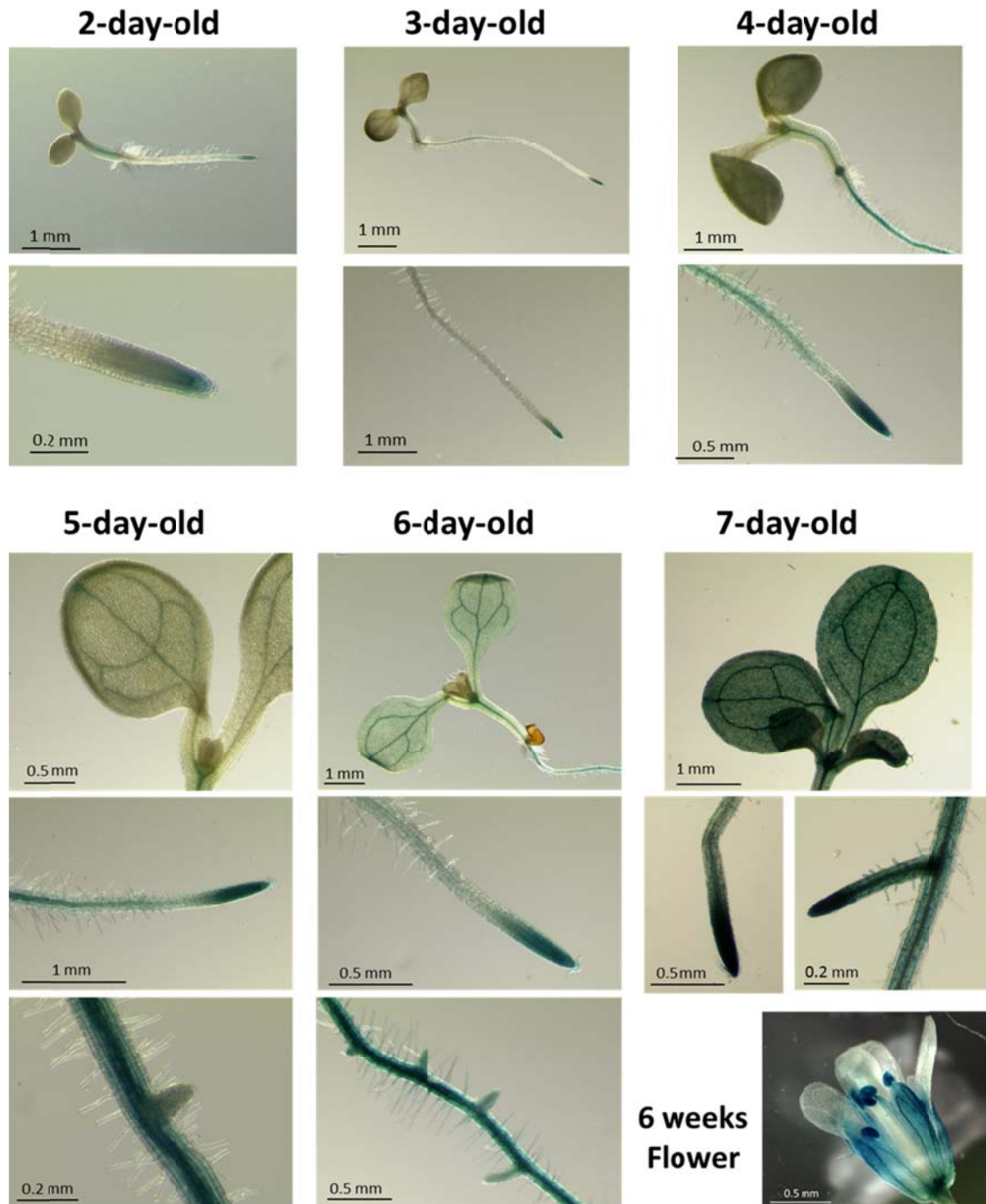


Figure 30. Developmental Stage-Specific Expression of Arabidopsis *SVL*.

The GUS reporter analyses of the promoter activities of Arabidopsis *SVL* show

that the expression of SVL in 2- to 3-day-old seedlings of Arabidopsis was restricted in root tips and hypocotyls. The expression of SVL becomes ubiquitous in the 7-day-old seedlings. SVL is also expressed in anthers and sepals.

3.2.3. SVL Null Mutant Showed no Apparent Phenotype

To reveal the physiological functions of SVL gene in Arabidopsis, three SALK insertion mutants of SVL were ordered from the Arabidopsis Biological Resource Center (ABRC). The three mutant lines were named *svl-1* (SALK_114298), *svl-2* (SALK_089824C) and *svl-3* (SALK_069071.25.70x) (Figure 31A). The homozygous lines were obtained by antibiotic screening and genotyping PCR. The RT-PCR analysis showed that *svl-1* was a null mutant, but the expression levels of SVL transcripts in *svl-2* and *svl-3* were similar to that of wild type (Figure 31B). The growth of the primary roots of *svl-2* and *svl-3* was the same as that of wild type in both normal and salt-stress conditions (Figure 31C). No phenotype could be observed in the two mutants. Moreover, the SVL knock-out mutant *svl-1* still showed no severe phenotype, even though the roots of *svl-1* grew slightly faster than that of wild type at the early seedling stage in normal condition (Figure 32A). Arabidopsis SVL has been shown to be a niacin transporter; however, our RT-PCR results showed the niacin treatment did not alter the expression levels of SVL in wild type Arabidopsis (Figure 31B). High concentration of niacin inhibited the growth of Arabidopsis; however, no significant difference was observed between the growth of *svl-1* and wild type under niacin treatment (Figure 32). No obvious phenotype in the SVL mutants was recorded from our experiments.

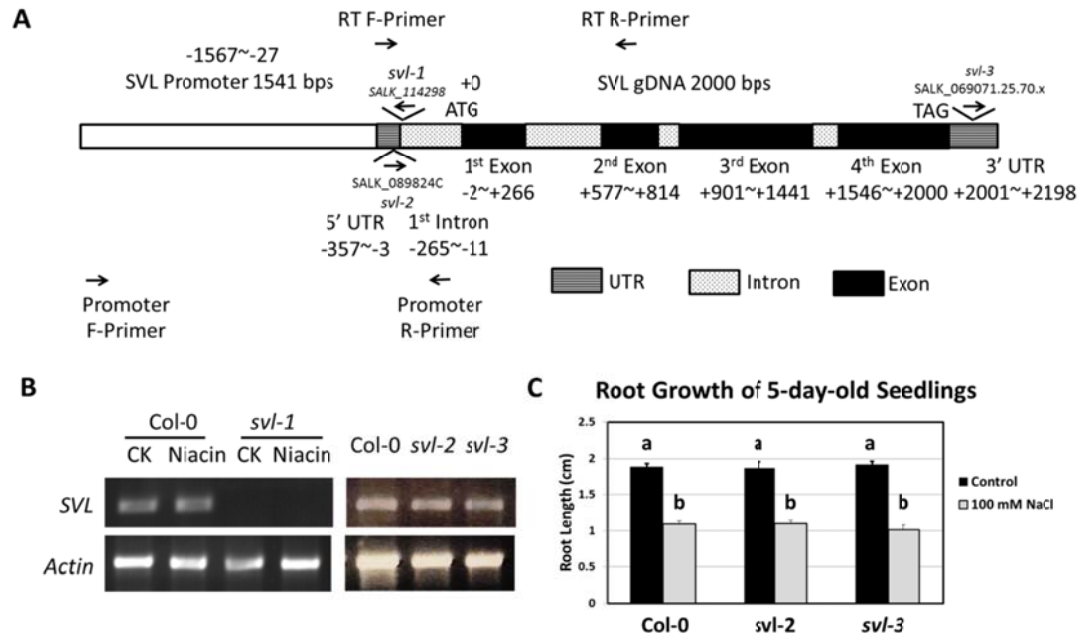


Figure 31. Identification of Arabidopsis SVL Mutants.

- (A) Schematic diagram of *SVL* gene structure. Three T-DNA insertion sites of the *SVL* mutants and the primers used for RT-PCR are indicated.
- (B) The RT-PCR analyses show that *svl-1* is a knock-out mutant. Wild type Col-0, *svl-2* and *svl-3* express similar levels of *SVL* transcripts. The seedlings grown on medium containing high concentration of niacin (50 mg/L) for 7 days show that the expression level of *SVL* was not affected by the niacin treatment. The *Actin* gene was used as an internal control.
- (C) The root lengths of 5-day-old Col-0, *svl-2* and *svl-3* seedlings are the same. Different letters indicate significant differences between groups (p -value < 0.05) according to the student t-test. Error bars = standard errors (SE).

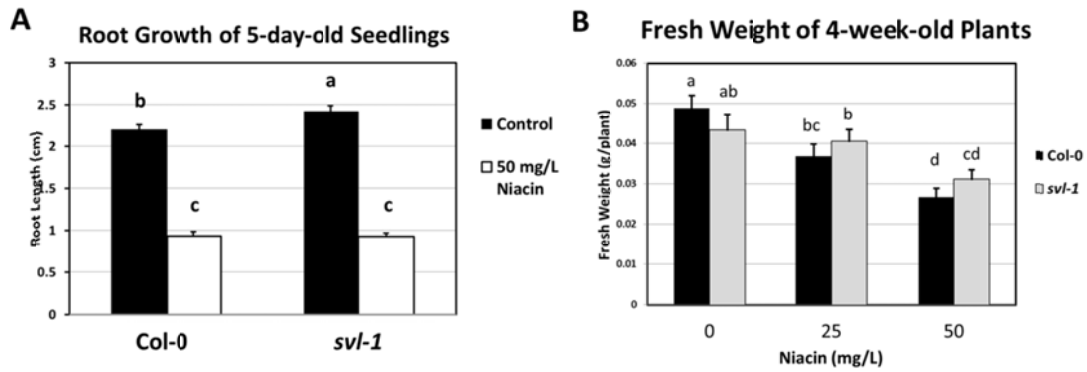


Figure 32. Arabidopsis SVL Null Mutant Seedlings Show no Obvious Differences in Growth Compared with Wild Type Seedlings.

(A) The roots of *svl-1* seedlings grow slightly faster than that of wild type in normal condition. Niacin treatment inhibited both the growth of primary roots of wild type and *svl-1* mutant.

(B) Niacin treatments reduce the fresh weight of wild type and *svl-1* plants. The fresh weight of wild type and *svl-1* shows no significant difference.

Different letters indicate significant differences between groups (p -value < 0.05) according to the student t-test. Error bars = standard errors (SE).

3.2.4. SVL is Localized on the Trans-Golgi Network

To reveal the subcellular localization of Arabidopsis SVL, co-expressions of SVL-GFP or SVL-mCherry with different fluorescent organelle markers were conducted using agroinfiltration in *N. benthamiana* leaves. The results showed that Arabidopsis SVL-GFP was localized on motile vesicle-like structures, which were not co-localized with the ER marker RFP-HDEL (Figure 33A) and the ER-PM contact site marker SYT1-mCherry (Figure 33B). The vesicles labeled with SVL-GFP often met and partly overlapped with the ST-RFP-labeled Golgi apparatus (Figure 34A), whose localization patterns resembled the trans-Golgi networks (TGN). The SVL-GFP was then

co-expressed with the TGN marker vesicle transport v-SNARE 12 (VTI12)-mCherry. The result showed that the SVL-GFP signals were largely overlapped with the VTI12-mCherry signals (Figure 34B), indicating that SVL was localized on the TGN and/or other post-Golgi vesicles.

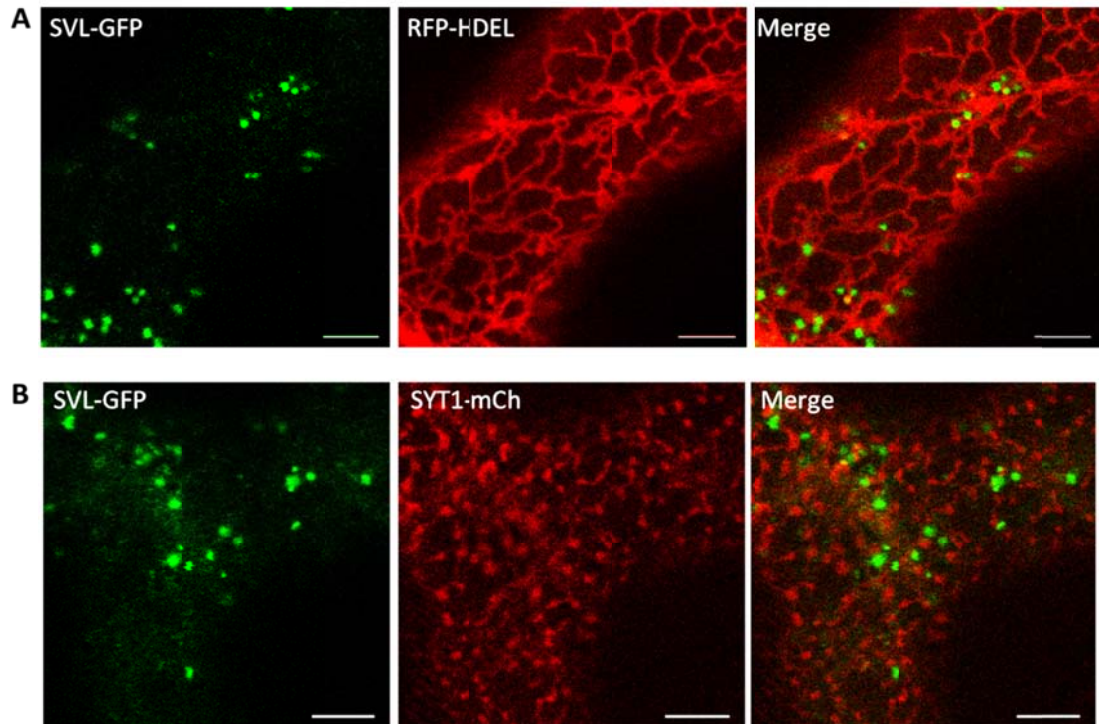


Figure 33. SVL-GFP is Localized on Vesicles in *N. benthamiana* Leaf Epidermal Cells.

(A) Co-expression of SVL-GFP and RFP-HDEL shows that SVL is not localized on the ER but on motile vesicles.

(B) Co-expression of SVL-GFP and SYT1-mCherry shows that SVL is not overlapped with the SYT1 puncta.

Scale bars = 5 μ m.

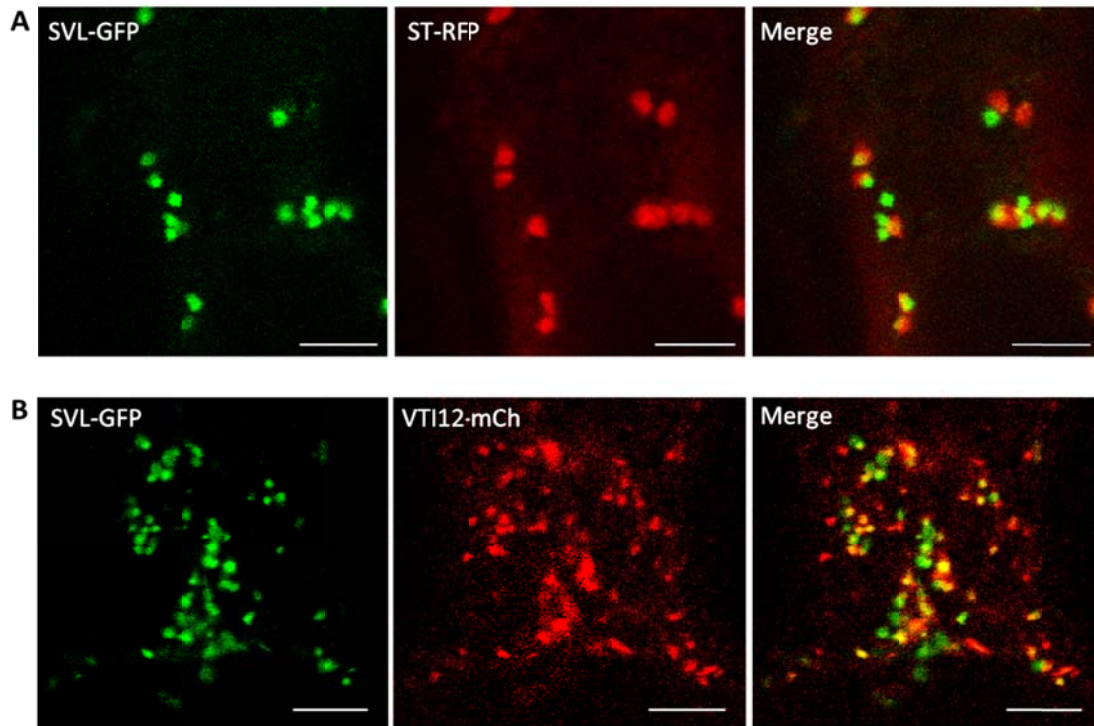


Figure 34. SVL is Localized on Trans-Golgi Network in *N. benthamiana* Leaf Epidermal Cells.

(A) Co-expression of SVL-GFP and ST-RFP shows that SVL-localized vesicles are often overlapped with the Golgi apparatus.

(B) Co-expression of SVL-GFP and VTI-mCherry shows that SVL-localized vesicles are largely overlapped with the VTI12-labeled trans-Golgi network.

Scale bars = 5 μm .

To further characterized the SVL-localized vesicles, SVL-GFP or SVL-mCherry was co-expressed with various early endosome and late endosome markers in tobacco leaves. The data showed that SVL was not co-localized with the clathrin light chain (CLC)-labeled endosomes (Figure 35A), indicating that SVL was not likely to be incorporated in the clathrin-mediated endocytosis. SVL was not localized on the Fab1, YOTB, Vac1, and EEA1 (FYVE)- and root handedness 1 (Rha1)-labeled prevacuolar

compartments/late endosomes (PVCs/LEs) (Figure 35B and 35C). However, SVL-labeled endosomes were partly co-localized with the Ara6-labeled vesicles, a subpopulation of multivesicular bodies/late endosomes (MVBs/LEs) distinct from the Rha1-labeled MVBs (Figure 36A). SVL protein was also partly co-localized with the early endosome/recycling endosome marker RabA1e-mCherry (Figure 36B). These data suggested that SVL was transported between TGN, MVBs, and recycling endosomes.

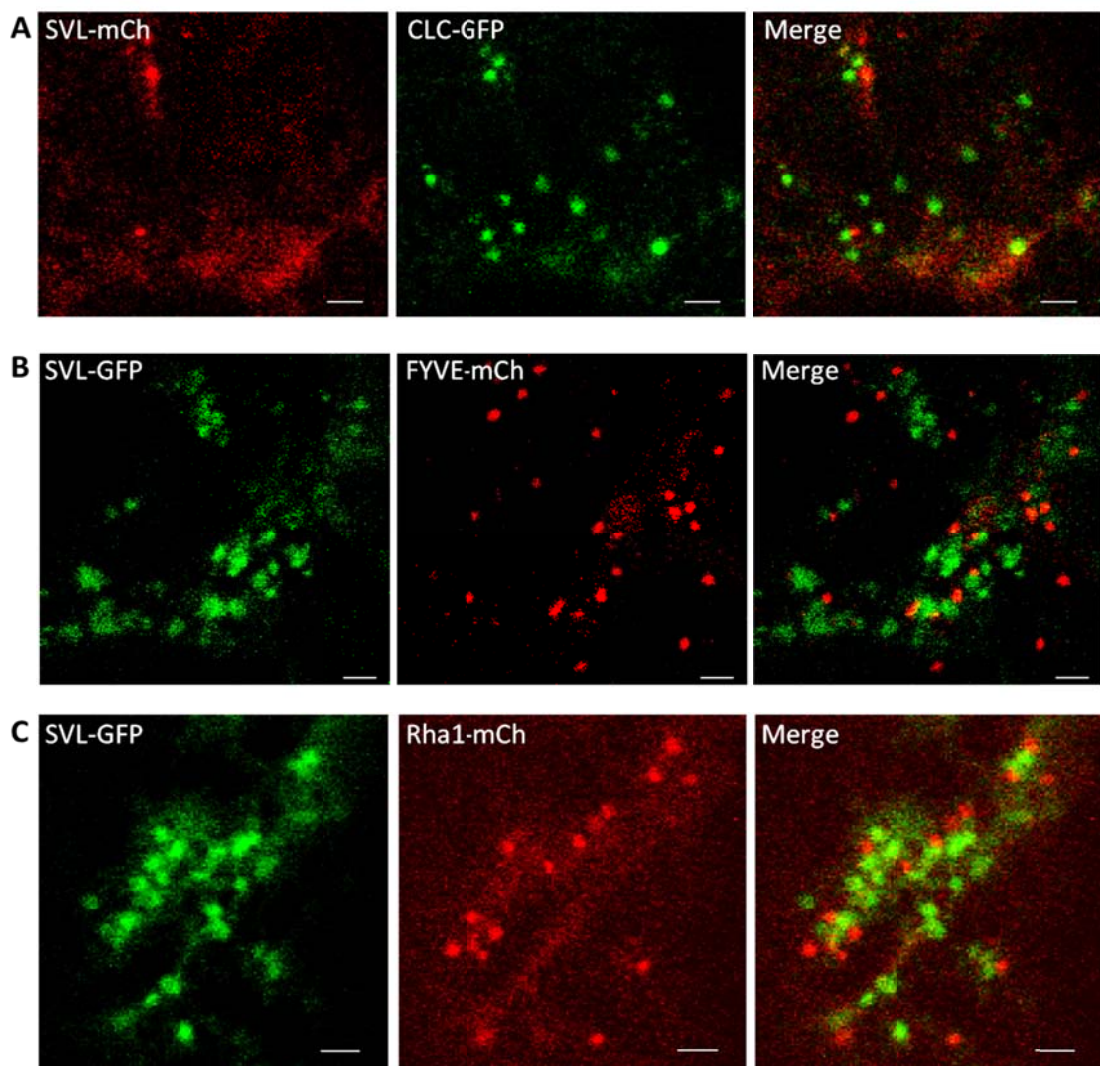


Figure 35. SVL is not Localized to CLC-Coated Vesicles and Prevacuolar Compartments in *N. benthamiana* Leaf Epidermal Cells.

(A) Co-expression of SVL-mCherry and CLC-GFP shows that SVL and CLC

are localized on different vesicles.

(B) Co-expression of SVL-GFP and FYVE-mCherry shows that SVL is not localized on the FYVE-labeled late endosomes.

(C) Co-expression of SVL-GFP and Rha1-mCherry shows that SVL is not transported to the Rha1-labeled prevacuolar compartments/late endosomes.

Scale bars = 2 μ m.

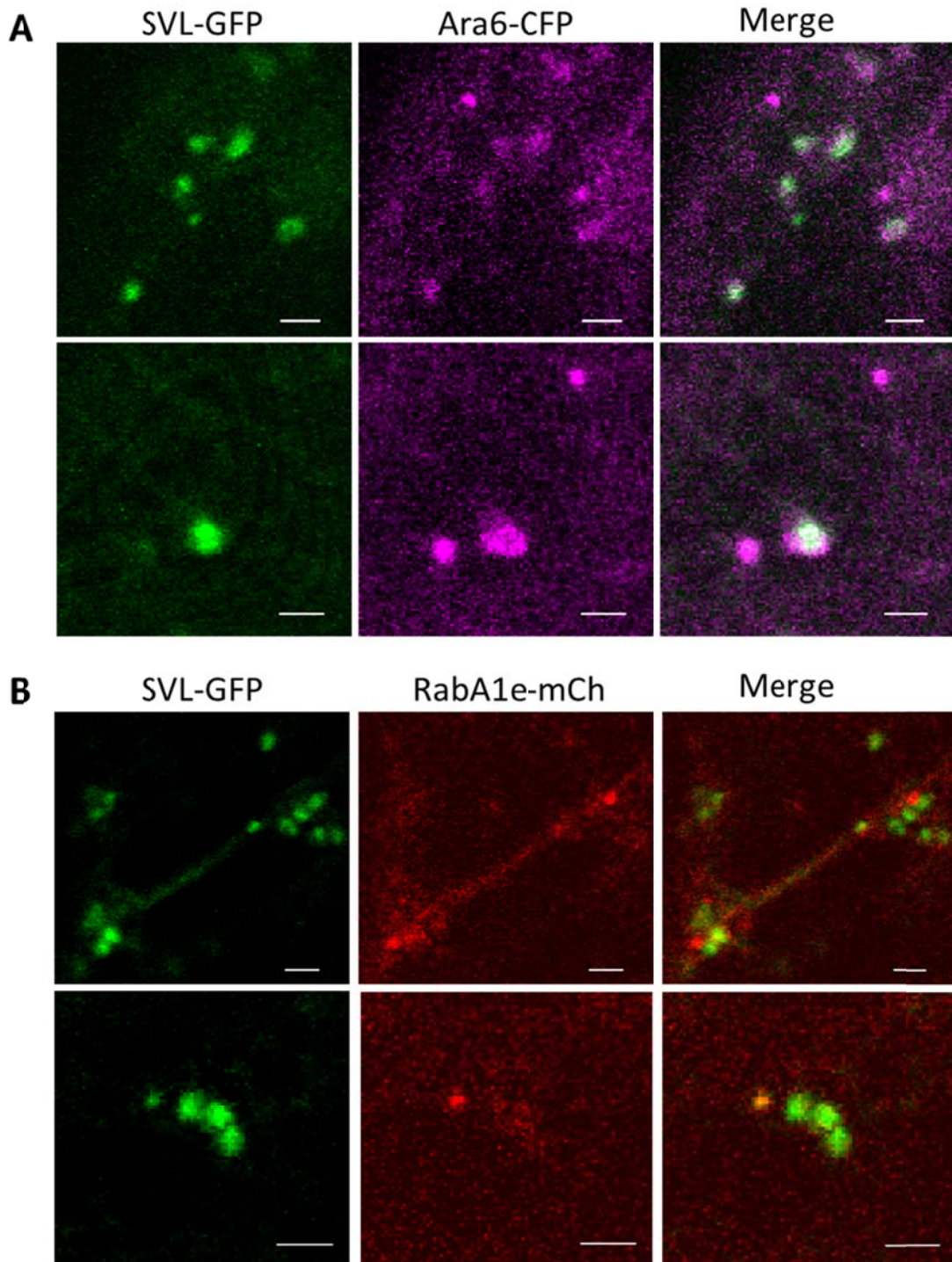


Figure 36. SVL is Partly Localized on the Multivesicular Bodies and Recycling Endosomes *N. benthamiana* Leaf Epidermal Cells.

(A) Co-expression of SVL-mCherry and Ara6-CFP shows that SVL is partly localized on the Ara6-labeled endosomes.

(B) Co-expression of SVL-GFP and RabA1e-mCherry shows that SVL is partly

overlapped with the RabA1e-labeled endosomes.

Scale bars = 2 μm .

In order to confirm the subcellular localization of SVL in Arabidopsis, SVL-GFP fusion construct driven by SVL native promoter was stably transformed into the SVL null mutant, *svl-1*. To investigate if SVL-GFP is incorporated into the early endosomes, the roots of SVL-GFP/*svl-1* homozygous transgenic Arabidopsis was stained with the endocytic tracer FM4-64 for 15 min. The result showed that SVL-GFP was largely overlapped with the FM4-64-stained early endosomes (Figure 37A). When the FM4-64 stained roots were treated with 35.6 μM of BFA for 60 min, SVL-GFP formed large aggregate and incorporated into the BFA compartments (Figure 37B). Some of the SVL-GFP vesicles decorated the periphery of the BFA compartments. This indicated that SVL was localized on the TGN and partly on the Golgi apparatus. When the roots were treated with 33 μM of wortmannin for 100 min, some of the FM4-64-stained vesicles, the late endosomes, became swelled. However, SVL-GFP was not co-localized with the enlarged multivesicular compartments induced by wortmannin (Figure 37C), indicating that SVL was probably not transported to the PVCs/LEs.

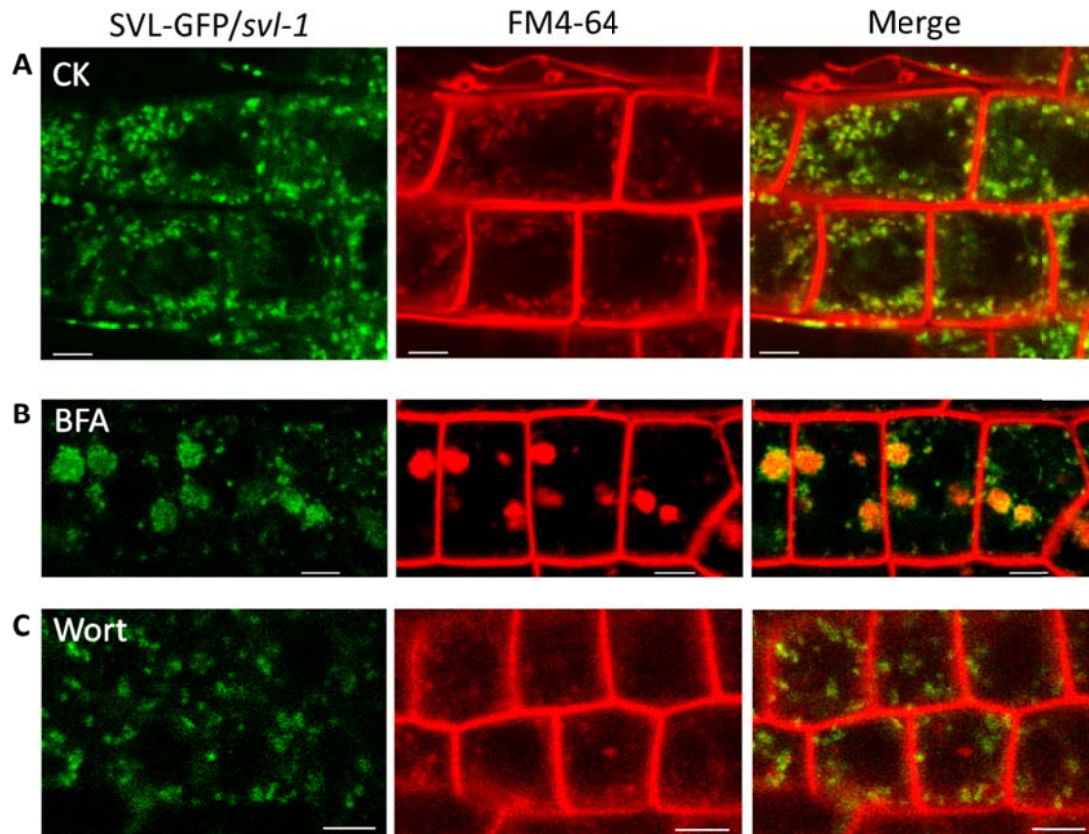


Figure 37. SVL is Localized on Trans-Golgi Networks/Early Endosomes in Arabidopsis Root Apex Cells.

(A) FM4-64 staining of the roots of *SVL-GFP/svl-1* transgenic line (4.1 μM of FM4-64 for 15 min) shows that SVL-GFP signals are mostly overlapped with the FM4-64-labeled vesicles.

(B) FM4-64 staining followed by BFA treatment (35.6 μM for 60 min) shows that SVL-GFP is localized to the BFA compartments.

(C) SVL-GFP is not incorporated into the wortmannin-induced (33 μM for 100 min) swollen late endosomes labeled by FM4-64.

Scale bars = 5 μm .

4. Discussion

4.1. Arabidopsis SYT1

4.1.1. Subcellular Localization of SYT1

Using expression of SYT1-GFP fusion in *N. benthamiana* and Arabidopsis, aqueous two-phase extraction followed by mass spectrometry or western blot, and immunogold electron microscopy, studies have shown that Arabidopsis Synaptotagmin 1 (SYT1) is a plasma membrane protein (Schapire et al., 2008; Yamazaki et al., 2008). Arabidopsis SYT1 has also been shown to be localized to the plasma membrane-derived endosomes in *N. benthamiana* protoplasts (Lewis and Lazarowitz, 2010). However, two recent studies have shown Arabidopsis Synaptotagmin 1 is an ER integral membrane protein localized on the ER-PM junctions (Levy et al., 2015; Perez-Sancho et al., 2015). The subcellular localization of Arabidopsis SYT1 is convoluted owing to i) the resemblance of the protein to human SYT1 and E-SYT1, ii) the phospholipid binding property of the C2 domains and the characteristic of the transmembrane domain (TM), and iii) the diverse morphology of the cortical ER in plant cells. Arabidopsis SYT1 was deemed functionally related to human SYT1 because both Arabidopsis SYT1 and human SYT1 possess a single N-terminal transmembrane domain and two tandem C2 domains (C2A-C2B) at the C-terminal. Human E-SYTs have a long N-terminal transmembrane domain that forms a hairpin-like structure, and three to five C2 domains at the C-terminal; however, human E-SYTs share with Arabidopsis SYT1 a conserved SMP domain located between their TM and the C2 domains (Kopec et al., 2010;

Levy et al., 2015). The respective lengths of Arabidopsis SYT1, human SYT1, and human E-SYT1 are 541 aa, 422 aa and 1104 aa. The protein architecture of Arabidopsis SYT1 is close to human SYT1; however, Arabidopsis SYT1 has been proposed to share the same origin in a common ancestor with human SYTs and E-SYTs (Craxton, 2010). The subcellular localization and the physiological functions of the Arabidopsis SYT family provide important information on the influence of evolution on these proteins.

Mammalian SYTs and E-SYTs are both highly expressed in neurons; however, the ability of SYTs to translocate through the exocytosis pathway and trigger the membrane fusion makes it functionally different from the ER-retaining E-SYTs. Mammalian SYTs are transported from the ER membrane to the Golgi apparatus, carrier vesicles, and then to the plasma membrane by calcium-regulated exocytosis whereas mammalian E-SYTs are retained on the ER membrane and attach to the plasma membrane by calcium-regulated binding (Min et al., 2007; Rizzoli, 2014). Mutations in the linker domain between the TM and the C2A domain or the short C-terminus inhibit the transport of human SYTs from the ER to the Golgi apparatus (Fukuda et al., 2001). Moreover, both linkers between C2A and C2B domains, and between the TM and the C2 domains, influence neurotransmission (Lee and Littleton, 2015; Liu et al., 2014). On the other hand, deletion or mutation in the C2C domain of human E-STY2 prevents its cortical localization, leading to a dispersion of E-SYT2 on the ER (Giordano et al., 2013). Apparently, the C2 domains and other regions throughout the cytosolic part play important roles in the localization and the function of SYTs and E-SYTs. This may explain why Arabidopsis SYT1 is localized to the ER-PM contact sites but the closely

related Arabidopsis SYT2 is localized to the Golgi apparatus and the plasma membrane (Wang et al., 2015a; Zhang et al., 2011a).

Human E-SYT2 has three C2 domains (C2A-C2B-C2C) and the C2C domain of E-SYT2 is indispensable for the protein's cortical localization and binding to the PM (Giordano et al., 2013). Arabidopsis SYT1, by comparison, contains only two C2 domains (C2A-C2B) but is still localized on the cortical ER and tethers to the PM. The SMP domain of Arabidopsis SYT1 has also been shown to be critical for the puncta localization (Perez-Sancho et al., 2015; Yamazaki et al., 2010); however, the deletion of SMP domain in human E-SYT2 has no apparent effect on its localization (Giordano et al., 2013). It seems that Arabidopsis SYTs and mammalian E-SYTs have evolved different sorting and anchoring mechanisms. Furthermore, Arabidopsis SYTs are type I transmembrane protein with the N-terminus in the non-cytosolic space and a single transmembrane domain consisting of 22 or 23 amino acids, which is very similar to that of mammalian SYTs (about 22 to 27 aa) (Craxton, 2004; Giordano et al., 2013; Yamazaki et al., 2010). It has been demonstrated and generally assumed that proteins with a transmembrane domain of these lengths are transported to the post-Golgi compartments or to the PM. On the other hand, proteins with shorter transmembrane domains (about 17 to 20 aa) are generally retained on ER in both animal and plant cells (Brandizzi et al., 2002; Giordano et al., 2013; Sharpe et al., 2010; Yamazaki et al., 2010). Arabidopsis SYT1 is a special case in this aspect, indicating other factors may determine the ER retention of Arabidopsis SYT1. In addition, Arabidopsis SYTs (SYT1-5) have a very short N-terminal amino acid residue (about 2 to 7 amino acids) in the non-cytosolic space and the predicted signal peptide is overlapped

with the TM domain. These N-terminal features of Arabidopsis SYT1 are different from that of mammalian SYTs (about 64 aa in the non-cytosolic space for SYT1) and E-SYTs (N-terminus in cytosolic space).

This study demonstrates that Arabidopsis SYT1 is localized mainly on the cortical ER by co-expressing SYT1-GFP fusion with SYT1 native promoter in *N. benthamiana* leaves with ER, Golgi, PM, and endosome markers. Whole-mount fluorescent immunocytochemistry and cryo-immunogold electron microscopy in Arabidopsis root tips further confirm the ER-PM localization of Arabidopsis SYT1. Nonetheless, it may be a concern that GFP fusion to the C-terminus of Arabidopsis SYT1 may affect the trafficking of the protein as suggested in previous studies (Fukuda et al., 2001; Kotzer et al., 2004; Sohn et al., 2003). As the anti-SYT1 antibody was generated against the peptides on the C2 domains (Schapire et al., 2008) and the distance between the ER and the PM membranes on the contact sites is approximately 30 nm, the SYT1-positive gold particles localized on the ER-PM contact sites become indistinguishable from those on the PM if there is no clear staining on the cortical ER observed by electron microscopy. However, no SYT1-positive signal was found on the Golgi apparatus and BFA compartments, showing that Arabidopsis SYT1 is not transported to the Golgi apparatus. No evidence has suggested that membrane fusion occurs on the ER-PM contact sites in animal cells, even though hemifusion on the ER-chloroplast contact sites has been suggested (Mehrshahi et al., 2013; Prinz, 2014). The existence of Arabidopsis SYT in the PM fraction isolated by aqueous two-phase partitioning shown by previous studies (Kawamura and Uemura, 2003; Schapire et al., 2008; Yamazaki et al., 2010) may be attributed to its strong phospholipid binding ability even in the

absence of calcium ions and its long transmembrane domain. Therefore, excluding the possibility of transient translocation of Arabidopsis SYT1 from the ER to the PM, Arabidopsis SYT1 is an ER integral membrane protein localized on the ER-PM contact sites.

4.1.2. Tethering of SYT1 and VAP27-1 on ER-PM Contact Sites

The relationships between Arabidopsis SYT1 and ER-PM tethering proteins VAP27-1 and NET3C have also been addressed in this study. Co-expression in tobacco leaves, double immunofluorescent staining, and double immunogold labeling together have confirmed that Arabidopsis SYT1 does not co-localize with VAP27-1 and NET3C on the ER-PM contact sites. The localization patterns of these proteins indicate that there are different types of ER-PM contact sites, which have been identified by our team. These contact sites may have different functions, but their functions are interrelated. From our observation, the VECs are always associated with the SECSs, but half of the SECSs are not attached to the VECs, suggesting that the VECs may be dependent on the SECSs. The expression of the mutant form of VAP27-1, which was unable to anchor to the PM has no effect on the stationary characteristic of SECSs; the mutation of three conserved amino acid residues of the calcium binding motif slightly reduces the stability of the SECSs. The SECSs remain intact either by photobleaching or by the depletion of cytosolic calcium after BAPTA-AM treatment. However, the protein can be removed by photobleaching with BAPTA-AM pre-treatment. These data indicate that the tethering of SYT1 to the PM is steady and the SECSs are

stable, which agrees with the results described previously (Perez-Sancho et al., 2015). Based on the above observation, it can be inferred that Arabidopsis SYT1 plays important roles in stabilizing the ER network or supporting the compartmentation of the cell cortex.

The tethering of VAP27-1 to the PM does not require SYT1 because the VECSs can still be found in *SYT1* null mutant. These results are compatible with the presence of the stable VECSs in the cells in which the SECSs are removed by BAPTA-AM pre-treatment and photobleaching. However, the ER tubules are more dynamic, the VECSs are less stable, and the turnover of VAP27-1 increases in *SYT1* null mutant. The ER network is less connected and the average number of three-way-junctions is decreased in the absent of SYT1, although cells with well-reticulated ER and those with extremely motile ER strands can be observed in the same leaf. This observation suggests that the organization of cortical ER varies from across cell types. Additionally, Arabidopsis SYT1 and other factors are vital in regulating the stability of cortical ER. The behaviour of the cortical ER and the ER-PM contact sites may be affected by other endogenous and exogenous factors. Possible endogenous factors include growth, health status, signaling, or other tethering proteins; exogenous factors include pathogens, osmotic stress, wounding, or mechanical stimuli. This may also explain the conflicting results that the ER network may be found to be either collapsed or intact in *SYT1* null mutant as described in previous studies (Levy et al., 2015; Perez-Sancho et al., 2015). Recently, different types of proteins localized on the ER-PM contact sites have also been discovered in yeast and human (Gatta et al., 2015; Henne et al., 2015). Further

studies on ER-PM anchor proteins in plants will help to reveal the complexity of ER-PM interactions.

This study has demonstrated that the fluorescence recovery of VAP27-1-YFP after photobleaching on the ER-PM contact sites is enhanced in *SYT1* null mutant. Such enhancement is restored after treated with the actin-depolymerizing drug latrunculin B. However, latrunculin B treatment only slightly affect the recovery of VAP27-1 in Col-0 background. Depolymerization of microtubule by oryzalin treatment increases the recovery of VAP27-1 in Col-0 background. This result is consistent with the previous results showing that microtubule stabilizes the VAP27-1 by direct physical interaction (Wang et al., 2014). However, oryzalin treatment has no significant effect on the dynamic of VAP27-1 in *SYT1* mutant. This indicates that the increased motile fraction of VAP27-1 resulted from *SYT1* mutation is actin-dependent. ER dynamics can be categorized into two types: i) directional ER remodeling and ii) diffusive movement. Directional ER remodeling is an actomyosin-based movement, which is hindered by latrunculin B treatment but not by oryzalin treatment (Griffing et al., 2014; Runions et al., 2006). The enhanced recovery of VAP27-1 couples with the enhanced ER remodeling in *SYT1* mutant. Therefore, it can be inferred that Arabidopsis *SYT1* restrains the ER remodeling by ER-PM tethering and stabilizes the VECSs without a direct interaction with VAP27-1.

4.1.3. ER-PM Contact Sites and Vesicle Trafficking

Roles of ER-PM contact sites in membrane trafficking have been documented recently. In yeast, the spatial distribution of the cortical ER in close contact with the PM regulates the endocytic and exocytic events by steric hindrance for vesicle formation and delivery (Stradalova et al., 2012). Furthermore, several enzymes and ion channels localized on ER-PM contact sites can also modulate the recognition sites of receptors and PIP content on the PM. For example, the internalization of ligand-bound ephrin (Eph) receptors and interferon receptor (IFNAR1) are regulated by the ER-anchored protein tyrosine phosphatase 1B (PTP1B) on ER-PM contact sites in human cells (Carbone et al., 2012; Nievergall et al., 2010). The ER-localized PIP phosphatase Sac1 together with VAP and oxysterol-binding protein related proteins (ORPs) regulates phosphatidylinositol 4-phosphate (PI4P) pools, a signaling molecule controlling the secretion and endocytic recycling, at ER-PM contact sites (Hammond et al., 2012; Short, 2015; Stefan et al., 2011). E-SYT1, VAP-A and the phosphatidylinositol-transfer protein Nir2 together regulate the replenishment of PM phosphatidylinositol 4,5-bisphosphate (PI(4,5)P₂), which play important roles in endocytosis and PM-actin interaction (Chang et al., 2013; Di Paolo and De Camilli, 2006). In addition, the E-SYT1-mediated contact sites, and the activity of voltage-gated Ca²⁺ channels, which can be inhibited by STIM1, have also been proposed to regulate the neurotransmission (Fernández-Busnadiego et al., 2015; Park et al., 2010; Stefan et al., 2013).

A previous study has shown that the formation of PM-derived endosomes is inhibited by the expression of truncated SYT1 lacking the C2B domain in *N.*

benthamiana leaf cells (Lewis and Lazarowitz, 2010). This study demonstrates that the accumulation of BFA compartments is attenuated in the root cells of *SYT1* null mutant. BFA treatment inhibits the endosomal recycling to the PM by targeting GNOM, an ADP-ribosylation factor-guanine nucleotide exchange factor (ARF-GEF), which mediates vesicle budding process in Arabidopsis roots (Beck et al., 2012; Naramoto et al., 2014). The BFA compartments, visualized by the fluorescent endocytic tracer FM4-64, consist of the FM dye-stained early endosomes and trans-Golgi networks. The reduced BFA compartments sizes may represent reduced endocytosis or less fusion of the early endosomes. In addition, the expression of SYT1-GFP driven by native *SYT1* promoter in tobacco leaves shows various patterns and sizes of the SECSs on the cell cortex. The immunofluorescent labeling of SYT1 in the root cells also shows that the SECS may occupy large area of the cell cortex. The ER-PM contact sites in nerve cells also display different forms and shapes: the ER-PM junctions show discrete punctate patterns at the synapses, whereas the width of the ER-PM contact area can extend up to 2 to 4 μm in other regions of the neurons (Hayashi et al., 2008; Rosenbluth, 1962; Stefan et al., 2013). Moreover, it has been shown that the sizes of the SECSs are increased by thigmostimuli (Perez-Sancho et al., 2015). The ER-endosome contact sites and the integrity of ER network have also been shown to regulate the endosome fission, endosome dynamics, and endocytosis (Rowland et al., 2014; Stefano et al., 2015). All these data suggest that Arabidopsis SYT1 play a role in vesicle trafficking by maintaining the ER stability and by regulating the extent of ER-PM contact sites.

4.2. Arabidopsis SVL

4.2.1. Physiological Functions of Arabidopsis SVL

The phylogenetic analysis shows that the division of SV2 and SV2-like proteins occurred prior to the divergence of eukaryotes into unikonts (animals, fungi, Choanozoa and Amoebozoa) and bikonts (plants, chromists and all other protozoa). SV2 proteins are preserved only in vertebrate animals while other eukaryotes lost the gene in evolution. It is unclear how these neuron-specific genes, loss of which produces lethal phenotype in mice, exist only in vertebrates but not in other invertebrates. SV2-like proteins are conserved in all eukaryotes and are abundant on the synaptic vesicles in mammals. Unlike SV2, SV2-like proteins are not glycosylated (Janz et al., 1998). The function of *SV2-like* in eukaryotes is still unknown. The promoter:GUS reporter assay in this study shows that the expression of Arabidopsis *SV2-like* is restricted in the root tips and the hypocotyls at germination and early growing stages. The expression of Arabidopsis *SV2-like* increases over time and spreads through the whole roots and leaves at later seedling stage (4 to 7 days after germination). This pattern is similar to that of *Xenopus SVOP/SV2-like* gene, whose expression also increases over time in the developing nervous system (Logan et al., 2005). The promoter activity of Arabidopsis SV2-like seems to be regulated by the salt stress in our preliminary data; however, all these data should be confirmed by RT-PCR in the future. Even though the SVL null mutant *svl-1* seems to grow faster at the early seedling stage (2 to 5 days after germination) in the control and salt stress conditions, no consistent and convincing results had been obtained. The phenotype of SVL mutants and the physiological function of SVL gene in

Arabidopsis remain to be clarified.

4.2.2. Subcellular Localization of Arabidopsis SVL

No evidence of the subcellular localization of Arabidopsis SVL has been published. This study demonstrates that Arabidopsis SVL is mainly localized on the TGN/EE using live-cell imaging of fluorescently tagged SVL in tobacco leaf cells and Arabidopsis root cells. The genomic sequence including the promoter of *SVL* was used in the expression vectors. The TGN/EE is a dynamic and complicated organelle that carries a variety of cargos from the endocytic and biosynthetic pathways. The TGN/EE receives the materials from the Golgi and the PM, and transports the materials to the MVBs or to the PM depending on the sorting processes. Many protein components are involved in the sorting and targeting processes, including receptors, adaptor proteins, clathrins, soluble-*N*-ethylmaleimide sensitive factor attachment protein receptor (SNAREs), and Rat sarcoma (Ras)-related proteins in brain (Rab) GTPases (Rutherford and Moore, 2002). This study shows that Arabidopsis SVL is largely co-localized with VTI12, a vesicle-associated SNARE protein mostly localized to the TGN in plant cells (Reyes et al., 2011). VTI12 is shown to be involved in the transport of vacuolar storage proteins to the vacuoles (Sanmartín et al., 2007) and *VTI12* mutants display accelerated leaf senescence under starvation conditions (Surpin et al., 2003). This phenotype is connected with the possible function of animal *SVOP* in aging, even though *SVOP* knockout mice show normal aging phenotype (Yao et al., 2013). This study also shows that Arabidopsis SVL is not localized to the clathrin-coated vesicles, indicating that the trafficking of SVL vesicles is clathrin-independent.

This result also supports the idea that VT112 is involved in the clathrin-independent pathway (Sanmartín et al., 2007).

Rha1/RabF2a belongs to the conventional Rab5-related GTPase which mediate the trafficking of soluble cargo from the PVC/MVB/LE to the lytic vacuole (Sohn et al., 2003). On the other hand, Ara6/RabF1 is a plant-unique Rab5-related GTPase which play a role in the trafficking from the PVC/MVB/LE to the PM (Ebine et al., 2012; Tsutsui et al., 2015). Rha1 and Ara6 are localized on distinct populations of PVC/MVB/LE with large overlap (Ebine et al., 2011). This study shows that Arabidopsis SVL partly co-localizes with Ara6, but does not overlap with Rha1 and the LE marker FYVE. In addition, Arabidopsis SVL is also partly co-localized with EE/RE marker RabA1e (Asaoka et al., 2013; Bar et al., 2013). Taken together, these data suggest that Arabidopsis SVL may play a role in the vesicle transport from endosomes to the PM.

5. Conclusions

This work addresses the spatial relationships between Arabidopsis SYT1, VAP27-1 and the cytoskeletons on the cell cortex, and the functional relevance of Arabidopsis SYT1 in ER dynamics and vesicle trafficking. By live-cell imaging, immunocytochemistry, and immunogold labeling, SYT1 and VAP27-1 are shown to be localized on distinct ER-PM contact sites. VAP27-1 is always in contact with SYT1 and often associated with microtubules, but SYT1 is often excluded by microtubules on the cell cortex and often arranged along thick actin filaments. Amino acid substitutions demonstrate that VAP27-1 mutant protein has no dominant-negative effect on the SYT1 anchoring to the PM, and the mutation on the C2A domain of SYT1 does not prevent SYT1 from accumulating on the ER-PM contact sites. Using transient and stable transformation of VAP27-1 in Arabidopsis, SYT1 is shown to be essential for maintaining the stability of ER network and the ER-PM contact sites. The dynamic of VAP27-1 on the ER-PM contact sites is restrained by microtubule through direct interaction and by SYT1 through indirect interaction. Time-course imaging shows that SYT1 influences the distribution of early endosomes on the cell cortex. Finally, by fluorescent endocytic dye FM4-64 staining and BFA treatment, the vesicle trafficking is shown to be attenuated in the lack of *SYT1*. In summary, this study shows that Arabidopsis SYT1 is critical for tethering the ER to the PM and plays roles in regulating the ER remodeling, VAP27-1-located ER-PM contact sites, and vesicle trafficking.

This study also shows that Arabidopsis SVL-GFP is mainly associated with the VTI12-labelled TGN and partly co-localized with the Ara6-labelled MVBs and RabA1e-labelled REs. Arabidopsis SVL-GFP is not overlapped with

the CLC-labelled EEs and the FYVE- and Rha1-labelled LEs. In addition, Arabidopsis SVL-GFP is incorporated into the BFA compartments but not the wortmannin-induced compartments in root cells. Taken together, Arabidopsis SV2-like is localized to a specific population of the TGN/EE that may participate in regulating the vesicle trafficking to the PM. Furthermore, the activity of *SVL* promoter is developmental-stage-dependent; however, the *SVL* null mutant shows no obvious phenotype. These characteristics of Arabidopsis *SVL* resemble that of mammalian *SVOP*. The function of *SV2-like* family in eukaryotes still remains mysterious and requires further investigation.

This study aimed at investigating functions of synaptic vesicle proteins in plants and, in turn, proving the existence of neurotransmission in plants. This research has discovered that Arabidopsis SYT1 bear functional similarities with E-SYTs in animals instead of SYTs. In both plants and animals, SV2-like proteins, whose physiological functions remain unknown, are located on vesicles. It still remains unknown how plants convert electric signals into chemical signals.

6. References

- Altschul, S.F., Madden, T.L., Schaffer, A.A., Zhang, J., Zhang, Z., Miller, W., and Lipman, D.J. (1997). Gapped BLAST and PSI-BLAST: a new generation of protein database search programs. *Nucl Acid Res* 25:3389-3402.
- Amarilio, R., Ramachandran, S., Sabanay, H., and Lev, S. (2005). Differential regulation of endoplasmic reticulum structure through VAP-Nir protein interaction. *J Biol Chem* 280:5934-5944.
- Asaoka, R., Uemura, T., Ito, J., Fujimoto, M., Ito, E., Ueda, T., and Nakano, A. (2013). Arabidopsis RABA1 GTPases are involved in transport between the trans-Golgi network and the plasma membrane, and are required for salinity stress tolerance. *Plant J* 73:240-249.
- Bacaj, T., Wu, D., Burré, J., Malenka, R.C., Liu, X., and Südhof, T.C. (2015). Synaptotagmin-1 and -7 are redundantly essential for maintaining the capacity of the readily-releasable pool of synaptic vesicles. *PLoS Biol* 13:e1002267.
- Bar, M., Leibman, M., Schuster, S., Pitzhadza, H., and Avni, A. (2013). EHD1 functions in endosomal recycling and confers salt tolerance. *PloS ONE* 8:e54533.
- Barajas, D., Xu, K., de Castro Martín, I.F., Sasvari, Z., Brandizzi, F., Risco, C., and Nagy, P.D. (2014). Co-opted Oxysterol-Binding ORP and VAP proteins channel sterols to RNA virus replication sites via membrane contact sites. *PLoS Pathog* 10:e1004388.
- Bashline, L., Li, S., Anderson, C.T., Lei, L., and Gu, Y. (2013). The Endocytosis of cellulose synthase in Arabidopsis is dependent on μ 2, a clathrin-mediated endocytosis adaptin. *Plant Physiol* 163:150-160.
- Batoko, H., Zheng, H.-Q., Hawes, C., and Moore, I. (2000). A Rab1 GTPase is required for transport between the endoplasmic reticulum and Golgi apparatus and for normal Golgi movement in plants. *Plant Cell* 12:2201-2217.
- Beck, M., Zhou, J., Faulkner, C., MacLean, D., and Robatzek, S. (2012). Spatio-temporal cellular dynamics of the Arabidopsis flagellin receptor reveal activation status-dependent endosomal sorting. *Plant Cell* 24:4205-4219.
- Berson, T., von Wangenheim, D., Takáč, T., Šamajová, O., Rosero, A., Ovečka, M., Komis, G., Stelzer, E.H.K., and Šamaj, J. (2014). Trans-Golgi

- network localized small GTPase RabA1d is involved in cell plate formation and oscillatory root hair growth. *BMC Plant Biol* 14:252.
- Bolte, S., Talbot, C., Boutte, Y., Catrice, O., Read, N.D., and Satiat-Jeunemaitre, B. (2004). FM-dyes as experimental probes for dissecting vesicle trafficking in living plant cells. *J Microsc* 214:159-173.
- Brandizzi, F., Frangne, N., Marc-Martin, S., Hawes, C., Neuhaus, J.M., and Paris, N. (2002). The destination for single-pass membrane proteins is influenced markedly by the length of the hydrophobic domain. *Plant Cell* 14:1077-1092.
- Carbone, C.J., Zheng, H., Bhattacharya, S., Lewis, J.R., Reiter, A.M., Henthorn, P., Zhang, Z.Y., Baker, D.P., Ukkiramapandian, R., Bence, K.K., et al. (2012). Protein tyrosine phosphatase 1B is a key regulator of IFNAR1 endocytosis and a target for antiviral therapies. *Proc Natl Acad Sci USA* 109:19226-19231.
- Chang, C.L., Hsieh, T.S., Yang, T.T., Rothberg, K.G., Azizoglu, D.B., Volk, E., Liao, J.C., and Liou, J. (2013). Feedback regulation of receptor-induced Ca²⁺ signaling mediated by E-Syt1 and Nir2 at endoplasmic reticulum-plasma membrane junctions. *Cell Rep* 5:813-825.
- Clough, S.J., and Bent, A.F. (1998). Floral dip: a simplified method for *Agrobacterium*-mediated transformation of *Arabidopsis thaliana*. *Plant J* 16:735-743.
- Contento, A.L., and Bassham, D.C. (2012). Structure and function of endosomes in plant cells. *J Cell Sci* 125:3511-3518.
- Craxton, M. (2004). Synaptotagmin gene content of the sequenced genomes. *BMC Genom* 5:1-14.
- Craxton, M. (2010). A manual collection of Syt, Esyt, Rph3a, Rph3al, Doc2, and Dblc2 genes from 46 metazoan genomes - an open access resource for neuroscience and evolutionary biology. *BMC Genom*. 37.
- Crowder, K.M., Gunther, J.M., Jones, T.A., Hale, B.D., Zhang, H.Z., Peterson, M.R., Scheller, R.H., Chavkin, C., and Bajjalieh, S.M. (1999). Abnormal neurotransmission in mice lacking synaptic vesicle protein 2A (SV2A). *Proc Natl Acad Sci USA* 96:15268-15273.
- Curtis, M.D., and Grossniklaus, U. (2003). A gateway cloning vector set for high-throughput functional analysis of genes in planta. *Plant Physiol* 133:462-469.
- Deeks, M.J., Calcutt, J.R., Ingle, E.K.S., Hawkins, T.J., Chapman, S., Richardson, A.C., Mentlak, D.A., Dixon, M.R., Cartwright, F., Smertenko, A.P., et al. (2012). A superfamily of actin-binding proteins at the

- actin-membrane nexus of higher plants. *Curr Biol* 22:1595-1600.
- Derelle, R., Torruella, G., Klimeš, V., Brinkmann, H., Kim, E., Vlček, Č., Lang, B.F., and Eliáš, M. (2015). Bacterial proteins pinpoint a single eukaryotic root. *Proc Natl Acad Sci USA* 112:E693-E699.
- Di Paolo, G., and De Camilli, P. (2006). Phosphoinositides in cell regulation and membrane dynamics. *Nature* 443:651-657.
- Dong, M., Yeh, F., Tepp, W.H., Dean, C., Johnson, E.A., Janz, R., and Chapman, E.R. (2006). SV2 is the protein receptor for botulinum neurotoxin A. *Science* 312:592-596.
- Ebine, K., Fujimoto, M., Okatani, Y., Nishiyama, T., Goh, T., Ito, E., Dainobu, T., Nishitani, A., Uemura, T., Sato, M.H., et al. (2011). A membrane trafficking pathway regulated by the plant-specific RAB GTPase ARA6. *Nat Cell Biol* 13:853-859.
- Ebine, K., Miyakawa, N., Fujimoto, M., Uemura, T., Nakano, A., and Ueda, T. (2012). Endosomal trafficking pathway regulated by ARA6, a RAB5 GTPase unique to plants. *Small GTPases* 3:23-27.
- Feany, M.B., Lee, S., Edwards, R.H., and Buckley, K.M. (1992). The synaptic vesicle protein SV2 is a novel type of transmembrane transporter. *Cell* 70:861-867.
- Fernández-Busnadiego, R., Saheki, Y., and De Camilli, P. (2015). Three-dimensional architecture of extended synaptotagmin-mediated endoplasmic reticulum–plasma membrane contact sites. *Proc Natl Acad Sci USA* 112:E2004-E2013.
- Friedman, J.R., and Voeltz, G.K. (2011). The ER in 3D: a multifunctional dynamic membrane network. *Trends Cell Biol* 21:709-717.
- Fukuda, M., Ibata, K., and Mikoshiba, K. (2001). A unique spacer domain of synaptotagmin IV is essential for Golgi localization. *J Neurochem* 77:730-740.
- Garbino, A., van Oort, R.J., Dixit, S.S., Landstrom, A.P., Ackerman, M.J., and Wehrens, X.H.T. (2009). Molecular evolution of the junctophilin gene family. *Physiol Genom* 37:175-186.
- Gatta, A.T., Wong, L.H., Sere, Y.Y., Calderón-Noreña, D.M., Cockcroft, S., Menon, A.K., and Levine, T.P. (2015). A new family of StART domain proteins at membrane contact sites has a role in ER-PM sterol transport. *eLife* 4:e07253.
- Geldner, N., Dénervaud-Tendon, V., Hyman, D.L., Mayer, U., Stierhof, Y.-D., and Chory, J. (2009). Rapid, combinatorial analysis of membrane compartments in intact plants with a multicolor marker set. *Plant J*

59:169-178.

- Geppert, M., Goda, Y., Hammer, R.E., Li, C., Rosahl, T.W., Stevens, C.F., and Südhof, T.C. (1994). Synaptotagmin I: a major Ca^{2+} sensor for transmitter release at a central synapse. *Cell* 79:717-727.
- Giordano, F., Saheki, Y., Idevall-Hagren, O., Colombo, S.F., Pirruccello, M., Milosevic, I., Gracheva, E.O., Bagriantsev, S.N., Borgese, N., and De Camilli, P. (2013). PI(4,5)P(2)-dependent and Ca^{2+} -regulated ER-PM interactions mediated by the extended synaptotagmins. *Cell* 153:1494-1509.
- Granger, C.L., and Cyr, R.J. (2001). Spatiotemporal relationships between growth and microtubule orientation as revealed in living root cells of *Arabidopsis thaliana* transformed with green-fluorescent-protein gene construct GFP-MBD. *Protoplasma* 216:201-214.
- Graumann, K., Irons, S.L., Runions, J., and Evans, D.E. (2007). Retention and mobility of the mammalian lamin B receptor in the plant nuclear envelope. *Biol Cell* 99:553-562.
- Griffing, L.R., Gao, H.T., and Sparkes, I. (2014). ER network dynamics are differentially controlled by myosins XI-K, XI-C, XI-E, XI-I, XI-1, and XI-2. *Front Plant Sci* 5:218.
- Gustavsson, N., Wei, S.-H., Hoang, D.N., Lao, Y., Zhang, Q., Radda, G.K., Rorsman, P., Südhof, T.C., and Han, W. (2009). Synaptotagmin-7 is a principal Ca^{2+} sensor for Ca^{2+} -induced glucagon exocytosis in pancreas. *J Physiol* 587:1169-1178.
- Hammond, G.R.V., Fischer, M.J., Anderson, K.E., Holdich, J., Koteci, A., Balla, T., and Irvine, R.F. (2012). PI4P and PI(4,5)P2 are essential but independent lipid determinants of membrane identity. *Science* 337:727-730.
- Han, S.M., Tsuda, H., Yang, Y., Vibbert, J., Cottee, P., Lee, S.-J., Winek, J., Haueter, C., Bellen, H.J., and Miller, M.A. (2012). Secreted VAPB/ALS8 major sperm protein domains modulate mitochondrial localization and morphology via growth cone guidance receptors. *Dev Cell* 22:348-362.
- Hawkins, T.J., Deeks, M.J., Wang, P., and Hussey, P.J. (2014). The evolution of the actin binding NET superfamily. *Front Plant Sci* 5:254.
- Hayashi, M., Raimondi, A., O'Toole, E., Paradise, S., Collesi, C., Cremona, O., Ferguson, S.M., and De Camilli, P. (2008). Cell- and stimulus-dependent heterogeneity of synaptic vesicle endocytic recycling mechanisms revealed by studies of dynamin 1-null neurons. *Proc Natl Acad Sci USA* 105:2175-2180.

- Helle, S.C.J., Kanfer, G., Kolar, K., Lang, A., Michel, A.H., and Kornmann, B. (2013). Organization and function of membrane contact sites. *Biochim Biophys* 1833:2526-2541.
- Henne, W.M., Liou, J., and Emr, S.D. (2015). Molecular mechanisms of inter-organelle ER–PM contact sites. *Curr Opin Cell Biol* 35:123-130.
- Herdman, C., Tremblay, M.G., Mishra, P.K., and Moss, T. (2014). Loss of Extended Synaptotagmins ESyt2 and ESyt3 does not affect mouse development or viability, but in vitro cell migration and survival under stress are affected. *Cell Cycle* 13:2616-2625.
- Ho, S.N., Hunt, H.D., Horton, R.M., Pullen, J.K., and Pease, L.R. (1989). Site-directed mutagenesis by overlap extension using the polymerase chain reaction. *Gene* 77:51-59.
- Hong, M.-G., Myers, A.J., Magnusson, P.K.E., and Prince, J.A. (2008). Transcriptome-wide assessment of human brain and lymphocyte senescence. *PloS ONE* 3:e3024.
- Jahn, R. (2006). A neuronal receptor for botulinum toxin. *Science* 312:540-541.
- Janz, R., Hofmann, K., and Südhof, T.C. (1998). SVOP, an evolutionarily conserved synaptic vesicle protein, suggests novel transport functions of synaptic vesicles. *J Neurosci* 18:9269-9281.
- Janz, R., and Südhof, T.C. (1999). SV2C is a synaptic vesicle protein with an unusually restricted localization: anatomy of a synaptic vesicle protein family. *Neuroscience* 94:1279-1290.
- Jeanguenin, L., Lara-Núñez, A., Rodionov, D.A., Osterman, A.L., Komarova, N.Y., Rentsch, D., Gregory, J.F., and Hanson, A.D. (2011). Comparative genomics and functional analysis of the NiaP family uncover nicotinate transporters from bacteria, plants, and mammals. *Funct Integr Genom* 12:25-34.
- Jin, X., Shah, S., Du, X., Zhang, H., and Gamper, N. (2016). Activation of Ca^{2+} -activated Cl^- channel ANO1 by localized Ca^{2+} signals. *J Physiol* 594:19-30.
- Katoh, K., and Standley, D.M. (2013). MAFFT multiple sequence alignment software version 7: improvements in performance and usability. *Mol Biol Evol* 30:772-780.
- Kawamura, Y., and Uemura, M. (2003). Mass spectrometric approach for identifying putative plasma membrane proteins of Arabidopsis leaves associated with cold acclimation. *Plant J* 36:141-154.
- Kopec, K.O., Alva, V., and Lupas, A.N. (2010). Homology of SMP domains to the TULIP superfamily of lipid-binding proteins provides a structural

- basis for lipid exchange between ER and mitochondria. *Bioinformatics* 26:1927-1931.
- Kotzer, A.M., Brandizzi, F., Neumann, U., Paris, N., Moore, I., and Hawes, C. (2004). AtRabF2b (Ara7) acts on the vacuolar trafficking pathway in tobacco leaf epidermal cells. *J Cell Sci* 117:6377-6389.
- Ku, C., Nelson-Sathi, S., Roettger, M., Sousa, F.L., Lockhart, P.J., Bryant, D., Hazkani-Covo, E., McInerney, J.O., Landan, G., and Martin, W.F. (2015). Endosymbiotic origin and differential loss of eukaryotic genes. *Nature* 524:427-432.
- Lee, H., Sparkes, I., Gattolin, S., Dzimitrowicz, N., Roberts, L.M., Hawes, C., and Frigerio, L. (2013). An Arabidopsis reticulon and the atlastin homologue RHD3-like2 act together in shaping the tubular endoplasmic reticulum. *New Phytol* 197:481-489.
- Lee, J., and Littleton, J.T. (2015). Transmembrane tethering of synaptotagmin to synaptic vesicles controls multiple modes of neurotransmitter release. *Proc Natl Acad Sci USA* 112:3793-3798.
- Levy, A., Zheng, J.Y., and Lazarowitz, S.G. (2015). Synaptotagmin SYTA forms ER-plasma membrane junctions that are recruited to plasmodesmata for plant virus movement. *Curr Biol* 25:2018-2025.
- Lewis, J.D., and Lazarowitz, S.G. (2010). Arabidopsis synaptotagmin SYTA regulates endocytosis and virus movement protein cell-to-cell transport. *Proc Natl Acad Sci USA* 107:2491-2496.
- Lin, C.-C., Seikowski, J., Pérez-Lara, A., Jahn, R., Höbartner, C., and Walla, P.J. (2014). Control of membrane gaps by synaptotagmin-Ca²⁺ measured with a novel membrane distance ruler. *Nat Commun* 5:5859.
- Liou, J., Fivaz, M., Inoue, T., and Meyer, T. (2007). Live-cell imaging reveals sequential oligomerization and local plasma membrane targeting of stromal interaction molecule 1 after Ca²⁺ store depletion. *Proc Natl Acad Sci USA* 104:9301-9306.
- Liu, H., Bai, H., Xue, R., Takahashi, H., Edwardson, J.M., and Chapman, E.R. (2014). Linker mutations reveal the complexity of synaptotagmin 1 action during synaptic transmission. *Nat Neurosci* 17:670-677.
- Logan, M.A., Steele, M.R., and Vetter, M.L. (2005). Expression of synaptic vesicle two-related protein SVOP in the developing nervous system of *Xenopus laevis*. *Dev Dynam* 234:802-807.
- Lynch, B.A., Lambeng, N., Nocka, K., Kensel-Hammes, P., Bajjalieh, S.M., Matagne, A., and Fuks, B. (2004). The synaptic vesicle protein SV2A is the binding site for the antiepileptic drug levetiracetam. *Proc Natl Acad*

- Sci USA 101:9861-9866.
- Mackler, J.M., Drummond, J.A., Loewen, C.A., Robinson, I.M., and Reist, N.E. (2002). The C2B Ca²⁺-binding motif of synaptotagmin is required for synaptic transmission in vivo. *Nature* 418:340-344.
- Madeo, M., Kovács, A.D., and Pearce, D.A. (2014). The human synaptic vesicle protein, SV2A, functions as a galactose transporter in *Saccharomyces cerevisiae*. *J Biol Chem* 289:33066-33071.
- Marc, J., Granger, C.L., Brincat, J., Fisher, D.D., Kao, T.-h., McCubbin, A.G., and Cyr, R.J. (1998). A GFP–MAP4 reporter gene for visualizing cortical microtubule rearrangements in living epidermal cells. *Plant Cell* 10:1927-1939.
- Mehrshahi, P., Stefano, G., Andaloro, J.M., Brandizzi, F., Froehlich, J.E., and DellaPenna, D. (2013). Transorganellar complementation redefines the biochemical continuity of endoplasmic reticulum and chloroplasts. *Proc Natl Acad Sci USA* 110:12126-12131.
- Min, S.W., Chang, W.P., and Südhof, T.C. (2007). E-Syts, a family of membranous Ca²⁺-sensor proteins with multiple C2 domains. *Proc Natl Acad Sci USA* 104:3823-3828.
- Moghadam, P.K., and Jackson, M.B. (2013). The functional significance of synaptotagmin diversity in neuroendocrine secretion. *Front Endocrinol* 4:124.
- Moriishi, K., and Matsuura, Y. (2012). Exploitation of lipid components by viral and host proteins for hepatitis C virus infection. *Front Microbiol* 3:54.
- Nalefski, E.A., and Falke, J.J. (1996). The C2 domain calcium-binding motif: structural and functional diversity. *Protein Sci* 5:2375-2390.
- Naramoto, S., Otegui, M.S., Kutsuna, N., de Rycke, R., Dainobu, T., Karampelias, M., Fujimoto, M., Feraru, E., Miki, D., Fukuda, H., et al. (2014). Insights into the localization and function of the membrane trafficking regulator GNOM ARF-GEF at the Golgi apparatus in *Arabidopsis*. *Plant Cell* 26:3062-3076.
- Nievergall, E., Janes, P.W., Stegmayer, C., Vail, M.E., Haj, F.G., Teng, S.W., Neel, B.G., Bastiaens, P.I., and Lackmann, M. (2010). PTP1B regulates Eph receptor function and trafficking. *J Cell Biol* 191:1189-1203.
- Park, C.Y., Shcheglovitov, A., and Dolmetsch, R. (2010). The CRAC channel activator STIM1 binds and inhibits L-type voltage-gated calcium channels. *Science* 330:101-105.
- Perez-Sancho, J., Vanneste, S., Lee, E., McFarlane, H.E., Esteban Del Valle, A., Valpuesta, V., Friml, J., Botella, M.A., and Rosado, A. (2015). The

- Arabidopsis synaptotagmin1 is enriched in endoplasmic reticulum-plasma membrane contact sites and confers cellular resistance to mechanical stresses. *Plant Physiol* 168:132-143.
- Porter, K.R., and Palade, G.E. (1957). Studies on the endoplasmic reticulum. III. Its form and distribution in striated muscle cells. *J Biophys Biochem Cytol* 3:269-300.
- Prinz, W.A. (2014). Bridging the gap: membrane contact sites in signaling, metabolism, and organelle dynamics. *J Cell Biol* 205:759-769.
- Pruitt, K.D., Tatusova, T., and Maglott, D.R. (2005). NCBI Reference Sequence (RefSeq): a curated non-redundant sequence database of genomes, transcripts and proteins. *Nucl Acid Res* 33:D501-D504.
- Renna, L., Hanton, S.L., Stefano, G., Bortolotti, L., Misra, V., and Brandizzi, F. (2005). Identification and characterization of AtCASP, a plant transmembrane Golgi matrix protein. *Plant Mol Biol* 58:109-122.
- Reyes, F.C., Buono, R., and Otegui, M.S. (2011). Plant endosomal trafficking pathways. *Curr Opin Plant Biol* 14:666-673.
- Rizzoli, S.O. (2014). Synaptic vesicle recycling: steps and principles. *EMBO J* 33:788-822.
- Robinson, D.G., and Pimpl, P. (2014). Clathrin and post-Golgi trafficking: a very complicated issue. *Trends Plant Sci* 19:134-139.
- Rosenbluth, J. (1962). Subsurface cisterns and their relationship to the neuronal plasma membrane. *J Cell Biol* 13:405-421.
- Rowland, A.A., Chitwood, P.J., Phillips, M.J., and Voeltz, G.K. (2014). ER contact sites define the position and timing of endosome fission. *Cell* 159:1027-1041.
- Runions, J., Brach, T., Kuhner, S., and Hawes, C. (2006). Photoactivation of GFP reveals protein dynamics within the endoplasmic reticulum membrane. *J Exp Bot* 57:43-50.
- Rutherford, S., and Moore, I. (2002). The Arabidopsis Rab GTPase family: another enigma variation. *Curr Opin Plant Biol* 5:518-528.
- Sanmartín, M., Ordóñez, A., Sohn, E.J., Robert, S., Sánchez-Serrano, J.J., Surpin, M.A., Raikhel, N.V., and Rojo, E. (2007). Divergent functions of VTI12 and VTI11 in trafficking to storage and lytic vacuoles in Arabidopsis. *Proc Natl Acad Sci USA* 104:3645-3650.
- Saraswati, S., Adolfsen, B., and Littleton, J.T. (2007). Characterization of the role of the Synaptotagmin family as calcium sensors in facilitation and asynchronous neurotransmitter release. *Proc Natl Acad Sci USA* 104:14122-14127.

- Saravanan, R.S., Slabaugh, E., Singh, V.R., Lapidus, L.J., Haas, T., and Brandizzi, F. (2009). The targeting of the oxysterol-binding protein ORP3a to the endoplasmic reticulum relies on the plant VAP33 homolog PVA12. *Plant J* 58:817-830.
- Schapiro, A.L., Voigt, B., Jasik, J., Rosado, A., Lopez-Cobollo, R., Menzel, D., Salinas, J., Mancuso, S., Valpuesta, V., Baluska, F., et al. (2008). *Arabidopsis* synaptotagmin 1 is required for the maintenance of plasma membrane integrity and cell viability. *Plant Cell* 20:3374-3388.
- Schauder, C.M., Wu, X., Saheki, Y., Narayanaswamy, P., Torta, F., Wenk, M.R., De Camilli, P., and Reinisch, K.M. (2014). Structure of a lipid-bound extended synaptotagmin indicates a role in lipid transfer. *Nature* 510:552-555.
- Schivell, A.E., Batchelor, R.H., and Bajjalieh, S.M. (1996). Isoform-specific, calcium-regulated interaction of the synaptic vesicle proteins SV2 and synaptotagmin. *J Biol Chem* 271:27770-27775.
- Schoberer, J., Runions, J., Steinkellner, H., Strasser, R., Hawes, C., and Osterrieder, A. (2010). Sequential depletion and acquisition of proteins during Golgi stack disassembly and reformation. *Traffic* 11:1429-1444.
- Schulz, T.A., and Creutz, C.E. (2004). The tricalbin C2 domains: lipid-binding properties of a novel, synaptotagmin-like yeast protein family. *Biochemistry* 43:3987-3995.
- Sharpe, H.J., Stevens, T.J., and Munro, S. (2010). A comprehensive comparison of transmembrane domains reveals organelle-specific properties. *Cell* 142:158-169.
- Short, B. (2015). PI(4)P gets Sac-rificed in the name of endocytic recycling. *J Cell Biol* 209:3.
- Sohn, E.J., Kim, E.S., Zhao, M., Kim, S.J., Kim, H., Kim, Y.-W., Lee, Y.J., Hillmer, S., Sohn, U., Jiang, L., et al. (2003). Rha1, an *Arabidopsis* Rab5 homolog, plays a critical role in the vacuolar trafficking of soluble cargo proteins. *Plant Cell* 15:1057-1070.
- Sparkes, I.A., Runions, J., Kearns, A., and Hawes, C. (2006). Rapid, transient expression of fluorescent fusion proteins in tobacco plants and generation of stably transformed plants. *Nat Protocols* 1:2019-2025.
- Stamatakis, A. (2006). RAxML-VI-HPC: maximum likelihood-based phylogenetic analyses with thousands of taxa and mixed models. *Bioinformatics* 22:2688-2690.
- Stathopoulos, P.B., Li, G.-Y., Plevin, M.J., Ames, J.B., and Ikura, M. (2006). Stored Ca²⁺ Depletion-induced Oligomerization of Stromal Interaction

- Molecule 1 (STIM1) via the EF-SAM Region: an initiation mechanism for capacitive Ca²⁺ entry. *J Biol Chem* 281:35855-35862.
- Stefan, C.J., Manford, A.G., Baird, D., Yamada-Hanff, J., Mao, Y., and Emr, S.D. (2011). Osh proteins regulate phosphoinositide metabolism at ER-plasma membrane contact sites. *Cell* 144:389-401.
- Stefan, C.J., Manford, A.G., and Emr, S.D. (2013). ER–PM connections: sites of information transfer and inter-organelle communication. *Curr Opin Cell Biol* 25:434-442.
- Stefano, G., Renna, L., Lai, Y., Slabaugh, E., Mannino, N., Buono, R.A., Otegui, M.S., and Brandizzi, F. (2015). ER network homeostasis is critical for plant endosome streaming and endocytosis. *Cell Discov* 1:15033.
- Stradalova, V., Blazikova, M., Grossmann, G., Opekarová, M., Tanner, W., and Malinsky, J. (2012). Distribution of cortical endoplasmic reticulum determines positioning of endocytic events in yeast plasma membrane. *PLoS ONE* 7:e35132.
- Sugita, S., Han, W., Butz, S., Liu, X., Fernández-Chacón, R., Lao, Y., and Südhof, T.C. (2001). Synaptotagmin VII as a plasma membrane Ca²⁺ sensor in exocytosis. *Neuron* 30:459-473.
- Surpin, M., Zheng, H., Morita, M.T., Saito, C., Avila, E., Blakeslee, J.J., Bandyopadhyay, A., Kovaleva, V., Carter, D., Murphy, A., et al. (2003). The VTI family of SNARE proteins is necessary for plant viability and mediates different protein transport pathways. *Plant Cell* 15:2885-2899.
- Sutter, J.-U., Campanoni, P., Blatt, M.R., and Paneque, M. (2006). Setting SNAREs in a different wood. *Traffic* 7:627-638.
- Südhof, T.C. (2002). Synaptotagmins: why so many? *J Biol Chem* 277:7629-7632.
- Südhof, T.C. (2012).. *Cold Spring Harbor Persp Biol* 4:a011353.
- Südhof, T.C. (2013). A molecular machine for neurotransmitter release: synaptotagmin and beyond. *Nat Med* 19:1227-1231.
- Takeshima, H., Komazaki, S., Nishi, M., Iino, M., and Kangawa, K. (2000). Junctophilins: a novel family of junctional membrane complex proteins. *Mol Cell* 6:11-22.
- Topping, J.F., Wei, W., and Lindsey, K. (1991). Functional tagging of regulatory elements in the plant genome. *Development* 112:1009-1019.
- Toulmay, A., and Prinz, W.A. (2012). A conserved membrane-binding domain targets proteins to organelle contact sites. *J Cell Sci* 125:49-58.
- Tsutsui, T., Nakano, A., and Ueda, T. (2015). The plant-specific RAB5 GTPase ARA6 is required for starch and sugar homeostasis in *Arabidopsis*

- thaliana*. Plant Cell Physiol 56:1073-1083.
- Uchiyama, A., Shimada-Beltran, H., Levy, A., Zheng, J.Y., Javia, P.A., and Lazarowitz, S.G. (2014). The Arabidopsis synaptotagmin SYTA regulates the cell-to-cell movement of diverse plant viruses. Front Plant Sci 5:584.
- Viotti, C., Bubeck, J., Stierhof, Y.-D., Krebs, M., Langhans, M., van den Berg, W., van Dongen, W., Richter, S., Geldner, N., Takano, J., et al. (2010). Endocytic and secretory traffic in Arabidopsis merge in the trans-Golgi network/early endosome, an independent and highly dynamic organelle. Plant Cell 22:1344-1357.
- Vogl, C., Tanifuji, S., Danis, B., Daniels, V., Foerch, P., Wolff, C., Whalley, B.J., Mochida, S., and Stephens, G.J. (2015). Synaptic vesicle glycoprotein 2A modulates vesicular release and calcium channel function at peripheral sympathetic synapses. Eur J Neurosci 41:398-409.
- Voigt, B., Timmers, A.C.J., Šamaj, J., Hlavacka, A., Ueda, T., Preuss, M., Nielsen, E., Mathur, J., Emans, N., Stenmark, H., et al. (2005a). Actin-based motility of endosomes is linked to the polar tip growth of root hairs. Eur J Cell Biol 84:609-621.
- Voigt, B., Timmers, A.C.J., Šamaj, J., Müller, J., Baluška, F., and Menzel, D. (2005b). GFP-FABD2 fusion construct allows *in vivo* visualization of the dynamic actin cytoskeleton in all cells of Arabidopsis seedlings. Eur J Cell Biol 84:595-608.
- Wang, H., Han, S., Siao, W., Song, C., Xiang, Y., Wu, X., Cheng, P., Li, H., Jasik, J., Micieta, K., et al. (2015a). Arabidopsis synaptotagmin 2 participates in pollen germination and tube growth and is delivered to plasma membrane via conventional secretion. Mol Plant 8:1737-1750.
- Wang, L., Li, H., Lv, X., Chen, T., Li, R., Xue, Y., Jiang, J., Jin, B., Baluška, F., Šamaj, J., et al. (2015b). Spatiotemporal dynamics of the BRI1 receptor and its regulation by membrane microdomains in living Arabidopsis cells. Mol Plant 8:1334-1349.
- Wang, P., Hawkins, T.J., Richardson, C., Cummins, I., Deeks, M.J., Sparkes, I., Hawes, C., and Hussey, P.J. (2014). The plant cytoskeleton, NET3C, and VAP27-1 mediate the link between the plasma membrane and endoplasmic reticulum. Curr Biol 24:1397-1405.
- Wang, P., Hummel, E., Osterrieder, A., Meyer, A.J., Frigerio, L., Sparkes, I., and Hawes, C. (2011). KMS1 and KMS2, two plant endoplasmic reticulum proteins involved in the early secretory pathway. Plant J 66:613-628.

- Wang, P., Richardson, C., Hawkins, T.J., Sparkes, I., Hawes, C., Hussey, P.J. (2016) Plant VAP27 proteins: domain characterization, intracellular localization and role in plant development. *New Phytol* in press.
- Wang, Q., Zhao, Y., Luo, W., Li, R., He, Q., Fang, X., Michele, R.D., Ast, C., von Wirén, N., and Lin, J. (2013). Single-particle analysis reveals shutoff control of the Arabidopsis ammonium transporter AMT1;3 by clustering and internalization. *Proc Natl Acad Sci USA* 110:13204-13209.
- Xu, T., and Bajjalieh, S.M. (2001). SV2 modulates the size of the readily releasable pool of secretory vesicles. *Nat Cell Biol* 3:691-698.
- Yamazaki, T., Kawamura, Y., Minami, A., and Uemura, M. (2008). Calcium-dependent freezing tolerance in Arabidopsis involves membrane resealing via synaptotagmin SYT1. *Plant Cell* 20:3389-3404.
- Yamazaki, T., Takata, N., Uemura, M., and Kawamura, Y. (2010). Arabidopsis synaptotagmin SYT1, a type I signal-anchor protein, requires tandem C2 domains for delivery to the plasma membrane. *J Biol Chem* 285:23165-23176.
- Yao, J., de la Iglesia, H.O., and Bajjalieh, S.M. (2013). Loss of the SV2-like Protein SVOP Produces No Apparent Deficits in Laboratory Mice. *PLoS ONE* 8:e68215.
- Yeh, F.L., Dong, M., Yao, J., Tepp, W.H., Lin, G., Johnson, E.A., and Chapman, E.R. (2010). SV2 mediates entry of tetanus neurotoxin into central neurons. *PLoS Pathog* 6:e1001207.
- Zhang, H., Zhang, L., Gao, B., Fan, H., Jin, J., Botella, M.A., Jiang, L., and Lin, J. (2011a). Golgi apparatus-localized synaptotagmin 2 is required for unconventional secretion in Arabidopsis. *PLoS ONE* 6:e26477.
- Zhang, X., Henriques, R., Lin, S.-S., Niu, Q.-W., and Chua, N.-H. (2006). Agrobacterium-mediated transformation of *Arabidopsis thaliana* using the floral dip method. *Nat Protocols* 1:641-646.
- Zhang, Z., Wu, Y., Wang, Z., Dunning, F.M., Rehfuss, J., Ramanan, D., Chapman, E.R., and Jackson, M.B. (2011b). Release mode of large and small dense-core vesicles specified by different synaptotagmin isoforms in PC12 cells. *Mol Biol Cell* 22:2324-2336.

7. Appendix

7.1. Abbreviation

aa	amino acid
ABD2	actin-binding domain 2
ABRC	Arabidopsis Biological Resource Center
ANO1	anoctamin 1
AP2	adaptor protein 2
AtSYT	<i>Arabidopsis thaliana</i> synaptotagmin
BAPTA-AM	1,2-Bis(2-aminophenoxy)ethane-N,N,N',N'-tetraacetic acid tetrakis(acetoxymethyl ester)
BFA	brefeldin A
BLAST	Basic Local Alignment Search Tool
BSA	bovine serum albumin
CC	coiled-coil
CFP	cyan fluorescent protein
CLC	clathrin light chain
CRAC	Ca ²⁺ release-activated Ca ²⁺
DNA	deoxyribonucleic acid
DAPI	4',6-diamidino-2-phenylindole
EDTA	Ethylenediaminetetraacetic acid
EE	early endosome
ER	endoplasmic reticulum
ERMES	ER-mitochondrion encounter structure
E-SYT	extended synaptotagmin
DMSO	dimethyl sulfoxide
FFAT	di-phenylalanine in an acidic tract
FYVE	Fab1, YOTB, Vac1, and EEA1
GFP	green fluorescent protein
GUS	β-glucuronidase
HRP	horseradish peroxidase
Ist2	increased sodium tolerance protein 2
JPH	junctionophilin
KKKK	poly-lysine patch
LatB	latrunculin B
LE	late endosome
HsSYT	<i>Homo sapiens</i> synaptotagmin

MAFFT	Multiple Alignment using Fast Fourier Transform
MAP4	microtubule-associated protein 4
MBD	microtubule-binding domain
MCS	membrane contact site
MFS	major facilitator superfamily
MORN	membrane occupation, and recognition nexus
MS	Murashige and Skoog
MSP	N-terminal major sperm protein
MTSB	microtubule stabilizing buffer
MVB	multivesicular body
NAB	NET actin-binding
NCBI	National Center for Biotechnology Information
NET3C	Networked 3C
Nir	PYK2 N-terminal domain-interacting receptors
Nvj2	nucleus–vacuole junction
ORP	OSBP-related protein
OSBP	oxysterol-binding protein
OSH	oxysterol binding homology
PBS	phosphate-buffered saline
PIP/PtdInsP	phosphoinositide
PIP2	phosphatidylinositol(4,5)-bisphosphate
PM	plasma membrane
PB	polybasic
PC	phosphatidylcholine
PCR	polymerase chain reaction
PI	phosphatidylinositol
PS	phosphatidylserine
PVC	prevacuolar compartment
PYK2	proline-rich tyrosine kinase 2
Rab	Ras-related proteins in brain
Ras	rat sarcoma
RE	recycling endosome
RFP	red fluorescent protein
Rha1	root handedness 1
RNA	ribonucleic acid
RNAi	RNA interference
RT-PCR	reverse transcription polymerase chain reaction
Sac1	phosphoinositide phosphatase

Scs2	suppressor of choline sensitivity
ScTcb	<i>Saccharomyces cerevisiae</i> Tricalbin
SECS	SYT1-enriched ER-PM contact sites
SMP	synaptotagmin-like mitochondrial and lipid-binding protein
SNARE	soluble-N-ethylmaleimide sensitive fusion factor attachment protein receptor
SOCE	store-operated Ca ²⁺ entry
SR	sarcoplasmic reticulum
ST	sialyltransferase
STIM1	stromal interaction molecule-1
SV2	synaptic vesicle protein 2
SVL	SV2-like
SVOP	SV2-related protein
SYT	synaptotagmin
TGN	trans-Golgi network
TM	transmembrane
TULIP	tubular lipid-binding
VAMP	vesicle-associated membrane protein
VAP	VAMP-associated protein
VECS	VAP27-1-enriched ER-PM contact sites
VSR	vacuolar sorting receptor
VT112	vesicle transport v-SNARE 12
YFP	yellow fluorescent protein

7.2. List of Figures

Figure 1. Protein Domains of <i>Arabidopsis thaliana</i> SYT1 (<i>AtSYT1</i>), <i>Homo sapiens</i> SYT1 (<i>HsSYT1</i>), <i>Homo sapiens</i> E-SYT1, 2 and 3 (<i>HsE-SYT1-3</i>), and <i>Saccharomyces cerevisiae</i> Tricalbin-1 and -2 (<i>ScTcb1/2</i>).	2
Figure 2. Domain Structure of Rat SYT1.....	4
Figure 3. Models of Lipid Transfer by Human E-SYT2.....	6
Figure 4. ER-PM Tethering Proteins in Mammals.....	9
Figure 5. Schematic Depiction of NET3C, VAP27-1 and Cytoskeleton on ER-PM Contact Sites.....	10

Figure 6.	Schematic Depiction of SYT1 on ER-PM Contact Sites.....	13
Figure 7.	Botulinum Neurotoxins Entry into Neurons via SV2..	14
Figure 8.	Endocytic and Exocytic Pathways in Plant Cells.	17
Figure 9.	SYT1 Unevenly Distributes on Cortical ER Elements and Forms Stable Attachments at PM of <i>N. benthamiana</i> Leaf Epidermal Cells.	31
Figure 10.	SYT1 and VAP27-1 Localize to Different Regions of ER-PM Contact Sites in <i>N. benthamiana</i> Leaf Epidermal Cells.....	33
Figure 11.	SYT1 and VAP27-1 Accumulate on Different Region of ER Elements in Arabidopsis Root Apex Cells.	35
Figure 12.	SYT1 and VAP27-1 Antibodies are Specific.....	36
Figure 13.	Double Immunogold Labeling of SYT1 and VAP27-1 in Arabidopsis Root Apex Cells.	38
Figure 14.	NET3C Co-Localize with VAP27-1 on VECs in <i>N. benthamiana</i> Leaf Epidermal Cells.	41
Figure 15.	Spatial Relationship between SYT1 and Plant Cytoskeleton in <i>N.</i> <i>benthamiana</i> Leaf Epidermal Cells.	42
Figure 16.	Spatial Relationship between SYT1, VAP27-1, and Microtubules in <i>N. benthamiana</i> Leaf Epidermal Cells.	43
Figure 17.	Anchoring of SYT1 to PM is not Affected by VAP27-1 Mutant in <i>N.</i> <i>benthamiana</i> Leaf Epidermal Cells.	45
Figure 18.	Mutation of SYT1 C2A Domain do not Disrupt SECSs and VECs in <i>N. benthamiana</i> Leaf Epidermal Cells.	46
Figure 19.	Removal of SECSs has Little Effect on Anchoring of VAP27-1 at Stable Puncta Structures in <i>N. benthamiana</i> Leaf Epidermal Cells.	48
Figure 20.	VAP27-1 Puncta and ER Networks are More Dynamic in Cells of Arabidopsis <i>syt1-2</i> Null Mutant.....	49
Figure 21.	SYT1 is Essential for Maintaining of Polygonal ER Networks in Arabidopsis Leaf Epidermal Cells.	51
Figure 22.	Motility of VAP27-1 at ER-PM Contact Sites is Restrained by Microtubules and SYT1 in Arabidopsis Epidermal Cells.....	52
Figure 23.	VAP27-1-Enriched ER-PM Contact Sites are Unstable Without SYT1 in Arabidopsis Leaf Epidermal Cells.....	53
Figure 24.	Tethering of SYT1 and VAP27-1 at PM is not Affected by BFA Treatment in Arabidopsis Root Apex Cells.....	56
Figure 25.	Vesicle Trafficking in Arabidopsis Root Apex Cells is Disturbed by the Loss of <i>SYT1</i>	58

Figure 26.	SYT1-Enriched ER-PM Contact Sites Show Various Patterns...	59
Figure 27.	Some Cell Cortex Areas are Free of SYT1, VAP27-1, and Microtubules in <i>N. benthamiana</i> Leaf Epidermal Cells.	61
Figure 28.	Spatial Relationship between SECSs and Early Endosomes in <i>N.</i> <i>benthamiana</i> Leaf Epidermal Cells.	62
Figure 29.	Phylogeny of SV2 and SV2-Like Proteins.	64
Figure 30.	Developmental Stage-Specific Expression of Arabidopsis <i>SVL</i>	65
Figure 31.	Identification of Arabidopsis <i>SVL</i> Mutants.	67
Figure 32.	Arabidopsis <i>SVL</i> Null Mutant Seedlings Show no Obvious Differences in Growth Compared with Wild Type Seedlings.....	68
Figure 33.	<i>SVL</i> -GFP is Localized on Vesicles in <i>N. benthamiana</i> Leaf Epidermal Cells.	69
Figure 34.	<i>SVL</i> is Localized on Trans-Golgi Network in <i>N. benthamiana</i> Leaf Epidermal Cells.	70
Figure 35.	<i>SVL</i> is not Localized to CLC-Coated Vesicles and Prevacuolar Compartments in <i>N. benthamiana</i> Leaf Epidermal Cells.....	71
Figure 36.	<i>SVL</i> is Partly Localized on the Multivesicular Bodies and Recycling Endosomes <i>N. benthamiana</i> Leaf Epidermal Cells....	73
Figure 37.	<i>SVL</i> is Localized on Trans-Golgi Networks/Early Endosomes in Arabidopsis Root Apex Cells.	75

7.3 List of Table

Table 1.	Primer List.	19
Table 2.	List of SV2-related proteins.	27
Table 3.	Statistical Analysis for Clustering of Gold Particles.	39
Table 4.	Spatial Relationship between VECs and SECSs.	40

Acknowledgements

I would like to express my deepest gratitude to Dr. Frantisek Basluska for his guidance throughout my PhD study. I have learned a lot from him. His expertise helped me overcome many difficulties during my study. I would like to thank him for giving me many opportunities to cooperate and communicate with other research groups and for letting me plan my own schedule freely. It is really delightful to study under Dr. Baluska. I would also like to extend my appreciation to Prof. Dr. Diedrik Menzel, Prof. Dr. Albert Haas, and Prof. Dr. Pavel Kroupa for presiding over my defence. The SYT1 work in this dissertation was done jointly with Prof. Patrick J. Hussey's group in Durham University, UK. I would like to express my sincere gratitude to Prof. Hussey for hosting my stay in Durham University in the summer of 2014. My thanks also goes to Dr. Pengwei Wang for the inspiring discussions and his kind help.

I would like to extend my sincere gratitude to Deutsche Akademischer Austauschdienst (DAAD) for supporting my PhD study in the Institut für zelluläre und Molekulare Botanik (IZMB) at the University of Bonn in Germany. Without this scholarship I would have not started my study in Germany and finished this dissertation. I would also like to thank our technicians, Ursula Mettbach, for her great assistance on immunogold labeling, and Claudia Heym, for the technical supports in the lab. My special thanks goes to Andrew Lai for English editing and his warm support. I also want to thank my friend Chuan Ku for helping me with the phylogenetic analyses. My lab mates also deserve my gratitude for discussing with me and helping me.

Finally, I would like to dedicate this dissertation to my family. I warmly appreciate for their love, concern and spiritual support all these years. Lastly, I would like to extend my appreciation to people I met during my PhD study! You have enriched my life!

Curriculum Vitae

Siao, Wei

siao@uni-bonn.de

Education

2012 - 2016 **PhD study in Molecular and Cellular Botany**, University of Bonn, Germany

2010 - 2012 **M. S. in Plant Biology**, National Taiwan University, Taiwan

2003 - 2007 **B. S. in Agronomy**, National Taiwan University, Taiwan

Specialization

Whole-mount Immunolabeling; Immunogold Labelling; Gene Gun Bombardment; Confocal Microscopy; Electron Microscopy; 2D gel; Western blot; Kinase assay; QCM analysis; Protein purification; Promoter Analysis; Rice Transformation; Arabidopsis Transformation; Real-Time RT PCR; Gene Construction; Enzyme Activity Assay (α -amylase, β -amylase, GUS and LUC); GUS Analysis; CFDA Labeling

Research and Work Experience

Jul. 2010 – Jun. 2012 **Graduate Student**, National Taiwan University

Dr. Hsu-Liang Hsieh's Lab, Institute of Plant Biology

1. Revealing the phospho-regulation of a protein involved in the light signaling and JA signaling pathways.
2. Identifying the kinase-substrate relationship between casein kinase 2 and a protein involved in far-red light and JA signaling.

Jan. 2009 – May. 2010 **Research Assistant**, National Taiwan University

Dr. Shu-Jen Wang's Lab, Department of Agronomy

1. Analyzed the transcription regulating elements controlling the sucrose transporter gene expression in rice by promoter deletion analysis.
2. Studied the subcellular localization of a rice sucrose transporter by transient expression of the protein fused with GFP.
3. Studied the organ- and tissue-specific expression of a rice sucrose transporter by generating promoter-reporter rice transformants.

Jul. 2008 – Jan. 2009 **Part-Time Research Assistant**, National Taiwan University

Dr. Shu-Jen Wang's Lab, Department of Agronomy

1. Studied hormone effects on sucrose transporter gene expression in rice embryos.
2. Analyzed the function of a salt-responsive gene in transgenic Arabidopsis.

Jul. 2007 – Jun. 2008 **Coast Guard Officer**, Mandatory Military Service
Su-Ao Harbor Inspection Office, Coast Guard Administration

1. Conducted security inspection of merchant vessels.
2. Cooperated in National Marine Pollution Mitigation Program.
3. Managed the internal affairs and training in the office.

Jul. 2006 – Jun. 2007 **Undergraduate Research Student**, National Taiwan University
Dr. Shu-Jen Wang's Lab, Phytotron, Department of Agronomy

1. Analyzed changes in starch amounts in germinating rice embryos.
2. Analyzed α -amylase and β -amylase enzyme activities in rice embryos.

Awards

1. DAAD Scholarship holder of Research Grants for Doctoral Candidates and Young Academics and Scientist
2. Dean Award of College of Life Science, Master Program, Institute of Plant Biology, NTU.
3. Outstanding Poster Presentation for Master Program, Institute of Plant Biology, NTU.
4. Six time Presidential Award winner in NTU with class ranking in the top 5%. (Bachelor's degree)
5. Dean's List Award, NTU, for providing consultation to students, with class ranking in the top 10%.
6. 1996 Agronomy Alumni Scholarship for senior students.
7. Fine Poster Presentation in Biology Program for Selected High Student, Academia Sinica.

Publications

1. Wang, H, Han, S, Siao, W, Song, C, Xiang, Y, Wu, X, Cheng, P, Li, H, Jásik, J, Mičičeta, K, Turňa, J, Voigt, B, Baluška, F, Liu, J, Wang, Y, Zhao, H (2015) Arabidopsis Synaptotagmin 2 participates in pollen germination and tube growth and is delivered to plasma membrane via conventional secretion. *Mol Plant* 8:1737-1750.
2. Siao, W, Chen, J, Hsiao, H, Chung, P, Wang, S (2011) Characterization of *OsSUT2* expression and regulation in germinating embryos of rice seeds. *Rice* 4:39-49.
3. Liu, S, Siao, W, Wang, S (2010) Changing sink demand of developing shoot affects transitory starch biosynthesis in embryonic tissues of germinating rice seeds. *Seed Sci Res* 20:137-144.
4. Chen, Y, Liu, S, Siao, W, Wang, S (2010) Hormone and sugar effects on rice sucrose transporter *OsSUT1* expression in germinating embryos. *Acta Physiol Plant* 32:749-756.